

Lawrence Berkeley National Laboratory

Recent Work

Title

THE QUEST FOR SUPERSYMMETRY

Permalink

<https://escholarship.org/uc/item/0v7504z2>

Author

Hinchliffe, I.

Publication Date

1985-12-01



Lawrence Berkeley Laboratory

UNIVERSITY OF CALIFORNIA

RECEIVED
LAWRENCE
BERKELEY LABORATORY

MAR 25 1986

LIBRARY AND
DOCUMENTS SECTION

Physics Division

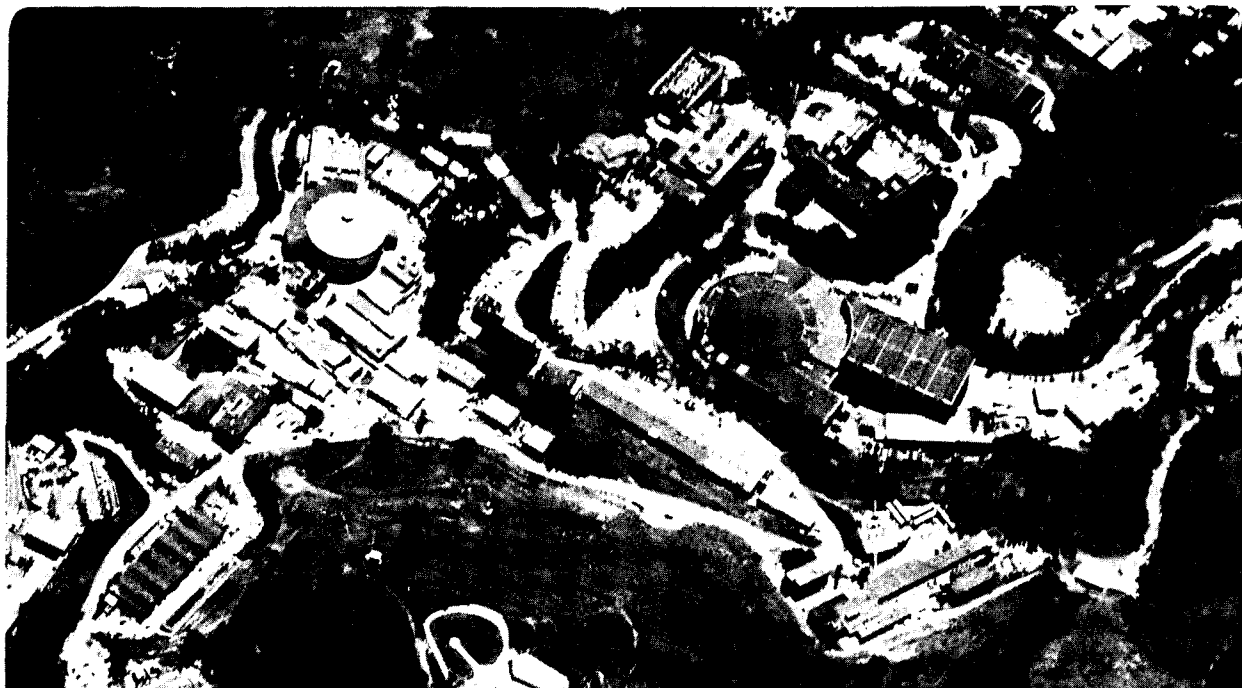
Lectures given at the Summer School on
'Architecture of Fundamental Interactions',
Les Houches, France, July-August 1985

THE QUEST FOR SUPERSYMMETRY

I. Hinchliffe

December 1985

For Reference
Not to be taken from this room



LBL-20747
e.1

DISCLAIMER

This document was prepared as an account of work sponsored by the United States Government. While this document is believed to contain correct information, neither the United States Government nor any agency thereof, nor the Regents of the University of California, nor any of their employees, makes any warranty, express or implied, or assumes any legal responsibility for the accuracy, completeness, or usefulness of any information, apparatus, product, or process disclosed, or represents that its use would not infringe privately owned rights. Reference herein to any specific commercial product, process, or service by its trade name, trademark, manufacturer, or otherwise, does not necessarily constitute or imply its endorsement, recommendation, or favoring by the United States Government or any agency thereof, or the Regents of the University of California. The views and opinions of authors expressed herein do not necessarily state or reflect those of the United States Government or any agency thereof or the Regents of the University of California.

THE QUEST FOR SUPERSYMMETRY*

Lectures given at the Summer School on 'Architecture of Fundamental Interactions' Les Houches France July-August 1985.

Ian Hinchliffe

*Lawrence Berkeley Laboratory
University of California
Berkeley, California 94720*

1. Introduction
2. Cosmological Bounds
3. Supersymmetry in e^+e^- Annihilation
4. Supersymmetry in Hadronic Reactions
5. Rare Processes
6. Summary and Outlook

*This work was supported by the Director, Office of Energy Research, Office of High Energy and Nuclear Physics, Division of High Energy Physics of the U.S. Department of Energy under contract DE-AC03-76SF00098.

I. Introduction

These lectures are concerned with the methods for searching for supersymmetric particles and the limits which have been set on their masses and couplings. Appealing as it may be to most theorists, there is no experimental evidence in favor of supersymmetry although much effort has been expended in the quest for it.* There are some problems, particularly in cosmology (e.g. the dark matter problem)⁵ which can be solved by the existence of some supersymmetric particles. Unfortunately, it may also be possible to solve them without invoking supersymmetry. I shall take the attitude that such indirect evidence is not reliable and shall use arguments based on such physics to place limits only. If positive evidence for supersymmetry is found elsewhere, then one may be more inclined to believe that supersymmetry could be helping with such problems.

The methods for constructing supersymmetric models have been discussed by Graham Ross in his lectures at this school⁶ and I shall rely upon much of his material. The remainder of this first section is devoted to the setting up of notation and to discussion of the assumptions that I will use throughout the rest of these lectures. Since there is no compelling model of supersymmetry, I shall attempt to keep my discussion as model independent as possible. Sometimes I will be forced to sacrifice generality for clarity.

Section two will discuss the limits from cosmology. In sections three and four I shall discuss the direct searches for supersymmetry in e^+e^- and hadron machines. Section five will deal with the constraints from rare processes, and finally in section six I shall give an overview of the prospects for future searches and comment upon some ways to evade existing limits.

I shall only discuss models based on $N = 1$ supersymmetry, in which case the minimal supersymmetric model must have three generations of quarks and leptons, and their superpartners, the squarks and sleptons, each of which contains the following representations under $SU(2) \times U(1)_Y$

$$\begin{array}{cccccc} L = \begin{pmatrix} \nu \\ e \end{pmatrix}_L & E^c = e_R^+ & Q = \begin{pmatrix} u \\ d \end{pmatrix}_L & u_R^c & d_R^c & \\ y = -1 & 2 & 1/3 & -4/3 & 2/3 & \end{array} \quad (1.1)$$

*See references 1-4 for earlier review material and more details of the material in this introductory section.

$$\begin{array}{cc} H_1 = \begin{pmatrix} H_0 \\ H^- \end{pmatrix}_L & H_2 = \begin{pmatrix} H^+ \\ H^0 \end{pmatrix} \\ Y = & -1 \quad 1 \end{array}$$

The subscripts L and R refer to helicity states and Y is normalized in the usual manner so that the particle's electric charge is given by

$$Q = T_3 + \frac{Y}{2}, \quad (1.2)$$

where T_3 is value of the weak isospin. In a supersymmetric model each of these fields is a superfield which has a fermionic component and a scalar component. I will usually suppress indices when writing the couplings and will use the same label for a superfield as for its scalar component. The fermionic component of a superfield A will be indicated by ψ_A .

The gauge fields are contained in supermultiplets which contain the spin 1 gauge fields themselves as well as a spin 1/2 Majorana gauginos.

In the minimal Weinberg-Salam model⁷ the gauge symmetry is broken to $U(1)_{em}$, and quark and lepton masses generated, via the vacuum expectation value of a single Higgs doublet. This is not possible in a supersymmetric model where at least two doublets are required.

The superpotential which contains the interactions between the quarks, leptons and Higgs multiplets must contain the following terms.

$$W_1 = \lambda_L L E^c H_1 + \lambda_d Q H_1 d^c + \lambda_u Q H_2 u^c. \quad (1.3)$$

The second term, which contains the Yukawa interaction $\psi_Q \psi_d H_0$, generates a mass for the down quark once H_0 obtains a vacuum expectation value $(vev)v_1$. In the non-supersymmetric model, the up quark's mass is generated from $\psi_Q \psi_u H_0^*$. This term is not available in a supersymmetric model since H^* cannot appear in the superpotential⁸, hence the need for H_2 whose $vev v_2$ will generate the appropriate mass.

The superpotential can also contain the term $\mu H_1 H_2$. If this term is not present then the theory contains a Peccei-Quinn symmetry⁹ under which H_1 and H_2 can have independent phase rotations. This symmetry will be broken when the Higgs fields obtain vevs and a phenomenologically unacceptable axion¹⁰ may result. If $\mu \neq 0$, the axion is eliminated. If the theory is grand unified then it may be

possible to expunge this axion even if $\mu = 0$, since radiative corrections may generate additional terms which violate the Peccei-Quinn symmetry.

The potential for the scalar fields will have the following contributions from W

$$\begin{aligned}
V \ni & |\mu H_2 + \lambda_L L E^c + \lambda_d Q d^c|^2 + |\mu H_1 + \lambda_u Q u^c|^2 \\
& + \lambda_L^2 \left[|E^c H_1|^2 + |L H_1|^2 \right] + |\lambda_d H_1 d^c + \lambda_u H_2 u^c|^2 \\
& + \lambda_d^2 |Q H_1|^2 + \lambda_u^2 |Q H_2|^2
\end{aligned} \tag{1.4}$$

and will contain the following D terms from the gauge interactions of $SU(2) \times U(1)_Y$. (I have suppressed that from $SU(3)_{color}$ which plays no role).

$$V \ni \frac{D^a D^a}{2} + \frac{D' D'}{2}$$

with

$$D^a = \frac{g_2}{2} \left[H_1^\dagger \tau^a H_1 + H_2^\dagger \tau^a H_2 + Q^\dagger \tau^a Q + L^\dagger \tau^a L \right] \tag{1.5}$$

and

$$D' = \frac{g'}{2} \left[H_2^\dagger H_2 - H_1^\dagger H_1 + y_a Q^\dagger Q + y_u u^\dagger u^c + y_d d^\dagger d^c - L^\dagger L + 2E^\dagger E^c \right].$$

Here y_i is the hypercharge of the representation i and g_2 and g' are the $SU(2)$ and $U(1)_Y$ coupling constants.

Supersymmetry must be broken in order to lift the degeneracy between quarks and squarks. I will assume that it is broken via the appearance of soft operators¹¹ in this potential which do not break $SU(3) \times SU(2) \times U(1)$. These can take the form of masses for all the scalars:

$$\tilde{m}_i^2 \phi_i^2 \tag{1.6}$$

and pieces proportional to the terms in the superpotential itself

$$A W_1 + B \mu H_1 H_2. \tag{1.7}$$

Low energy supersymmetry is usually motivated by the desire to provide the solution to the hierarchy problem.¹² It does this by removing the quadratic divergences appearing in the Higgs mass renormalization. These divergences are cut off at the mass of the scalar partners. Therefore, the masses appearing in the soft operators should be of order M_W and are unlikely to be more than a few TeV if the Higgs system is naturally to maintain the correct mass scale.

Supersymmetry breaking can also be manifested in mass terms for the gauginos

$$M_i \tilde{g}_i \tilde{g}_i. \tag{1.8}$$

In the most popular types of supersymmetric models, those based on the coupling to supergravity¹³ the mechanism which breaks supersymmetry treats all the matter fields equally and consequently all the scalar masses are equal when the potential is evaluated at the scale where this mechanism operates. This scale is of order the Planck mass ($M_P \approx 10^{19} GeV$) and, therefore, renormalization effects will be important and the masses will not be equal when they are evaluated at low energy ($0(M_W)$). The relevant renormalization group equations are given in Appendix A. The most important renormalization effects are due to gaugino masses and any large Yukawa couplings present in the superpotential.¹⁴

If the gaugino masses are comparable to, or larger than, scalar masses at M_P then, since over most of the range between M_P and M_W the strong coupling (α_s) is larger than the weak and electromagnetic couplings, squark masses will be affected more than slepton or Higgs masses by radiative corrections and will be larger at low energy. This renormalization effect is so strong that it prevents the gaugino masses from being much greater than the squark masses in models where such effects are important.

The only Yukawa coupling which is known to be large is that of the top quark. This enters in the evolution of the masses $m_{\tilde{t}_L}$, $m_{\tilde{t}_R}$ and m_{H_2} . It usually makes the top squark appreciably lighter than the other squarks, and can reduce the Higgs mass squared sufficiently so that the breaking of weak interactions is triggered.¹⁵

After the two neutral members of the Higgs doublets have obtained *vevs* v_1 and v_2 , the slepton mass matrix will have the following form

$$\begin{pmatrix} \tilde{e}_L \\ \tilde{e}_R \end{pmatrix}^\dagger \begin{pmatrix} L^2 \tilde{m}^2 + m_e^2 & A m_e + \mu m_e \frac{v_2}{v_1} \\ A m_e + \mu m_e \frac{v_2}{v_1} & R^2 \tilde{m}^2 + m_e^2 \end{pmatrix} \begin{pmatrix} \tilde{e}_L \\ \tilde{e}_R \end{pmatrix} \tag{1.9}$$

The off-diagonal terms which cause mixing between the partners of the left and right handed leptons arise from the terms in the scalar potential coming from W_1 . Hence the dependence on the lepton mass (m_e). The mixing is therefore likely to be small for the partners of all known leptons and it is reasonable to assume that the eigenstates are the partners of the left and right handed leptons. I have introduced a mass scale \tilde{m} so that L and R are dimensionless.

The terms L^2 and R^2 arise from two sources. Firstly, there are the soft masses. In the renormalization to low scales L^2 evolves more slowly than R^2 due to the presence of Yukawa couplings (see Appendix A) leading to $L > R$ at low energy. However, these effects are proportional to the lepton's Yukawa coupling and are therefore small for the known leptons. The effects of gaugino masses are larger for L than R since the winos can act in the former case. Again this tends to make L^2 larger than R^2 at low energy if they are equal at M_P .

Secondly there are the contributions to L and R from the D terms

$$\pi\alpha_{em} (v_2^2 - v_1^2) \left(\frac{2\tilde{e}_R\tilde{e}_R}{\cos^2\theta_W} - \tilde{e}_L\tilde{e}_L \left(\frac{1}{\cos^2\theta_W} - \frac{1}{\sin^2\theta_W} \right) \right) \quad (1.10)$$

If the weak interaction breaking is triggered by a large t-quark Yukawa coupling then $m_{H_2}^2 < m_{H_1}^2$ and it is likely that $v_2 > v_1$. Hence R is greater than L . This effect is likely to overwhelm the effect from the renormalization group scaling unless the gaugino masses are large, so it is reasonable to expect $R > L$ in the slepton mass matrix. Notice that these splittings are quite small unless v_1/v_2 is much different from one, so that one may expect approximate degeneracy between the left and right partners of all the sleptons, although this will not be one of my standard assumptions.

In the standard model, the absence of neutrino masses is sufficient to ensure that there is separate lepton number conservation for the electron, the muon, and the tau. In a supersymmetric model, since the sneutrinos have mass, the individual lepton number conservation may be lost. Of course, it can always be imposed as a global symmetry. Failure to observe processes such as $\mu \rightarrow e\gamma$ leads to tight constraints on lepton number violating processes. These will be discussed briefly in section five. In the meantime I shall neglect lepton number non-conserving effects.

It is natural for the sneutrino masses to be comparable with the slepton masses. If they are to be appreciably different, the difference must be produced by the mechanism which generated supersymmetry breaking, since renormalization effects

associated with Yukawa couplings, are very small for the sleptons and sneutrinos of the first three generations.

In the case of squark masses, the situation is slightly more complicated owing to the presence of Yukawa couplings which connect different generations. After diagonalization of the quark mass matrix these off diagonal couplings are responsible for the Kobayashi-Maskawa¹⁶ mixing angles. The mixing between partners of left and right handed quarks is similar to that discussed above for sleptons.

If there were no renormalization effects, all the soft squark masses would be equal and the squark mass matrix would have the following form³

$$\tilde{m}_{ij}^2 = (m_q^+ m_q)_{ij} + \tilde{m}^2 \mathbf{1}_{ij} \quad (1.11)$$

where m_q is the quark mass matrix and $\mathbf{1}$ is a unit matrix. The squark mass matrix is then diagonalized by the same rotation among flavors which diagonalizes the quark mass matrix. The mixing angles appearing in the couplings of the squarks to the W ('Skobayashi-Maskawa' angles) will be equal to the usual Kobayashi-Maskawa angles. The constraints from the absence of flavor changing neutral currents on squark mixing will be discussed in detail later (section five).

I will conclude this discussion of the mass spectrum with some comments on gaugino masses. The gaugino mass is controlled by its value at M_P and by renormalization effects. If the wino ($M_{\tilde{W}}$) and gluino ($M_{\tilde{g}}$) mass terms (equation 1.8) are equal at M_P and the theory is grand unified¹⁷ then

$$\frac{M_{\tilde{g}}}{M_{\tilde{W}}} = \frac{\alpha_s(M_W)}{\alpha_2(M_W)} \quad (1.12)$$

where α_s is the strong coupling constant. One can also expect that the gluino will be much heavier than the photino.

If the gaugino masses are zero at M_P , they can arise through graphs of the type shown in figure 1.1. There is a cancellation between the contributions from left and right handed squarks in the loop.¹⁸ The dominant contribution for gluinos will come from the top squarks, where this splitting is expected to be largest.

$$M_{\tilde{g}} = \frac{\alpha_s}{8\pi} m_t F(m_t, m_{\tilde{L}}, m_{\tilde{R}}) \quad (1.13)$$

Here m_t is the top quark mass, $m_{\tilde{L}}$ and $m_{\tilde{R}}$ are the masses of the left and right handed top squarks and F is given by

$$F(\mu, \mu_1, \mu_2) = -\frac{\mu_1^2}{(\mu^2 - \mu_1^2)} \log\left(\frac{\mu_1^2}{\mu^2}\right) + \frac{\mu_2^2}{\mu^2 - \mu_2^2} \log\left(\frac{\mu_2^2}{\mu^2}\right) \quad (1.14)$$

This radiative gluino mass is rather small so that models of this type will predict light gluinos and can be more easily ruled out. Notice that, once again, the photino is expected to be lighter than the gluino.*

The mass matrix of the remaining gauginos is complicated by the breaking of electro-weak symmetry. The charged winos (\tilde{W}) mix with the Higgsinos (ψ_{H_1} and ψ_{H_2}) to give the following mass matrix**

$$g_2(v_1\psi_{H_1}\tilde{W}^+ + v_2\psi_{H_2}\tilde{W}^-) + M_{\tilde{W}}\tilde{W}^+\tilde{W}^- + \mu\psi_{H_1}\psi_{H_2} + h.c. \quad (1.15)$$

The eigenvalues are

$$M_{\pm}^2 = \frac{1}{2}(M_{\tilde{W}}^2 + \mu^2 + 2M_{\tilde{W}}^2 \pm A) \quad (1.16)$$

with

$$A = \left((M_{\tilde{W}}^2 - \mu^2)^2 + 4M_{\tilde{W}}^4 \cos^2 2\theta + 4M_{\tilde{W}}^2 (M_{\tilde{W}}^2 + \mu^2 + 2M_{\tilde{W}} \mu \sin 2\theta) \right)^{1/2}$$

and $\tan \theta = v_1/v_2$. The interactions of the physical states depend on the values of the parameters in equation 1.15. A model independent analysis is very difficult. In the case where $\mu = 0$, and $v_1 = v_2$, the physical states are two Dirac spinors

$$\chi_1 = \begin{pmatrix} -\tilde{W}^+ \cos \phi + \psi_{H_1} \sin \phi \\ \tilde{W}^- \cos \phi + \psi_{H_2} \sin \phi \end{pmatrix}, \text{ mass } M_+ \quad (1.17)$$

$$\chi_2 = \begin{pmatrix} -\tilde{W}^+ \sin \phi - \psi_{H_1} \cos \phi \\ \tilde{W}^- \sin \phi + \psi_{H_2} \cos \phi \end{pmatrix}, \text{ mass } M_-$$

*A contribution from gravitino loops is also possible (figure 1.2), but is much smaller. ($\alpha m_{3/2}^2/M_p$).

**A detailed analysis is given in Ref. 1.

with

$$\cos \phi = \left(\frac{M_+}{M_+ + M_-} \right)^{1/2}$$

If the wino mass $M_{\tilde{W}}$ is zero then one of the eigenvalues is less than M_W .¹⁹ Even when the wino mass is not zero it is still likely that this will be true. This observation is rather important since it is one of the few relatively model independent statements which can be made about sparticle masses.

The neutral gaugino mass matrix is even more complicated. We can write the mass matrix in terms of the photino, ($\tilde{\gamma}$) zino (\tilde{Z}) (the partners of the photon and the Z boson) and neutral Higgsinos.

$$\begin{aligned} & \left(\frac{g_1^2 + g_2^2}{2} \right)^{1/2} \tilde{Z} (v_1\psi_{H_1} - v_2\psi_{H_2}) + \frac{1}{2} (M_{\tilde{W}} \cos^2 \theta_W + M_1 \sin^2 \theta_W) \tilde{Z} \tilde{Z} \\ & + (M_{\tilde{W}} - M_1) \sin \theta_W \cos \theta_W \tilde{Z} \tilde{\gamma} + \frac{1}{2} (M_1 \cos^2 \theta_W + M_{\tilde{W}} \sin^2 \theta_W) \tilde{\gamma} \tilde{\gamma} \\ & + \mu\psi_{H_1}\psi_{H_2} + h.c. \end{aligned} \quad (1.18)$$

M_1 is the mass associated with the $U(1)_v$ gaugino (\tilde{B}). The eigenstates will be labeled χ^i . The general analysis is rather messy, so I will discuss some typical cases. The 'Bino mass' (M_1) and 'wino mass' will be related if they arise either by radiative corrections or by renormalization scaling from a scale at which the theory is grand unified. I will use the relation which arises when the latter mechanism is operative

$$M_1 = \frac{5}{3} M_{\tilde{W}} g^2 / g_2^2. \quad (1.19)$$

This relation is true, for example, if the theory is unified into $SU(5)$ ¹⁷ so that

$$\tan \theta_W(M_p) = \frac{3}{5}. \quad (1.20)$$

In the limit $\mu \rightarrow 0$ the lightest eigenstate (χ_0) is made up of the Higgsinos

$$\chi_0 = \frac{v_2\psi_{H_1} + v_1\psi_{H_2}}{\sqrt{v_1^2 + v_2^2}} \quad (1.21)$$

and has mass

2. Cosmological Bounds.

In this section I shall discuss the various limits which can be applied to supersymmetric models from cosmological considerations. In the very early universe, when the temperature (T) was high, all particles with masses much less than T were in thermal equilibrium. As the temperature fell, particles whose interactions were strong enough to keep them in thermal equilibrium became rarer since their number density (n_i) followed the Boltzmann distribution ($n_i \propto e^{-m_i/T}$). A particle whose interactions are feeble, will not stay in equilibrium and will have a much larger density. If the particle is stable, it will exist in the present universe and its number density may be sufficiently large for it to make a significant contribution to the mass density of the universe.

We have seen that in a supersymmetric model, the lightest sparticle is likely to be absolutely stable and hence may still exist as a relic of the Big Bang. Some simple relations from cosmology are required before we can proceed.²⁶ If we assume that the universe is described by Robertson-Walker metric with scale factor R, then the evolution of R is given by

$$\frac{1}{2} \left(\frac{dR}{dt} \right)^2 = \frac{G_N M}{R} + k + \frac{\Lambda R^2}{3} \quad (2.1)$$

Here t is the age of the universe, Λ is the cosmological constant and k is the curvature factor which is 1 if the universe is closed -1 if it is open and zero if it is asymptotically flat. M is the mass inside a comoving volume

$$M = \frac{4\pi R^3 \rho}{3} \quad (2.2)$$

where ρ is the matter density. Conservation of energy implies that the density and pressure (p) in the matter are related by

$$d(\rho R^3) + p d(R^3) = 0 \quad (2.3)$$

In order to proceed further we need an equation of state. For a fluid composed of non-interacting relativistic particles we have

$$3p = \rho, \quad (2.4)$$

and for a gas of non-relativistic particles of mass m

$$\rho = mn, \quad p = nkT. \quad (2.5)$$

Here, k is Boltzmann's constant; I shall use natural units in which $\hbar = c = k = 1$ in what follows. The number density n_i and the mass density ρ_i are given by

$$\begin{aligned} n_i &= \frac{g}{2\pi^2} T^3 \int_0^\infty [\exp \epsilon/T \pm 1]^{-1} z^2 dz \\ \rho_i &= \frac{g}{2\pi^2} T^4 \int_0^\infty [\exp \epsilon/T \pm 1]^{-1} \frac{\epsilon}{T} z^2 dz \end{aligned} \quad (2.6)$$

where the +(-) sign applies to Bose (Fermi) particles, $\epsilon = (z^2 T^2 + m^2)^{1/2}$, and g is spin degeneracy factor (2 for a photon, 1 for a scalar, etc.) In the relativistic limit it is useful to write these quantities in terms of the density of a gas of photons.

$$n_\gamma = \frac{2\zeta(3)}{\pi^2} T^3, \quad \rho_\gamma = \frac{\pi^2}{15} T^4 \quad (2.7)$$

then

$$n = g_n n_\gamma / 2 \text{ and } \rho = g_\rho \rho_\gamma / 2$$

$$g_n = (n_B + \frac{3}{4} n_F)$$

and

$$g_\rho = (n_B + \frac{7}{8} n_F) \quad (2.8)$$

are the effective numbers of degrees of freedom. $n_B (n_F)$ is the numbers of Bosonic (Fermionic) degrees of freedom. The numbers g_ρ and g_n depend upon temperature, at the present time the only particles which contribute are neutrinos and photons but in the minimal supersymmetric model $g_\rho = 915/4$ at temperature above 1 TeV. If we use the equation of state for relativistic matter then equation 2.3 implies that $\rho \propto \frac{1}{R^4}$ and hence

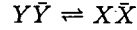
$$T \propto \frac{1}{R} \quad (2.9)$$

which gives, using 2.4, and neglecting Λ and k,

$$\left(\frac{\dot{R}}{R}\right) = -\left(\frac{\dot{T}}{T}\right) = \left(\frac{8g_p\pi^3 G_N}{90}\right)^{1/2} T^2 \quad (2.10)$$

where the dots denote derivatives with respect to t .

Let us now consider the behavior of a particle (Y) of mass M_Y as the universe cools. I will assume that Y is stable so that it can be produced and disappear only via the reaction



where X is any other particle. If the annihilation cross section is σ , the number (N) of Y in a comoving volume (V) will be reduced due to annihilations at the following rate.²⁷

$$\frac{dN}{dt} |_{ann} = -\langle\sigma v\rangle n^2 V \quad (2.11)$$

v is the relative velocity of Y and \bar{Y} and $\langle \rangle$ denotes a thermal average. If the particle is in thermal equilibrium, N will be constant, since $Y\bar{Y}$ pairs are created at the same rate. Hence we may write

$$\frac{dN}{dt} = \langle\sigma v\rangle (n_0^2 - n^2) V \quad (2.12)$$

where n_0 is the equilibrium density given by equation 2.6. Using equation 2.10 we can rewrite equation 2.12 in terms of the variable $f = n/T^3$

$$\frac{df}{dx} = m_Y \left(\frac{8\pi^3 g_p}{90M_p^2}\right)^{-1/2} \langle\sigma v\rangle (f^2 - f_0^2) \quad (2.13)$$

and we have introduced $x = T/m_Y$.

Once the cross-section σ has been calculated, this equation can be solved numerically subject to the boundary condition $f = f_0$ at $x = \infty$. As T approaches zero, f will approach some value f_1 . The qualitative behavior of the solution is easy to understand. The particle remains in equilibrium as the temperature drops provided the reaction rate given by

$$\langle\sigma v\rangle n^2 \quad (2.14)$$

exceeds the expansion rate of the universe given by equation 2.10. At some temperature T_d the reaction rate becomes equal to the expansion rate. Then, at succeeding times, the interactions are too weak to maintain equilibrium and the particle decouples. The density at later times is therefore larger than the equilibrium density.

At current times the particle is non-relativistic so that it will contribute to the observed mass density

$$\rho_Y = m_Y n = m_Y f_1 T^3 \quad (2.15)$$

In order to evaluate this we need the temperature of the gas of particles. This is not equal to the temperature (T_γ) of the microwave background (2.7 K) since the photons were reheated when other particles such as electrons annihilated.²⁶ (Y has decoupled by this time so it is not reheated). We can estimate this reheating as follows if we assume that the universe expanded isentropically. The entropy density S is

$$S = \frac{1}{T}(\rho + p) = \frac{2\rho_\gamma}{3T} g_p \quad (2.16)$$

At high temperature $g_p = g_I$. As the temperature falls below the mass of a particle g_p decreases and the remaining gas reheats slightly so that entropy is conserved. If the particle Y dropped from equilibrium at $T)M_W$ (when $g_I \sim 915/4$) then its temperature is given by $T_Y = T_\gamma \left(\frac{2}{g_I}\right)^{1/3}$. Hence

$$\rho_Y = m_Y f_1 T_\gamma^3 \left(\frac{2}{g_I}\right) \quad (2.17)$$

The mass density observed in baryons at present is $\sim 2 \times 10^{-31} g \text{ cm}^{-3}$. There is evidence that the universe may contain non-luminous matter,²⁶ but data indicate that the mass density is less than the density ρ_c required to close the universe.

$$\rho_c = \frac{3H_0^2}{8\pi G_N} \quad (2.18)$$

where H_0 is the Hubble constant. If we use $H_0 = 100 h_0 \text{ km/sec} / M_{\text{psec}}$ then

$$\rho_c = 2 \times 10^{-29} h_0^2 g \text{ cm}^{-3} \approx 10^{-48} h_0^2 \text{ GeV}^4.$$

The exact value of h_0 is not known,^{26,5} I will take $h_0 = 1$.

In order to make an estimate of the type of constraint that we can obtain on a relic particle, suppose that the interaction rate is very low so that the particle suddenly dropped out of equilibrium. Then we have $f_1 = f_0$ and the particle makes a contribution to the current mass density of

$$\rho_Y = m_Y \frac{2\zeta(3)}{\pi^2} T_Y^3. \quad (2.19)$$

(I have taken $g_Y = 2$). $\rho_Y < \rho_c$ implies that

$$m_Y \lesssim 1 \text{KeV}. \quad (2.20)$$

The method that I have just described was developed and first applied to a heavy neutrino by Lee and Weinberg.²⁷ I will discuss this case briefly since it is familiar, before passing on to the supersymmetric particles of interest. Neutrino-antineutrino pairs can annihilate into other weakly interacting particles via the Z^0 , or into charged leptons of the same generation via W exchange (see figure 2.1). The cross-section has the following form.

$$\langle \sigma v \rangle \sim G_F^2 m_\nu^2 \frac{N_A}{2\pi} \quad (2.21)$$

where N_A is a factor to account for the number of open channels and the non-relativistic approximation has been used. This approximation is valid as can be seen by evaluating T_d and noting that it is much less than the neutrino mass. Equation 2.12 becomes

$$\frac{df}{dx} = \left(\frac{16\pi^5 g_\rho}{45M_p^2} \right)^{-1/2} G_F^2 m_\nu^3 (f^2 - f_0^2) N_A. \quad (2.22)$$

The solution of this equation is shown for various choices of the masses and constants in figure 2.2. An approximate analytic solution is given below. This figure can be used to set a bound given below. This figure can be used to set a bound on the neutrino mass.

$$m_\nu \lesssim 100 \text{eV} \text{ or } m_\nu \gtrsim 2 \text{GeV}. \quad (2.23)$$

The qualitative picture is easy to understand. When the mass is very low, the annihilation rate is so slow that practically all the neutrinos survive, and so the

lower bound is similar to the estimate given above. The bound is tighter because the neutrino decouples late so the factor $(2/g_I)$ is smaller than in the case discussed above. As the mass increases, the annihilation rate rises and eventually few enough survive so that they cannot dominate the mass density.

In the supersymmetric case the analysis can be used to bound the mass of the lightest sparticle.²⁸ Since the χ_0 is in general a mixture of photino, zino and Higgsino, the analysis can be complicated, so I shall begin by assuming that it is the photino. Photino pairs can annihilate via graphs of the type shown in figure 2.3 into final states of lepton anti-lepton or quark anti-quark pairs. The cross-section has the following form²⁹

$$\langle \sigma v \rangle = \frac{e^2}{4\pi} \sum_f \frac{Q_f^4}{m_f^4} \left[\frac{4}{3} (m_{\tilde{\tau}}^2 - m_f^2) \left(\frac{v}{2} \right)^2 + m_f^2 \right] \quad (2.24)$$

Here m_f is the mass of the final state fermion of charge Q_f and $m_{\tilde{\tau}}$ is that of the exchanged sparticle.

The origin of the two terms on the right hand side of equation 2.24 can be understood simply. In the limit of large slepton and squark masses, we can write an effective vertex which couples two photinos to a fermion anti-fermion pair as follows

$$\frac{e^2}{2m_{\tilde{f}}^2} Q_f^2 (\bar{\psi}_{\tilde{\tau}} \gamma^\mu \gamma_5 \psi_{\tilde{\tau}}) (\bar{f} \gamma_\mu \gamma_5 f) \quad (2.25)$$

I have assumed that the left and right handed sparticles are degenerate. If the fermion mass is zero then helicity conservation forces the final state to have angular momentum $J = 1$. The photino is a Majorana fermion and so Fermi statistics force the initial state into a p-wave, resulting in an angular momentum barrier which generates the factor of v^2 . This factor can be avoided if the final state fermion has mass since helicity is no longer conserved, hence the term proportional to m_f^2 in equation 2.24. Replacing v^2 by its thermal average in the non relativistic limit,

$$\langle v^2 \rangle = 6T/m_{\tilde{\tau}}, \quad (2.26)$$

We have

$$\frac{df}{dx} = (a + bx)(f^2 - f_0^2) \quad (2.27)$$

where

$$a = c \sum_f \frac{m_f^2 Q_f^4}{m_{\tilde{\gamma}}^4}$$

and

$$b = 2c \sum_f (m_{\tilde{\gamma}}^2 - m_f^2) \frac{Q_f^4}{m_f^4} \quad (2.28)$$

with

$$c = \alpha \left(\frac{4\pi^3 g_\rho}{45 M_p^2} \right)^{-1/2} m_{\tilde{\gamma}}$$

This equation can be solved numerically or via the following approximation.

Assume that the particles stay in equilibrium until a freezeout temperature (x_f) given by

$$\frac{df_0}{dx} = (a + bx) f_0^2 \quad \text{at } x = x_f. \quad (2.29)$$

Then neglect the term f_0 on the right of equation 2.26 and solve it subject to the boundary condition

$$f = f_0 \quad \text{at } x = x_f.$$

We then have

$$f(0) = \frac{1}{ax_f + \frac{b}{2}x_f^2}. \quad (2.30)$$

The contribution of photinos to the mass density is then

$$\rho_{\tilde{\gamma}} = T^3 f(0) m_{\tilde{\gamma}}. \quad (2.31)$$

The limit on the photino mass depends on the fermion and sfermion masses (see figure 2.4),

$$\begin{aligned} m_{\tilde{\gamma}} &\gtrsim 1 \text{ GeV} & \text{for } m_{\tilde{q}} &\approx 20 \text{ GeV} \\ m_{\tilde{\gamma}} &\gtrsim 5 \text{ GeV} & \text{for } m_{\tilde{q}} &\approx 70 \text{ GeV.} \end{aligned} \quad (2.32)$$

I have assumed that all squarks and sleptons have a common mass. As in the case of the neutrino, there is a window if the photino is very light.

$$m_{\tilde{\gamma}} \lesssim 100 \text{ eV} \quad (2.33)$$

If the photino and squark masses are such that the photinos are contributing to the current mass density, then annihilations could still be occurring at a very small rate.³⁰ Reactions of the type

$$\begin{aligned} \tilde{\gamma}\tilde{\gamma} &\rightarrow \tau^+\tau^- (\rightarrow e^+e^- + X) \\ &\rightarrow c\bar{c} (\rightarrow \bar{p} + X, e^+ + X) \end{aligned} \quad (2.34)$$

could yield reasonable cosmic ray fluxes of anti-protons, positrons or high energy gamma rays. This could produce a bound which is slightly tighter than that given above.³⁰

If the χ_0 is a Higgsino then the graphs of figure 2.5 contribute to annihilations. The first graph involves Yukawa couplings and is small unless $m_{\tilde{H}} \gg m_t$, so that the process $\tilde{H}\tilde{H} \rightarrow t\bar{t}$ is allowed. The p-wave suppression remains resulting in a bound²⁸

$$m_{\tilde{H}} \gtrsim m_b = 5.5 \text{ GeV}. \quad (2.35)$$

If $v_1 = v_2$ then the second graph of figure 2.5 vanishes since the coupling of \tilde{H} to the Z^0 is zero and we need²⁸

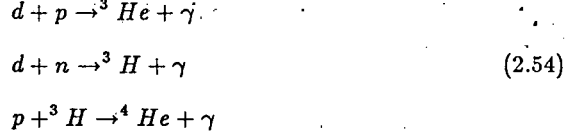
$$m_{\tilde{H}} > m_t \quad (2.36)$$

If the χ_0 is a general linear combination of $\tilde{\gamma}$, \tilde{Z} and \tilde{H} then the bound on its mass will clearly still be of order a few GeV.

Are there any other options for the lightest sparticle? If a particle (A) has non-zero electric charge, the annihilation rate is so high that very few will survive. Approximately, we have³¹

When the temperature reaches T_F , of order 1 MeV, the weak interaction rates become too slow to maintain equilibrium and the neutron to proton ratio is frozen.

There are now two competing effects, neutron decay and the formation of deuterium via $p + n \rightarrow d + \gamma$. As the temperature reaches 0.2 MeV the deuterium is processed into helium via reactions of the type



As T drops still further, these nuclear reactions stop and any remaining unprocessed neutrons decay.

According to astrophysical observations, the fraction of mass in ${}^4\text{He}$ is $23\% \pm 2\%$, and that in D and ${}^3\text{He}$ is less than 10^{-4} .³⁸

This picture is upset if the mass density, and hence the expansion rate, is changed. If ρ increases then \dot{R}/R will increase so that weak interactions will go out of equilibrium earlier, i.e. T_F rises, and we get more neutrons. The increase in expansion rate could be sufficiently great that the reactions 2.54 are not able to process all the deuterium and ${}^3\text{He}$ into ${}^4\text{He}$.

The detailed analysis is complicated since there are so many coupled channels and a numerical simulation is required. In the case of stable heavy neutrino such an analysis was performed by Kolb and Scherrer.³⁹ Their result can be used to obtain a constraint. It is clear from the above discussion that nucleosynthesis will be unaffected if the contribution to ρ at the time of nucleosynthesis is small. I will require that $\rho_{\text{gravitinos}} < \frac{1}{10} \rho_{\text{everything else}}$ at $T \sim 1 \text{ MeV}$. Then

$$\rho_{\text{everything else}} = \rho_\gamma + \rho_{e^+} + \rho_{e^-} + \rho_{\text{neutrinos}} \approx \frac{\pi^2}{3} T^4. \quad (2.55)$$

Comparing with equation 2.48 at $T = 1 \text{ MeV}$ we get

$$T_R \lesssim 3 \times 10^{12} \left(\frac{100 \text{ GeV}}{m_{3/2}} \right) \text{ GeV}. \quad (2.56)$$

The most severe constraints arise if the gravitino is unstable and decays very late in the evolution of the universe. Since the decay occurs when the gravitinos are out of equilibrium, the entropy of universe is increased by it. The baryon to

entropy ratio measured now is consistent with that which predicts the correct value of the Helium abundance during nucleosynthesis. A large release in entropy since nucleosynthesis is therefore not allowed. This yields a constraint³⁵ similar to that given in equation 2.56.

The tightest constraint comes from considering the fate of the decay products of the gravitino.^{35,40,41} If the gravitino is heavy enough it will decay into strongly interacting particles via

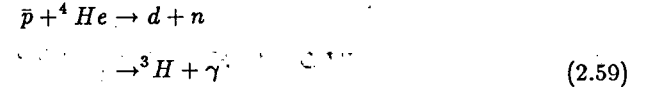
$$\begin{aligned} \tilde{G} &\rightarrow \tilde{g} + g \\ &\rightarrow \tilde{q} + q \end{aligned} \quad (2.57)$$

In this case, the ultimate decay products will include anti-protons. We would expect to obtain of the order of one anti-proton per decay. (Recall that there is approximately one anti-proton per hadronic event seen at PEP.⁴²) Even if these decay modes are not available because the gravitino is too light, the decay

$$\begin{aligned} \tilde{G} &\rightarrow \tilde{\gamma} + \gamma \\ &\rightarrow e + \tilde{e} \end{aligned} \quad (2.58)$$

will generate final state photons. The number of photons per decay and their energy spectrum is not easy to obtain. A full shower Monte-Carlo is required.⁴¹

The produced anti-protons and photons are able to initiate the break up of nuclei through reactions of the type



$$\downarrow {}^3\text{He} + e^- + \bar{\nu}.$$

The abundance of ${}^4\text{He}$ will be reduced while that of ${}^3\text{He}$ and deuterium is increased. The tight limit on the amount of ${}^3\text{He}$ can be used to bound the number of decaying gravitinos. A complete numerical simulation has been given in reference 41. Here, I shall only consider the effect of the anti-protons⁴⁰ and will make some simplifying assumptions. The production rate of ${}^3\text{He}$ via the destruction of ${}^4\text{He}$ by anti-protons is given by

$$\frac{dN_{{}^3\text{He}}}{dt} = n_{{}^4\text{He}} n_{\bar{p}} (\sigma v (\bar{p} + {}^4\text{He} \rightarrow {}^3\text{He}, {}^3\text{H} + X)) V. \quad (2.60)$$

The annihilation cross-section has been measured at CERN and is approximately 23% of the total.⁴³ If I assume that not much ${}^4\text{He}$ is destroyed and therefore that $N_{{}^4\text{He}}$ is constant. Equation 2.60 can be written as

$$\frac{dX}{dT} = \langle\sigma v\rangle \frac{n_p(T)}{T^3} M_p \left(\frac{90}{32\pi^3 g_p}\right)^{1/2} \quad (2.61)$$

where

$$X = n_{\bar{p}}/n_{{}^4\text{He}}$$

I will make the drastic assumption that there is one anti-proton produced for each decaying gravitino, and that each one is energetic enough to initiate the disintegration reaction. Furthermore I will assume that all the anti-protons appear when the age of the universe is the same as the lifetime of the gravitino. The ${}^3\text{He}$ abundance is then given by

$$X = \langle\sigma v\rangle T_x \left(\frac{90}{32\pi^3 g_p}\right)^{1/2} M_p \frac{n_{3/2}(T_x)}{T_x^3} \quad (2.62)$$

where T_x is the temperature corresponding to the gravitino lifetime.

Requiring $X < 10^{-4}$ gives $T_R \lesssim 10^8 \text{ GeV}$ for a gravitino mass of 100 GeV. The more careful analysis of Ref. 41, which applies even if there are no produced anti-protons since it relies on photo-dissociation, gives a similar result.

The tight constraint on the reheating temperature could be avoided if the gravitino were heavier than 10^6 GeV so that it could have decayed before nucleosynthesis. Alternatively, if the gravitino decay released enough energy so that all the helium was destroyed and nucleosynthesis restarted, there would be no problem. This occurs if the gravitino mass is larger than 10^4 GeV.³⁴ Gravitinos lighter than about 10 MeV will have survived to the present time and will dominate the mass of the universe. We can conclude, therefore, that if we require a reheat temperature greater than 10^{10} GeV and a successful Big Bang cosmology, gravitinos in the mass range 1 KeV to 10^4 GeV are excluded.

Why are we so interested in the reheat temperature? The conventional mechanism for generating the baryon asymmetry⁴⁴ of the universe relies upon the decay of superheavy gauge bosons and Higgs particles in a Grand Unified theory. The mass of these particles is of order the unification scale, $M_G \sim 10^{14}$ GeV. As the universe cools through temperatures of this order, these particles go out of thermal

equilibrium. Baryon and CP invariance are broken by their interactions so a net baryon asymmetry can be generated. It is one of the successes of Grand Unification that the required baryon to entropy ratio of order 10^{-11} can be generated in this way.⁴⁵

After the universe has inflated and reheated, the superheavy gauge bosons and Higgs bosons cannot reach thermal equilibrium unless $T_R \sim M_G$. In view of the constraints discussed above we must give up on this conventional mechanism if we wish to have gravitino mass of order M_W . Several alternate mechanisms for generation baryon number have been suggested. The decay of particles with masses less than 10^8 GeV is one option.⁴⁶ Models based on this idea have been constructed but they are very ugly. A better alternative is for the superheavy gauge bosons to be produced during the phase transition from the inflationary phase or by the decay of the scalar field responsible for inflation, the inflation.⁴⁷ Recently, it has also been suggested that squark and slepton fields could have non-zero vacuum expectation values⁴⁸ at temperatures in excess of a few hundred GeV. As these fields relaxed to zero and baryon and lepton number became good symmetries, the net baryon number of the universe could be created.

Cosmological investigations have proved an important tool in constraining the mass spectrum of supersymmetric models. The results are extremely model dependent. Light photinos are a possible solution to the dark matter problem. However, since other non-supersymmetric particles, such as axions could be responsible, we cannot draw any positive conclusion.

3. Supersymmetry in e^+e^- Annihilation

In this section I shall discuss the supersymmetric phenomenology of e^+e^- annihilations. The cross section for the production of a pair of squarks or sleptons is due to the exchange of the photon or Z in the s channel and is given by

$$\sigma = \frac{\pi\alpha^2}{3s} k\beta^3 \left(Q_0^2 - 2\chi Q_i p(1 - 4\sin^2\theta_W) + p^2\chi^2(1 + (1 - 4\sin^2\theta_W)^2) \right) \quad (3.1)$$

where $k = 3$ for squarks and 1 for sleptons and

$$\chi = \frac{s}{(s - M_Z^2)} \frac{1}{16\sin^2\theta_W \cos^2\theta_W}$$

For the partners of left handed fermions

$$p = 4Q_i \sin^2 \theta_W - 2I_3$$

and for the partners of right handed fermions

$$p = 4Q_i \sin^2 \theta_W$$

where Q_i is the fermion charge and I_3 is its weak isospin. The sparticles are produced with a $\sin^2 \theta$ angular distribution (θ is the angle between the beam and the sparticle).

An exception to this formula occurs when the sparticle is a selectron. In this case there is a contribution from zino and photino exchange in the t channel, see figure 3.1. In general the photino and zino are not mass eigenstates (see section 1), but assuming that this is the case, in the limit $m_{\tilde{\gamma}} = 0$, the neglect of the Z and zino contributions gives the following cross-section⁴⁹

$$\frac{d\sigma}{d\cos\theta} = \frac{\pi\alpha^2\beta^3\sin^2\theta}{8s} \left[1 + \left(1 - \frac{4}{1 - 2\beta\cos\theta + \beta^2} \right)^2 \right] \quad (3.2)$$

The rate for left and right handed sleptons is equal. Notice the peaking at small angle which is characteristic of t-channel processes.

The final state from a pair of sleptons will be a lepton pair and two χ 's. Since the Yukawa couplings of the known leptons are small the decay will be into the χ state which is dominantly photino or zino even if this state is not the χ_0 . The lifetime of the sleptons will be too short for the decay vertex to be visible, see table 1. If the χ is the lightest sparticle it will leave the detector without interacting so that the final state will consist of a lepton anti-lepton pair with unbalanced momenta.

Searches for such final states at PETRA yield the limits shown in figure 3.2.⁵⁰ The only backgrounds arise from two-photon production of a fermion anti-fermion pair and from tau pair production. The former can be eliminated by taking events where the missing momentum vector does not point along the beam direction. The latter produces lepton antilepton pairs which are back to back, since the tau is light, and μe final states which cannot be produced by the slepton pair decay.

If the χ is not the lightest sparticle it may decay inside the detector. If it decays to a photon and χ_0 , which then exits, the final state will consist of a lepton anti-lepton pair and two photons with unbalanced momenta. A search for this channel has also been carried out and the resultant limits are similar to those in the case of the stable χ .⁵¹

It is difficult to criticize these direct searches, which exclude sleptons with masses less than 20 GeV or so. They are rather model independent, being insensitive to the detailed properties of the χ states. The unlikely decay chain

$$\tilde{e} \rightarrow e + \tilde{\gamma} \rightarrow e + q + \bar{q} + \tilde{H}^0 \quad (3.3)$$

is the only obvious possible loophole.

A selectron can be produced singly in association with a photino via the graphs shown in figure 3.3. The cross-section is given by⁵²

$$\begin{aligned} \sigma(e^+e^- \rightarrow \tilde{e}^+\tilde{\gamma}e^-) = & \frac{\alpha^2}{9s} \left[\frac{2}{x} + 18 - 54x + 34x^2 \right. \\ & + 3(3 - 3x - 4x^2) \log x \\ & \left. - 9x \log^2 x \right] \log(E/m_e) \end{aligned} \quad (3.4)$$

where m_e is the electron mass, E is the beam energy and

$$x = m_{\tilde{e}}^2/s$$

the equivalent photon approximation⁵³ has been used in this estimate. The final state consists of a wide angle electron, from the selectron decay, whose transverse momentum is not balanced by visible tracks. The positron is scattered at a very small angle and consequently is unlikely to be detected. A search for this process has been carried out and yields the constraint⁵⁴

$$m_{\tilde{e}} > 23 \text{ GeV} \quad (3.5)$$

if $m_{\tilde{\gamma}=0}$ and it is assumed that the two selectrons corresponding to the two electron chirality states are degenerate. Notice that this limit depends critically upon the photino coupling and is therefore more model dependent than that from the direct searches discussed above.

In the case of squark pair production the situation is not so good. There are two possible decay modes.

$$\begin{aligned}
& \tilde{q} \rightarrow q + \chi_0 \\
& \tilde{q} \rightarrow \tilde{g} + q \\
& \quad \hookrightarrow q\tilde{q}\chi_0
\end{aligned}
\tag{3.6}$$

The latter will dominate if the gluino is lighter than the squark. In either case the final state consists of hadrons with missing energy/momentum.*

If all the squark flavors were degenerate then the onset of squark pair production could be detected by a rise in the total hadronic cross-section. The rise due to the crossing of a single squark threshold could be too small to see, particularly if the squark had charge $1/3$. In this case, one must look at specific final states. Searches have been carried out for the mode $\tilde{q} \rightarrow q + \chi$ on the assumption that the χ is stable (its detailed properties are irrelevant).⁵⁵ The final state consists of two jets with unbalanced momenta. Squarks of mass less than 14 GeV are excluded. The rather unlikely case of a stable squark is also excluded if its mass is in the same region.⁵⁵ I am aware of no search which is sensitive to the mode $\tilde{q} \rightarrow q + \tilde{g}$, indeed the situation with regard to squark searches in e^+e^- annihilation is rather unsatisfactory.

Let us now turn to the pair production of pairs of neutral sparticles which takes place by the processes shown in figure 3.4.⁵⁶ If both of the produced χ 's are stable then there will be nothing observable in the final state. If one, or both, of the χ 's decays then a signal is possible. The analysis is very model dependent. Searches have been carried out for final states with photons⁵⁷ and missing energy which could arise from the decay chain

$$e^+e^- \rightarrow \chi + \chi \rightarrow \chi_0 + \chi_0 + \gamma + \gamma \tag{3.7}$$

A search for the final state $\tilde{Z}\tilde{\gamma}$ ⁵⁸ has also been carried out.⁵⁹ Experiments have looked for the decays of the zino into $\gamma\tilde{\gamma}$ or $e^+e^-\tilde{\gamma}$.

If a photon is produced along with the χ pair then the final state may be observable even if the χ 's are stable. I shall discuss one specific case which has received some attention. If χ is a photino, then a photino pair can be produced in association with a photon via the graphs of figure 3.5. In the limit the single photon differential cross section is given by⁶⁰

*Hadronization will be discussed in the next section

$$\begin{aligned}
\frac{d\sigma}{dx_\gamma d\cos\theta} &= \frac{2\alpha^3}{3m_\pm^4} \frac{s}{x_\gamma \sin^2\theta} \left[(1-x_\gamma) \left(\frac{1-x_\gamma^2}{2} \right) + \frac{1}{4} x_\gamma^2 (1-x_\gamma) \cos^2\theta \right] \\
&\quad \times \left(1 - 4 \frac{m_\pm^2}{s(1+x_\gamma)} \right)^{3/2}
\end{aligned}
\tag{3.8}$$

where

$$x_\gamma = 2E_\gamma/\sqrt{s}.$$

Notice that the cross-section peaks at small angle and energy, so that an effective search will have to be sensitive to soft photons. The principal background is due to radiative Bhabha scattering, where the transverse momentum of the photon is balanced by an electron (see figure 3.6). A dedicated experiment at SLAC⁶¹ has set a limit on this process which translates into the constraint on photino and selectron masses shown in figure 3.7. The limit is extremely model dependent; the experiment produces no constraint if χ is a higgsino. The result of this experiment can also be used to set a limit on the number of neutrinos (N_ν) produced via $e^+e^- \rightarrow \nu\bar{\nu} + \gamma$.⁶² The cross-section can be obtained from equation 3.5 by means of the substitution

$$\frac{2\alpha^3}{3m_\pm^4} \rightarrow \frac{G_F^2 \alpha}{6\pi^2} [N_\nu \left(\frac{1}{2} - 2\sin^2\theta_W \right) + 4\sin^2\theta_W]. \tag{3.9}$$

The pair production of winos is also possible if they are sufficiently light. Recall from section 1 that in a class of models, those with small Majorana gaugino masses, there is an eigenstate (a mixture of wino and Higgsino, see equation 1.17) with mass less than the mass of the W boson. The production process

$$e^+e^- \rightarrow \tilde{W}^+ \tilde{W}^- \tag{3.10}$$

occurs at a rate similar to that for the production of the charged particles. There are two distinct possibilities for the decay of a wino. If the channel

$$\tilde{W} \rightarrow e + \tilde{\nu} \tag{3.11}$$

is allowed, it will dominate. Decays with squarks in the final state are unlikely given the limits on their masses. In this case the signal will depend upon the behaviour of the sneutrino⁶³ which will be discussed below. A limit⁵⁹ exists only in the case

where the sneutrino leaves the detector before decaying or decays into unobservable states.

If the sneutrino is too heavy for the channel 3.11 to be open, then the decays

$$\begin{aligned}\tilde{W} &\rightarrow \ell\nu + \chi \\ \tilde{W} &\rightarrow q + \bar{q} + \chi\end{aligned}\tag{3.12}$$

will occur. The leptonic decays lead to a final state with two charged leptons and missing energy. The branching ratio for the decay $\tilde{W} \rightarrow e + \nu + \chi$ is model dependent but a value of 10% seems reasonable. In this case a search by the MARK-J collaboration⁵⁹ has excluded winos up to about 20 GeV, provided to χ exits the detector without decaying.

Final states involving sneutrinos are also possible.⁶³ They can be produced in pairs via an intermediate Z boson. This process is too small to produce a measurable rate at current energies but could be important in the forthcoming generation of e^+e^- machines. The signal depends upon the decay of the sneutrino. The two body decay into a neutrino and a χ proceeds via the graph of figure 3.8. This decay produces nothing observable unless the χ decays. The four body final states $\ell q \bar{q} \tilde{g}$ or $\ell\nu\ell\chi_0$ are also possible, see figure 3.9. These decay rates are very model dependent but the two body mode is likely to dominate unless the gluino channel is open.⁶³ A measurement of the Z width will be able to constrain sneutrino masses respective of their decay products. The contribution of each pair $(\tilde{\nu}_L, \tilde{\nu}_R)$, assumed degenerate to the Z width is

$$\Gamma = 80\beta^3 MeV.\tag{3.13}$$

I have not discussed the production of gluinos in e^+e^- annihilation since they have no electro-weak charges. Three jet events will arise from the final state $q\bar{q}\tilde{g}$, but will only be clear when the energy is far above the threshold. It may also be possible to detect a gluino from the decays onium $\rightarrow \tilde{g}\tilde{g}$,⁶⁴ onium $\rightarrow g\tilde{g}\tilde{g}$ or onium $\rightarrow \gamma\tilde{g}\tilde{g}$ where onium is a bound state of a heavy quark and its antiquark.⁶⁵ None of these searches are easy and are superceded by the limits from hadronic searches to which we now turn.

I will close this section with a brief summary of the limits from e^+e^- annihilation. Sleptons and Winos with masses less than 20 GeV are ruled out unless very bizzare decay modes dominate. In the special case where χ_0 is a photino, selectron masses

up to 50 GeV are excluded. There are no limits on sneutrino masses at present. The squark mass limits are poor since the searches do not appear to be sensitive to the decay mode $q + \tilde{g}$. Nevertheless probably at most two squark flavors are allowed with masses below 15 GeV. We shall see in the next section that better limits on squark masses are to be obtained from hadron colliders.

4. Supersymmetry in Hadronic Reactions.

The searches for supersymmetry in hadronic reactions are more complicated, and more model dependent than those in e^+e^- annihilation. Detailed limits usually depend upon uncertainties beyond those inherent in the supersymmetric models.

I shall first discuss the searches for sleptons in hadron colliders. Fixed target experiments at CERN and FNAL have nothing to contribute in view of the limits quoted in the previous section. There are only two relevant sources of new leptons and sleptons in hadron colliders; pair production via the Drell-Yan⁶⁶ mechanism and the decay of W's and Z's. The luminosity of a collider must be large before the former can be exploited effectively and so we are left with the latter mechanism as the only one relevant at the $S\bar{p}\bar{p}S$ and Tevatron colliders. Charged sleptons can be pair produced in the decay of the Z at the following rate⁶⁷

$$\frac{\Gamma(Z \rightarrow \tilde{e}\tilde{e})}{\Gamma(Z \rightarrow e^+e^-)} = \frac{1}{2} \left(\frac{2p}{M_Z} \right)^3 \quad (4.1)$$

where p is momentum of the slepton in the Z rest frame. I have assumed that \tilde{e}_L and \tilde{e}_R are degenerate and have summed. The sleptons will decay and will produce a final state of consisting of a lepton pair with unbalanced momentum, provided χ exits or decays into unobserved particles. The rate is shown in figure 4.1 for various ranges of the lepton pair invariant mass. There is no published limit from this process since there are, as yet, insufficient produced Z's. The detection of 100 decays of the type $Z \rightarrow e^+e^-$ should be sufficient to be sensitive to slepton masses less than 35 GeV.

The decay $W \rightarrow \tilde{e}\tilde{\nu}$ will occur at a rate⁶³

$$\frac{\Gamma(W \rightarrow \tilde{e}\tilde{\nu})}{\Gamma(W \rightarrow e\nu)} = \frac{1}{2} \left(1 - \frac{(m_{\tilde{e}}^2 + m_{\tilde{\nu}}^2)}{M_W^2} - 4 \frac{m_{\tilde{e}}^2 m_{\tilde{\nu}}^2}{M_W^4} \right)^{3/2} \quad (4.2)$$

The signal depends on the behaviour of the sneutrino. As I discussed in the last section it is possible that it will decay into invisible particles. In this case the final state will consist of a single lepton unbalanced in transverse momentum with a transverse momentum spectrum which is much softer than that from the decay $W \rightarrow e\nu$, see figure 4.2. Again a few hundred decays of the type $W \rightarrow e\nu$ should be sufficient to set a limit of order 40 GeV on the slepton and sneutrino masses.⁶³

The only other supersymmetric particles which can be searched for at hadron colliders are those which have strong interactions. The estimates of the production

rates of these particles are more ambiguous. All estimates are based on the QCD parton model which is illustrated in figure 4.3 for the production of a pair of massive particles X. The production rate is given by

$$\sigma = \sum_{ij} \int dx_1 dx_2 f_i(x_1, Q^2) f_j(x_2, Q^2) \sigma_{ij \rightarrow X\bar{X}} \quad (4.3)$$

Where the sum i runs over quarks anti-quarks and gluons and $f_i(x, Q^2)$ is the parton distribution functions for parton of type, which is extracted from deep inelastic scattering. In order to calculate the production rate one must first calculate the partonic cross sections. Gluino pairs can be produced from initial states of quark anti-quark or gluon-gluon with the following rates^{68,69,70}

$$\begin{aligned} \frac{d\sigma}{dt}(gg \rightarrow \tilde{g}\tilde{g}) = & \frac{9\pi\alpha_s(Q^2)}{4s^2} \left\{ \frac{2(t - m_{\tilde{g}}^2)(u - m_{\tilde{g}}^2)}{s^2} \right. \\ & + \left[\left[\frac{(t - m_{\tilde{g}}^2)(u - m_{\tilde{g}}^2) - 2m_{\tilde{g}}^2(t + m_{\tilde{g}}^2)}{(t - m_{\tilde{g}}^2)^2} \right. \right. \\ & \left. \left. + \frac{(t - m_{\tilde{g}}^2)(u - m_{\tilde{g}}^2) + m_{\tilde{g}}^2(u - t)}{s(t - m_{\tilde{g}}^2)} \right] + [t \rightarrow u] \right\} \\ & + \frac{m_{\tilde{g}}^2(s - 4m_{\tilde{g}}^2)}{(t - m_{\tilde{g}}^2)(u - m_{\tilde{g}}^2)} \left. \right\} \quad (4.4a) \end{aligned}$$

$$\begin{aligned} \frac{d\sigma}{dt}(q_i\bar{q}_i \rightarrow \tilde{g}\tilde{g}) = & \frac{8\pi\alpha_s^2(Q^2)}{3s^2} \left[\frac{[(t - m_{\tilde{g}}^2)^2 + (u - m_{\tilde{g}}^2)^2 + 2m_{\tilde{g}}^2s]}{s^2} \right. \\ & + \frac{4(t - m_{\tilde{g}}^2)^2}{9(t - m_{\tilde{g}}^2)^2} + \frac{4(u - m_{\tilde{g}}^2)^2}{9(u - m_{\tilde{g}}^2)^2} \\ & + \frac{[(t - m_{\tilde{g}}^2)^2 + m_{\tilde{g}}^2s]}{(t - m_{\tilde{g}}^2)s} \\ & \left. + \frac{m_{\tilde{g}}^2s}{9(t - m_{\tilde{g}}^2)(u - m_{\tilde{g}}^2)} + \frac{(u - m_{\tilde{g}}^2)^2 - m_{\tilde{g}}^2s}{(u - m_{\tilde{g}}^2)s} \right] \quad (4.4b) \end{aligned}$$

where s, t and u are the usual Mandelstam variables. Squarks can be pair produced from the same initial states.

$$\frac{d\sigma}{dt}(gg \rightarrow \tilde{q}\tilde{q}) = \frac{\pi\alpha_s(Q^2)}{s^2} \left[\frac{7}{48} + \frac{3(u-t)^2}{16s^2} \right] \left\{ 1 + \frac{2m_q^2 t}{(t-m_q^2)^2} + \frac{2m_q^2 u}{(u-m_q^2)^2} + \frac{4m_q^4}{(t-m_q^2)(u-m_q^2)} \right\}, \quad (4.5a)$$

$$\frac{d\sigma}{dt}(q_i\bar{q}_j \rightarrow \tilde{q}_i\tilde{q}_j) = \frac{4\pi\alpha_s^2(Q^2)}{9s^2} \left\{ \left(\frac{ut-m_q^4}{s^2} \right) \left[\delta_{ij} \left(2 - \frac{2s}{3(t-m_q^2)} \right) + \frac{s^2}{(t-m_q^2)^2} \right] + \frac{m_q^2 s}{(t-m_q^2)^2} \right\}. \quad (4.5b)$$

Squarks can also be produced in quark quark scattering

$$\frac{d\sigma}{dt}(q_i q_j \rightarrow \tilde{q}_i \tilde{q}_j) = \frac{4\pi\alpha_s(Q^2)}{9s^2} \left[-\frac{(t-m_q^2)^2 + st}{(t-m_q^2)^2} - \delta_{ij} \frac{(u-m_q^2)^2 + su}{(u-m_q^2)^2} + \frac{sm_q^2}{(t-m_q^2)^2} + \frac{\delta_{ij} sm_q^2}{(u-m_q^2)^2} - \frac{2sm_q^2 \delta_{ij}}{3(t-m_q^2)(u-m_q^2)} \right] \quad (4.6)$$

Finally a squark and a gluino can be produced from an initial state of gluon-quark^{69,70,71}

$$\frac{d\sigma}{dt}(gq_i \rightarrow \tilde{g}\tilde{q}_i) = \frac{\pi\alpha_s^2(Q^2)}{s^2} \left[4 \frac{(m_g^2 - t)}{9s} + \frac{[(m_g^2 - t)s + 2m_g^2(m_q^2 - t)]}{(t - m_g^2)^2} + \frac{4(u - m_g^2)(u + m_q^2)}{9(u - m_q^2)^2} - \frac{[(s - m_q^2 + m_g^2)(t - m_q^2) - m_g^2 s]}{s(t - m_g^2)} + \frac{[s(u + m_q^2) + 2(m_q^2 - m_g^2)(m_q^2 - u)]}{18s(u - m_q^2)} \right]$$

$$+ \left\{ \frac{(m_q^2 - t)(t + 2u + m_g^2)}{4(t - m_g^2)(u - m_q^2)} + \frac{(t - m_g^2)(s + 2t - 2m_q^2)}{4(t - m_g^2)(u - m_q^2)} + \frac{(u - m_g^2)(t + m_g^2 + 2m_q^2)}{4(t - m_g^2)(u - m_q^2)} \right\} \quad (4.7)$$

The initial states with gluons are the most important since the cross sections are larger (compare 4.4a and 4.4b), and the gluon distribution function is bigger than that of quarks over most of the relevant range of x , see figure 4.4. There is some uncertainty in these structure functions and in the value of α_s (or Λ), so it is important to check that the ones being used are reasonable. Figure 4.5 shows a comparison of the jet data⁷² from the $Spp\bar{S}$ collider with the predictions of the structure functions which will be used in this section.^{73,74}

There is some uncertainty surrounding the choice of scale Q which appears in both the structure functions and in the cross-section formulae. It should be of the same order as the mass of the produced object, or its transverse momentum if that is larger. The precise value cannot be determined until higher order QCD corrections to the production processes are calculated.

These higher order corrections are not known for most processes. An exception is the case of W production⁷⁵ where they increase the expected rate by 30% or so*. The effect of these corrections is to improve the agreement between the expected and measured values as shown in table 3. The size of this correction can perhaps be taken as an indication of those to be expected in the cross-sections for the production of new particles of similar mass. It is also worth remarking that the estimates for charm production via gluon-gluon and quark anti-quark annihilation at the ISR, and fixed target experiments at FNAL are below the measured values by a factor of three or so.⁷⁶ However the data are confused, and it is not clear how reliable are the QCD estimates for the production of a such low mass objects.

If the new particles are produced with transverse momenta much greater than their mass, then other production mechanisms can become important.⁷⁷ Figure 4.6 shows a mechanism whereby a pair of gluinos are emitted at large transverse momentum which is balanced by the emission of a gluon. This process is more important at large transverse momentum than the pair production processes discussed above in which the transverse momenta of the new particles balance each other. This

*The discrepancy between the theoretical prediction and the observed rate is not large in view of the errors but could indicate some problem with the valence quark distributions of ref. 73.

result is surprising but can be easily understood. The cross-section for $gg \rightarrow gg$ is larger by about a factor of 200 than the corresponding process $gg \rightarrow q\bar{q}$ if both are evaluated at 90 degrees in the center of mass frame. In the former process the gluon can ‘decay’ into a quark anti quark pair at the cost of a factor of order α_s/π . Provided that the transverse momentum of the gluon is much larger than the quark mass, there is no substantial phase space inhibition of this ‘decay’, and so it can dominate the direct pair production.

If a new particle is very light then it can appear as a component of the proton’s wavefunction. This intrinsic component, which is generated as the structure functions are evolved in Q^2 , can then be used to produce other new particles. This evolution is determined by the Altarelli-Parisi equations⁷⁸, up to some uncertainties associated with the implementation of thresholds. There is some confusion concerning the role of these intrinsic particles.

I will discuss the case of squark production⁷⁹ in a model where the squark is much heavier than the gluino. The squark can be produced in association with a gluino as described in equation 4.7. It is also possible to generate a single squark via the fusion of a quark and a gluino, which exists in the proton, see figure 4.7. It is common to add these two contributions together. This is an error as I will now demonstrate.

The differential cross-section for the production of a squark and a gluino, equation 4.7 peaks in the forward direction at high energy. In the limit of small gluino mass dominant part of the total cross-section will come from the term with a t channel pole viz.,

$$\frac{\pi\alpha_s^2(Q^2)}{st} \left[1 - \frac{2m_{\tilde{q}}^2}{s} \left(1 - \frac{m_{\tilde{q}}^2}{s} \right) \right] \quad (4.8)$$

which yields the following total cross-section

$$\sigma(gq \rightarrow \tilde{g}\tilde{q}) \approx \frac{\pi\alpha_s^2}{s} \left[\left(1 - \frac{m_{\tilde{q}}^2}{s} \right) + \left(\frac{m_{\tilde{q}}^2}{s} \right)^2 \right] \log\left(\frac{s}{2t_{\min}}\right) \quad (4.9)$$

where $|t_{\min}|$ is the smallest value of $|t|$ allowed, which is of order $m_{\tilde{q}}^2$. We can rewrite this cross-section in the following form

$$\sigma(s) = \int dx P_{g \rightarrow \tilde{g}}(x) \sigma_{\tilde{g}q \rightarrow \tilde{q}}(xs) \quad (4.10)$$

where the formation cross-section $\sigma_{\tilde{q} \rightarrow \tilde{q}}$ is given by

$$\sigma_{\tilde{g}q \rightarrow \tilde{q}} = \frac{2\pi^2}{P_{cm}^2} \frac{(2J+1)}{(2s_1+1)(2s_2+1)} \Gamma_E \delta(\hat{s} - m_{\tilde{q}}^2) \quad (4.11)$$

where J is the spin of the squark, s_1 , and s_2 are the spins of the quark and gluino, P_{cm} is the momentum of the quark in the squark rest frame of Γ_E is the width $\tilde{q} \rightarrow q + \tilde{g}$. Comparing equation 4.9 and equation 4.10, we conclude that

$$P_{g \rightarrow \tilde{g}}(x) = \frac{3\alpha_s}{2\pi} \log\left(\frac{s}{m_{\tilde{q}}^2}\right) ((1-x)^2 + x^2). \quad (4.12)$$

The hadronic cross-section (equation 4.3) has the following form

$$\sigma(pp \rightarrow \tilde{g} + \tilde{q}) = \int f_q(x_1) f_{\tilde{q}}(x_2) dx_1 dx_2 \sigma(\tilde{g} + q \rightarrow \tilde{g} + \tilde{q}) \quad (4.13)$$

which we can rewrite as

$$\int f_q(x_1) f_{\tilde{q}}(x_2) dx_1 dx_2 \sigma_{q\tilde{q} \rightarrow \tilde{q}} \quad (4.14)$$

with

$$f_{\tilde{q}}(x) = \frac{3\alpha_s}{2\pi} \log\left(\frac{m_{\tilde{q}}}{m_{\tilde{g}}}\right) \int \frac{dy}{y} P_{g \rightarrow \tilde{g}}\left(\frac{x}{y}\right) f_g(y) \quad (4.15)$$

which is nothing more than the solution of the Altarelli-Parisi equation for the gluino structure function^{68,80} if the running of $\alpha_s(Q^2)$ is ignored and if the generation of gluinos from other gluinos is neglected.

It is now apparent that an overcounting takes place if one includes contributions from both $gq \rightarrow \tilde{g}\tilde{q}$ and $\tilde{g}q \rightarrow \tilde{q}$ in the estimate of squark production. In the limit of very small gluino mass, the logarithm in equation 4.9 can become large and the expansion of the cross-section as a power series in α_s breaks down; the next order will contain term of order $\alpha_s^3 \log^2$ etc. The intrinsic part contains a resummation of all these logarithms, i.e. all terms of the form $\alpha_s^{n+1} \log^n$. The complete result is obtained by removing the dominant piece, equation 4.8, from the pair production cross section, evaluating the rates from the rest and then adding it to the intrinsic component.⁸¹

That procedure is complicated, let us try to see whether one mechanism is a reasonable approximation for the interesting cases. Taking a squark mass of 100 GeV, I show in figure 4.9 the cross-section from as a function of gluino mass in $p\bar{p}$ collisions at 630 GeV. The rate from the ‘dominant’ term equation 4.9 is shown

separately. It is clear that the log term is not dominant and indeed overestimates the rate by a large factor. At very small gluino masses the 'dominant' term indeed gives a reasonable estimate of the rate. The conclusion is inescapable; the estimates from intrinsic gluinos will overestimate the rate. In the subsequent discussion I shall ignore them.

The signals for supersymmetry at a hadron collider are missing momentum arising for example, from the decay

$$\tilde{g} \rightarrow q\bar{q}\chi$$

The lifetime of the gluino is much longer than the characteristic time of strong interactions (see table 1). Consequently the decay is not of a free gluino but rather of one bound inside a hadron. The predictions will therefore depend upon how the gluino hadronizes.⁸²

In order to understand the problem more clearly, consider the case of a c quark produced in an e^+e^- collider. The quark is bound into a D meson by hadronization effects, and the meson will have less energy than the quark. Some data⁸³ are shown in figure 4.9. If there is a semileptonic decay some energy is lost (carried off by the neutrino). The estimate of this missing energy will be too high if the hadronization effect is ignored, since it is the quark inside the meson which decays. This fragmentation effect is non-perturbative and so cannot be reliably calculated at present.

We can define a fragmentation function $D(z, Q^2)$ which is the probability that a charm momentum p quark of will hadronize into a D meson with momentum pz. The scale Q is the same order as the energy E. The energy dependence is predicted by perturbative QCD,^{78,85} so that we have no problem; the measured form can simply be extrapolated to any desired energy. The fragmentation function will become softer (i.e. have more support at small x) as the energy is increased. The following form⁸⁶ provides a reasonable parameterization of the fragmentation function shown in figure 4.9.

$$D(z) = \frac{N(1-z)}{((1-z)^2 + \epsilon_c z)^2} \quad (4.16)$$

where ϵ_c is a constant, and N is chosen so that $\int_0^1 dz D(z) = 1$. Since no one has seen a gluino, its fragmentation function is not known. It is clear that the effects will not be important if most of the production cross-section comes from near threshold

where the fragmentation function can be expected to be very hard. A reasonable guess is to take the form above at $Q = 2m_{\tilde{g}}$ with

$$\epsilon_{\tilde{g}} = \epsilon_b \left(\frac{m_b}{m_{\tilde{g}}}\right)^2 \text{ or } \epsilon_{\tilde{g}} = \frac{9}{4} \epsilon_b \left(\frac{m_b}{m_{\tilde{g}}}\right)^2. \quad (4.17)$$

ϵ_b is taken from a fit to the data⁸⁸ on b fragmentation. This is then extrapolated to the relevant energies using QCD. The mass dependence is expected in some models and is consistent with the differences between b and c quarks. The factor of 9/4 is motivated by the larger color charge of the gluino, and applies only if perturbation theory can be used as a guide to this non-perturbative process. The fragmentation function given by this prescription is shown in figure 4.10 for two choices of gluino mass.

We now have all the ingredients needed to discuss hadronic reactions. Can fixed target experiments at CERN or FNAL make a useful contribution? If the squark mass limits quoted in the previous section are to be believed, then the energies will be too low to produce squark pairs. The rate of gluino pair production is shown in figure 4.11. These rates are probably reliable to a factor of 5 or so. Most of the production takes place close to threshold so that the fragmentation effects are unimportant. The decay of such light gluinos is unlikely to result in a clear direct signal at these low energies. However, the decay of the gluinos which are moving rapidly in the direction of the incident beam will produce a beam of χ 's which may be detected by their interactions downstream. An experiment will then place a limit on the product of the gluino cross-section and the interaction cross-section of and χ . The discussion is model dependent so I will specialize to the case where χ is a photino which is also the lightest sparticle.

In this case the interaction cross-section is described by figure 1.3 where the exchanged particle is a squark and is given by⁸⁹

$$\sigma_{\tilde{\gamma}+N \rightarrow z} = \sum_{\text{quarks}} \int dx f_q(x, Q^2) \sigma_p. \quad (4.18)$$

with

$$\sigma_p = 2 \times 10^{37} E_{\tilde{\gamma}} \left(\frac{m_W}{m_{\tilde{q}}}\right)^4 e_q^2 x \left(1 - \frac{m_{\tilde{g}}^2}{2m_p E_{\tilde{\gamma}} x}\right) \left(1 + \frac{m_{\tilde{g}}^2}{16m_p E_{\tilde{\gamma}} x}\right) cm^{-2} \quad (4.19)$$

Here m_p is the proton mass e_q is the charge of a quark of type q and $E_{\tilde{\gamma}}$ is the energy

of the incoming photino beam in GeV. The events produced by this interaction will look similar to a neutral current neutrino events. The cross-section depends upon the squark mass, so that the experimental limit can be translated into a coupled bound on squark and gluino masses shown in figure 4.12.⁹⁰ If the gluino is light enough to that its lifetime is long, it will be scattered in the target before it can decay and the energy of the photino will be degraded. This effect explains the loophole at small gluino masses which is indicated on the figure.

Such 'beam dump' experiments are difficult to interpret if they obtain a positive result. Confirmation that the effect is due to supersymmetry requires further study.

Could a very light gluino have escaped detection elsewhere? If the gluino is lighter than 2 GeV or so it could live long enough to leave a track if the shadron containing it is charged. A model of hadronic binding is required in order to decide whether the charged shadron (made up of $\tilde{g}u\bar{d}$) or the neutral shadron (made up of $\tilde{g}g$) is stable with respect to strong interactions. Bag model calculations indicate that the charged one is stable if the gluino mass is less than 2 GeV.⁹¹ Such a charged stable particle should probably have been seen in charm searches in bubble chambers. However, no definitive statement is possible in the absence of a dedicated search. A search for contamination in a neutral beam at FNAL⁹² also constrains neutral shadrons. A gluino with a lifetime of more than 2×10^{-8} seconds and a production rate of more than $20\mu b$ in proton nucleon collision at \sqrt{s} of 28 GeV is excluded. This constraint excludes the region $m_{\tilde{g}} \approx 1\text{GeV}$ provided $m_{\tilde{q}} \geq 500\text{GeV}$ (see figures 4.11 and table 1). It is difficult to believe such a very light gluino could have escaped detection, but precise limits are difficult to set.

I will now discuss the searches at the $S\bar{p}\bar{p}S$ collider. The characteristic signature is that of missing energy arising from the decays

$$\tilde{g} \rightarrow q + \bar{q} + \chi \quad (4.20a)$$

$$\tilde{q} \rightarrow q + \tilde{g} \quad (4.20b)$$

$$\tilde{q} \rightarrow q + \chi \quad (4.20c)$$

The precise nature of χ is not critical. It is usually taken to be a photino, but provided it exits the detector without interacting or decaying the signal is unaffected. The relative branching ratio of the channels 4.20b and 4.20c is sensitive to the couplings of χ . While the first channel will dominate if it is open, it produces

more hadrons and less missing energy than the decay 4.20c. Consequently it is less likely to produce events which will pass the cuts discussed below.

In the case of a gluino decay to a quark anti-quark pair, if the gluino mass is large and its momentum small, the two quarks will be well separated and the final state will consist of two jets. As the gluino momentum is increased, the angle between the two jets will be reduced and eventually they will coalesce. The structure visible in the final state also depends critically upon the detector and in particular upon its ability to separate nearby jets and to resolve soft ones. There are a large number of theoretical papers on this subject.⁹³

I shall base my discussion upon a theoretical analysis⁹⁴ which attempts to compare with the data from the UA1 collaboration. Although I believe that the results of this analysis are a good representation of the supersymmetric limits available from the experiment, I should emphasize that the only people who can really set limits are the experimenters themselves!

The events are required to pass the following cuts.

- (a) There be a jet with transverse energy (E_T) * greater than 15 GeV.
- (b) There be at least 15 GeV of missing (unbalanced) E_T .
- (c) There be no jet within 30° of the missing E_T vector. This cut reduces the background from QCD two jet events where one jet is mismeasured, or from three jet events where one jet is missed.
- (d) Nearby jets are merged according to the UA1 jet algorithm.
- (e) There is no jet within 30° of a direction opposite to the leading jet. This is again helps to reduce the QCD background.
- (f) The average missing energy in a two jet QCD event is determined (σ), and the event is rejected if the missing E_T is less than 4σ . This cut is effective only for events which just pass the cut (b).
- (g) An attempt has been made to simulate the effects of a fluctuation in the so called minimum-bias background. This is the host of hadrons which are produced with a rather flat rapidity distribution and limited transverse momentum, and are present in all events, irrespective of whether or not they contain jets. There is a problem here since this minimum bias is not well understood and there seem to be more such particles in events with jets than in events without.⁹⁵

* E_T is a two dimensional vector defined in the plane orthogonal to the beam direction.

Figure 4.13 shows contours of the number of events passing these cuts as a function of gluino and squark masses. All squark flavors have been taken to be degenerate. The discontinuity along the line $m_{\tilde{q}} = m_{\tilde{g}}$ is caused by the abrupt change in the allowed decay chains.

The cuts are very effective in reducing the predicted number of supersymmetric events. Figure 4.15 shows the total cross section for the production of gluino pairs. A comparison with figure 4.14 show the dramatic effect of the cuts. The UA1 collaboration⁹⁶ reports a small number of monojets (23 in the 1984 data which corresponds to an integrated luminosity of 260 nb⁻¹ at 630 GeV) which pass these cuts. Of these, some are due to the decay $W \rightarrow \tau\nu$; others to the production of jets in association with W's or Z's, where the Z decays to neutrinos and the W to $e\nu$ with the lepton being missed; or others to the production of heavy quarks. The estimates of^{96,97} backgrounds from these sources may account for all the events. It seems that there are fewer than 5 events/100 nb⁻¹ which could be due to supersymmetry.

This appears to exclude squark and gluino masses below 60 GeV. A close examination of the figure reveals the possibility of an allowed region where $m_{\tilde{g}} \approx 3\text{GeV}$, $m_{\tilde{q}} \approx 100\text{GeV}$. The possibility of this so-called window for light gluinos has been much discussed.^{82,77,98} The total cross-section for the pair production of gluinos is very large in this region but very few of the events pass the cuts.* In an event where the gluinos are back to back, they must have large energy in order that there be a jet which can pass the cut (a). In this case fragmentation become important. On the average the missing transverse momenta cancel so that the events will fail to pass cut (b). This cancellation does not take place when the final state is $g\tilde{g}\tilde{g}$, since the gluinos tend to be moving in the same direction. The exclusion of this latter process reduces the event rate by approximately a factor of three.⁷⁷

A significant fraction of the events in this region come from the reaction

$$p\bar{p} \rightarrow \tilde{g} + \tilde{q} \quad (4.21)$$

$$\quad \quad \quad \downarrow$$

$$\quad \quad \quad q + \tilde{\chi}$$

The cross-section is small but the final state readily passes the cuts since it has one hard jet and an energetic photino from the squark decay. In view of the strong dependence upon the cuts which are imposed on theoretical calculations some caution is needed. Nevertheless I think that is extremely unlikely that this window is open.

*Approximately one gluino pair event in 10⁶ passes the cuts in this region of very small gluino mass.

Once there is evidence for some signal it should be fairly easy to distinguish the sources. For example if the gluino mass is much larger than the squark mass which is of order 60 GeV, the missing E_T events will mostly have two jets from

$$p\bar{p} \rightarrow \tilde{q}\tilde{q} \rightarrow q + \bar{q} + \chi + \chi \quad (4.22)$$

Occasionally one jet will be lost in the beam fragments resulting in a monojet event. Events with three jets and missing E_T cannot arise directly.

On the other hand, if the gluino mass is of order 60 GeV and the squark is much heavier, the events will tend to have a higher jet multiplicity, since the decay chain will be

$$p\bar{p} \rightarrow \tilde{g} + \tilde{g} + X \quad (4.23)$$

$$\quad \quad \quad \downarrow$$

$$\quad \quad \quad q + \bar{q} + q + \bar{q} + \chi + \chi$$

If all the squarks are not degenerate then the limit quoted on the squark mass will be modified. Likewise, if the photino decays via either of the mechanisms discussed in section 1 (see equation 1.32), the missing momentum signature will be diluted. It is not clear whether the UA1 data provide any limit in this case.

At present there are too few events in the UA1 data to be able to search for other final states such as $\tilde{g}\tilde{\gamma}$, $\tilde{W}\tilde{W}$ etc. Some of these have clearer signatures, I shall return to them in section 6 when I survey the prospects for a future discovery of supersymmetry.

5. Rare Processes

In this section I shall discuss the the impact of low energy experiments upon supersymmetric models. The results that are obtained can be used to constrain models, but, as was the case with most of the cosmological discussion, a positive result from one of these experiments can be difficult to interpret. There can be other sources of the effect apart from supersymmetry.

One of the most accurately known, and predicted, quantities in physics is the anomalous magnetic moment of the muon. Calculations in quantum electrodynamics⁹⁹ agree with the measured value¹⁰⁰ so well that

$$|(g-2)_{QED} - (g-2)_{\text{experiment}}| < 2 \times 10^{-8} \quad (5.1)$$

In a supersymmetric model there are contributions to the magnetic moment from the graphs shown in figure 5.1. If $\tilde{\mu}_L$ and $\tilde{\mu}_R$ are degenerate then the contribution is proportional to the square of the muon mass. The effective vertex has the form

$$\frac{e}{2m_\mu} F(q^2) \bar{u} \sigma_{\mu\nu} q^\nu a \quad (5.2)$$

where q is the momentum of the photon. The contribution to $g-2$ is proportional to $F(0)$, which contains one power of the muon mass as a consequence of the definition 5.2. The second power arises since the contribution must violate chirality. Consequently we can get no useful constraint from the measurement of $g-2$ for the electron. Equation 5.1 translates into the following constraint.¹⁰¹

$$m_{\tilde{\mu}}, m_{\tilde{\nu}} \gtrsim 15 \text{ GeV}. \quad (5.3)$$

This is of no great impact in view of the limits from e^+e^- annihilation discussed in section 3. If $\tilde{\mu}_L$ and $\tilde{\mu}_R$ are not degenerate then a contribution is possible which is proportional to $m_\mu(m_{\tilde{\mu}_L} - m_{\tilde{\mu}_R})$. Even so, the process cannot yield anything relevant.¹⁰²

An experimental constraint on the mass difference between the partners of left and right handed quarks and leptons would enable a bound to be placed on the relative sizes of the elements in the mass matrix of equation 1.9. Once the squarks and sleptons are discovered a detailed measurement of the production rates and decay modes will determine the elements of the matrix.

However, experiments which search for parity violation can constrain the elements even though they have insufficient energy to produce the sparticles directly. In the case of selectrons, the best limit comes from the measurements of asymmetry in the scattering of polarized electrons from deuterium. (See figure 5.2) The cross-section difference is sensitive to the difference in the slepton masses,⁴ viz.

$$\frac{\sigma_L - \sigma_R}{\sigma_L + \sigma_R} \propto \frac{1}{m_{\tilde{e}_L}^2} - \frac{1}{m_{\tilde{e}_R}^2} \quad (5.4)$$

where $\sigma_L(\sigma_R)$ is the cross-section for the scattering of left (right) handed electrons from deuterium. The measurement of the asymmetry¹⁰³ is consistent with the value expected from electro-weak theory¹⁰⁴ and can be used to set the bound

$$\left| \frac{1}{m_{\tilde{e}_L}^2} - \frac{1}{m_{\tilde{e}_R}^2} \right| \lesssim 10^{-2} \text{ GeV}^{-2} \quad (5.5)$$

For simplicity I have assumed that e_L and e_R are mass eigenstates, i.e. that the off-diagonal elements in equation 1.9 are zero. Notice that this constraint is weak in view of the limit discussed in the previous sections.

In the case of squarks, the best limit arises from nuclear parity violation.¹⁰⁵ Graphs of the type shown in figure 5.3 result in short range, parity violating, four-fermion interactions. The graph of figure 5.3a would appear not to be of this type since it contains a gluon exchange. The gluon could be soft, so that the operator is not short range, and is not calculable since we do not have a reliable technique for calculating QCD at long distances. This is not the case as can be seen by considering effective $gq\bar{q}$ vertex arising from the top half of figure 5.3a

$$G_a^\mu \bar{q}_i \left[\gamma^\mu \gamma^5 F^A(g^2) + q^\mu \gamma^5 F_p(q^2) \right] \lambda_{ij}^a q_i \quad (5.6)$$

Here λ^a is an SU(3) matrix and q is the momentum transfer from the gluon to the quark.. Only the γ^5 pieces are relevant since the complete operator must violate parity and the bottom vertex in figure 5.3a is parity concerning.

Gauge invariance requires that

$$F^A(q^2) \rightarrow 0 \text{ as } q^2 \rightarrow 0 \quad (5.7)$$

and hence the $1/q^2$ from the gluon propagator is cancelled yielding the following form for the four-fermion operator.

$$\alpha_s^2 (\bar{q}\gamma^\mu \lambda^a q) (\bar{q}\gamma^\mu \gamma^5 \lambda^a q) f(m_{\tilde{q}}^2, m_{\tilde{g}}^2) \quad (5.8)$$

The prediction is reasonably reliable since it is not dominated by soft gluon exchange. Some parity violating nuclear transitions have been seen. For example

$${}^{18}F(J^P = 1^-, I = 0) \rightarrow {}^{18}F(J^P = 1^+, I = 0) + \gamma \text{ (circularly polarized)}$$

Or the back forward asymmetry (Δ) in the decay

$${}^{19}F(J^P = 1/2^-) \rightarrow {}^{19}F(J^P = 1/2^+) + \gamma \quad (5.9)$$

The standard electroweak theory predicts¹⁰⁶

$$\Delta_{\text{theory}} = -15 \times 10^{-5}$$

while the data are give¹⁰⁷

$$\Delta_{\text{exp}} = -26 \pm 12 \times 10^{-5}$$

In order to get a constraint, require that the operators equation of 5.8 from supersymmetry be smaller than the corresponding ones from the electro-weak theory. The particular result depends upon the isospin structure of the effective operator equation 5.8. The $\Delta I = 0$ operator gives¹⁰⁵

$$\frac{1}{4} \alpha_s^2 \left| \left(\frac{c(x_{Lu})}{m_{\tilde{u}_L}^2} - \frac{c(x_{Ru})}{m_{\tilde{u}_R}^2} \right) + \left(\frac{c(x_{Ld})}{m_{\tilde{d}_L}^2} - \frac{c(x_{Rd})}{m_{\tilde{d}_R}^2} \right) \right| < 10\sqrt{2}G_F \sin^2 \theta_W \quad (5.10)$$

where the $\Delta I = 1$ term gives

$$\alpha_s^2 \left| \left(\frac{c(x_{Lu})}{m_{\tilde{u}_L}^2} - \frac{c(x_{Ru})}{m_{\tilde{u}_R}^2} \right) - \left(\frac{c(x_{Ld})}{m_{\tilde{d}_L}^2} - \frac{c(x_{Rd})}{m_{\tilde{d}_R}^2} \right) \right| < \sqrt{2}G_F \sin^2 \theta_W \quad (5.11)$$

In equations 5.10 and 5.11, I have assumed that $\tilde{u}_L, \tilde{u}_R, \tilde{d}_L$ and \tilde{d}_R are mass eigenstates. x is given by

$$x_a = m_a^2/m_{\tilde{g}}^2$$

and $c(x)$ is a dimensionless function. We can consider two limits. Firstly $m_{\tilde{g}} \sim m_{\tilde{q}}$, then

$$c \approx \frac{3}{2}$$

or $m_{\tilde{q}} \gg m_{\tilde{g}}$ when

$$c(x) \sim \log x.$$

In the first case the constraint of 5.10 becomes

$$\frac{1}{m_{\tilde{u}_L}^2} - \frac{1}{m_{\tilde{u}_R}^2} + \frac{1}{m_{\tilde{d}_L}^2} - \frac{1}{m_{\tilde{d}_R}^2} < \left(\frac{1}{100\text{GeV}} \right)^2. \quad (5.12)$$

whereas in the latter case we get

$$\begin{aligned} & \frac{\log(m_{\tilde{u}_L}^2/m_{\tilde{g}}^2)}{m_{\tilde{u}_L}^2} - \frac{\log(m_{\tilde{u}_R}^2/m_{\tilde{g}}^2)}{m_{\tilde{u}_R}^2} \\ & + \frac{\log(m_{\tilde{d}_L}^2/m_{\tilde{g}}^2)}{m_{\tilde{d}_L}^2} - \frac{\log(m_{\tilde{d}_R}^2/m_{\tilde{g}}^2)}{m_{\tilde{d}_R}^2} < \left(\frac{1}{80\text{GeV}} \right)^2 \end{aligned} \quad (5.13)$$

In order to understand the implications of this bound consider the mass matrix for the up squarks (c.f. equation 1.7) which takes the following form in the limit $m_u = 0$

$$\begin{pmatrix} \tilde{u}_L \\ \tilde{u}_R \end{pmatrix}^\dagger \begin{pmatrix} m_{\tilde{u}_L}^2 & 0 \\ 0 & m_{\tilde{u}_R}^2 \end{pmatrix} \begin{pmatrix} \tilde{u}_L \\ \tilde{u}_R \end{pmatrix} \quad (5.14)$$

There are two sources of contributions to $m_{\tilde{u}_L}^2$ and $m_{\tilde{u}_R}^2$ one comes from the soft operators (equation 1.6) and the renormalization group scaling. The other comes from the difference of the vacuum expectations values of the two Higgs fields v_1 and v_2 (c.f. equation 1.10). If we include this term alone, equation 5.12 becomes

$$\frac{(v_1^2 - v_2^2)}{m_{\tilde{q}}^4} < \frac{1}{(20\text{GeV})^2} \quad (5.15)$$

where $m_{\tilde{q}}$ is the average squark mass. This is not particularly restrictive once we recall the limits on the squark masses discussed earlier $m_{\tilde{q}} \gtrsim 50\text{GeV}$ implies that

$$|(v_1^2 - v_2^2)| < (225 GeV)^2 \quad (5.16)$$

which of no importance since $v_1^2 + v_2^2 = (175 GeV)^2$.

As discussed in Section 1, there is the potential for lepton number violation through a supersymmetry breaking soft mass terms of the type

$$m_{\text{mix}}^2 E_R \mu_R^c, \quad m_{\text{mix}}^2 E_R \tau_R^c \text{ etc.} \quad (5.17)$$

The tightest bound on terms of the type applies to the one involving the muon and the electron. The transition $\mu \rightarrow e\gamma$ can occur as described in the Feynman diagrams of figure 5.4. The failure to observe this process with a branching ratio of 1.7×10^{-10} or more¹⁰⁸, results in the constraint¹⁰⁹

$$m_{\text{mix}} < 7 \times 10^{-4} m_\mu \left(\frac{m_{\tilde{e}}}{100 GeV} \right)^2 \left(\frac{m_{\tilde{e}}}{m_{\tilde{\gamma}}} \right) \quad (5.18)$$

where m_μ is the muon mass. If lepton number is violated, there is no reason why the soft mass term (m_{mix}) should be smaller than the other slepton masses. Since all the slepton masses must be less than 1 TeV or so if supersymmetry is to be relevant to the hierarchy problem, this constraint looks rather unnatural. Models should probably therefore, have a symmetry to forbid the appearance of such a term.

There are very tight limits on the existence of flavour changing neutral currents. The most restrictive data come from the kaon system.¹¹⁰ There are contributions to the $K_L - K_S$ mass matrix from the processes shown in figure 5.5. If the exchanged gauginos are winos, this graph is simply the supersymmetric analog of the usual contribution involving W bosons and the charm and top quarks. The contribution to the mass mixing implies^{110,111}

$$\frac{g^4}{64\pi^2} \left(\frac{\Delta m_{\tilde{q}_{ij}}^2}{m_{\tilde{q}}^2} \right) \frac{\Gamma_{ij}}{M^2} < 5 \times 10^{-13} GeV^{-2} \quad (5.19)$$

Here g is the appropriate coupling constant and M is the larger of the squark and gaugino masses. $\Delta m_{\tilde{q}_{ij}}^2$ is the mass difference between squarks of flavors i and j . This mass difference is assumed to be much smaller than the average value $m_{\tilde{q}}^2$. The quantity Γ_{ij} depends upon the mixing angles appearing at the vertices in figure 5.5.

The squark-quark gluino vertex can be written as

$$g_s \bar{\psi}_j^a \phi_i(\lambda_a) A_{ij} \psi_j + h.c. \quad (5.20)$$

where ϕ_i and ψ_j are a squark and quark of flavors i and j , and ψ_j^a is a spinor representing the gluino. The matrix A is given by

$$A = U_\phi^\dagger U_\psi \quad (5.21)$$

where U_ϕ and U_ψ are those matrices which rotate between the weak interaction eigenstates and the mass eigenstates for the squarks and quarks respectively. I will neglect any mixing between \tilde{q}_L and \tilde{q}_R . If the quark and squark mass matrices are diagonalized by the same rotation among flavors, which will be the case if the soft masses are all equal (see section 1), then the gluino vertex is diagonal and there is no contribution to the $K_L - K_S$ mass matrix from gluino exchange.

If, in the case of the wino diagrams, we assume that the mixing angles are equal to the Kobayashi-Maskawa angles¹⁶, then we get¹¹¹

$$\frac{1}{M^2} \frac{\Delta m_{\tilde{q}_{ij}}^2}{m_{\tilde{q}}^2} < 10^{-7} GeV^2 \quad (5.22)$$

for squarks of the first two generations. Here M is the larger of the squark and wino masses. This implies that the squark flavors of the first two generations must be almost degenerate if the squarks and winos have masses near the bounds discussed in the previous sections. The bounds on the masses of the third generation squarks are weaker since the mixing angles are correspondingly smaller.

The contribution from gluino exchange could be much larger^{113,112} than that from winos, since the couplings are larger. Unfortunately the values of the Γ_{ij} are critical and it is not possible to discuss the gluino contribution without reference to a specific model. I will therefore specialize to the case of a model based on the coupling to supergravity.¹¹³ I shall assume that the terms A and B in equation 1.7 are zero and that all the squark masses terms are diagonal in flavor and equal to $m_{\tilde{q}}$ when evaluated at some large scale, corresponding either to the Planck mass or the scale of grand unification.

If there were no renormalization effects, the squark mass matrices for the charge $2/3$ ($m_{\tilde{u}}$) and charge $1/3$ ($m_{\tilde{d}}$) squarks would have the following form

$$\begin{aligned}
m_u^2 &= m_y^2 1 + m_u^\dagger m_u \\
m_d^2 &= m_y^2 1 + m_d^\dagger m_d
\end{aligned}
\tag{5.23}$$

where m_u and m_d are the corresponding quark mass matrices, 1 is a unit matrix. Hence, m_u would be diagonal and m_d^2 would be diagonalized by the same rotation which diagonalized m_d . The gluino couplings would be flavor diagonal and there would be no contribution from gluinos to the $K_L - K_S$ mass matrix.

Once renormalization effects are taken into account this simple picture will change. Graphs of the type shown in figure 5.6 which involve the exchange of charged Higgs fields can cause mixing between the charge 2/3 and charge 1/3 squark mass matrices.^{3,113}

$$m_d^2 = m_d^\dagger m_d + \alpha m_u^\dagger m_u + 1 m_y^2 \tag{5.24}$$

Now m_d^2 is not diagonalized by the same rotation which diagonalizes m_d . How big is α ? It is likely to be $O(1)$, since the renormalization group scaling from the unification scale produces shifts in the scalar masses which are of the same order as the starting values. This is true at least for the Higgs masses if weak interactions are to be broken as a result of this scaling. Notice that the Yukawa couplings present on the vertices have been absorbed into the quark masses.

It is then apparent that the mixing angles present in equation 5.18 are of the same order as the Kobayashi-Maskawa angles, and the splitting between different flavors $m_{q_i}^2 - m_{q_j}^2$ is of order $m_{q_i}^2 - m_{q_j}^2$. Using the first two generations for which $\Delta m^2 = 2GeV^2$ and leads to the bound*

$$m_{\tilde{q}} \gtrsim 0(35) GeV \tag{5.25}$$

if I assume that $m_{\tilde{q}} = m_{\tilde{q}}$. The box graph with top squarks for which $\Delta m^2 \sim (40GeV)^2$ and $\Gamma \sim \sin^4 \theta_c$. yields

$$m_{\tilde{q}} > 0(100) GeV \tag{5.26}$$

*The estimates quoted here rely upon a perturbative estimate of the box graphs of figure 5.5. It has been claimed that effects involving gluino bound states results in much tighter bound.¹¹⁴ The result of reference 114 appear to be in error since the contribution from such bound states must vanish when the momentum flow through the graph goes to zero. I am grateful to R. Barbieri for a discussion of this point.

These bounds are competitive with those obtained from the direct searches in the previous section, but their model dependence cannot be overemphasized. It is also possible to obtain constraints by considering the CP violating terms in the $K_L - K_S$ system.^{115,116} Again the constraints are model dependent.

Rare decays of the kaons can also provide constraints. An analysis of $K \rightarrow \pi +$ missing neutrals can be sensitive to the existence of very light photinos.^{117,118} The graph of figure 5.7 yields¹¹⁷

$$BR(K \rightarrow \pi \tilde{\gamma} \tilde{\gamma}) = 7 \times 10^{-11} \left(\frac{20GeV}{m_{\tilde{c}}} \right)^4 \left[1 + 0.43 \log \left(\frac{m_{\tilde{c}}}{20GeV} \right) \right] \tag{5.27}$$

where $m_{\tilde{c}}$ is the mass of the charm squark. Experiments under at Brookhaven¹¹⁹ can expect to be sensitive to branching ratios of order 10^{-10} , so that they are unlikely to make a significant contribution. If the photino is sufficiently light then

$$\begin{aligned}
K &\rightarrow \pi^+ \pi^0 \\
&\quad \searrow \tilde{\gamma} \tilde{\gamma}
\end{aligned}$$

which occurs with a branching ratio of¹¹⁷

$$2 \times 10^{-11} \left(\frac{20GeV}{m_{\tilde{c}}} \right)^4 \left(\frac{m_{\tilde{\gamma}}}{1MeV} \right)^2 \tag{5.28}$$

may be observable. Recall however that a stable photino in this mass range is excluded by the cosmological arguments of Section 2 unless its mass is less than 100 ev.

Transitions involving B mesons may ultimately provide some constraints on supersymmetric theories.¹¹⁹ If $m_{\tilde{q}} \gtrsim 80GeV$ and $m_{\tilde{q}} \gtrsim 25GeV$, there could be observable mixing in the $B_d^0 - \bar{B}_d^0$ system, leading to final states of like sign muons from initial $b\bar{b}$ configurations. An effect at the 25% level is produced if the masses are in the above range¹²⁰ The limits from rare processes, impressive though they may be, are easily accommodated in the most fashionable models, those based on supergravity. It is therefore likely that we will have to look to future direct searches for supersymmetric particles.

6. Summary and Outlook

I shall begin this section with a brief review of all the limits from the previous sections and their implications for supersymmetric models. I shall then discuss some options for future quests.

We have seen that the cosmological bounds imply that the lightest sparticle, if it is stable, is unlikely to be strongly interacting or to have electric charge. If this sparticle is a sneutrino we have no bound, otherwise it must be a linear combination of Higgsino, Zino and photino (see equation 1.29), in which case it must be heavier than a few GeV, or lighter than 100 eV. This is sufficient to invalidate the supersymmetric signals in $K \rightarrow \pi +$ missing neutrals of section five unless the photino is very light.

The other limits from section five are easiest to satisfy if all the squark flavors are degenerate. It was precisely this assumption that was made in extracting bounds on squark masses from the searches for missing energy events at the $SppS$ collider in section four. These bounds could be invalidated if the Higgsino is lighter than the photino so that the photino emitted in squark and gluino decay could decay within the detector, so diluting the missing energy signal.

It is difficult to be absolutely certain that a very light gluino is excluded. The constraints from the beam dump experiments discussed in Section four are model dependent. Although the production cross section of such light gluinos at the $SppS$ collider is enormous, very few events pass the cuts, and the resulting excluded mass region is uncertain. However, in most models a gluino with mass in this dubious region also implies the existence of photinos with masses in the region excluded by the cosmological arguments.

The limits are summarized in Table 4. In view of the good limits from the $SppS$ collider, models with radiative gaugino masses in which $m_{\tilde{q}} \gg m_{\tilde{g}}$ are disfavored.¹²¹ Since they would require very large squark masses. Recall that the squark masses cannot be much larger than the scale of electroweak symmetry breaking if supersymmetry is to be relevant to the hierarchy problem.

Most of the limits can be evaded if the lightest sparticle is not stable. In order for this to occur the model must have a broken R parity.¹²² The R parity of a particle of spin S, baryon number B and lepton number L is given by

$$R = (-1)^{2S+L+3B} \quad (6.1)$$

Hence, if R parity is to be broken the model must also violate baryon or lepton number. Models of the former type will have proton decay via

$$p \rightarrow e^+ + \tilde{\gamma} \quad (6.2)$$

or will have neutron anti-neutron oscillations. Since the scale of breaking of the R parity will be of the same order as that of supersymmetry breaking, transitions of this type will occur at a disastrous rate.

Lepton number can be broken in two ways. A non-zero vev for the sneutrino field results in the spontaneous breaking of lepton number.¹²³ The theory will now have a Goldstone boson, the Majaron,¹¹² which couples to leptons via a term proportional to $g_2 m_\ell/m_W$, where m_ℓ is the lepton mass. Consequently the Majaron cannot be emitted in K or μ decays since it has no coupling to the neutrino current. If the Majaron is a truly massless it will cause Red Giants to lose energy at an unacceptable rate.¹²⁴ The second mechanism, explicit breaking, must be present in order to give the Majaron a small mass. Once its mass exceeds the temperature of a Red Giant, about 10 MeV, there is no further constraint.

If the non-zero vev is that of the tau sneutrino then there is very little constraint on its value. The vev causes a mixing between the bare tau, wino and charged Higgsino states, so that the physical 'tau' is a linear combination of the wino, the bare τ and the charged Higgsino.^{126,127} The mixing of \tilde{w} is very small, proportional to

$$\frac{m_{\tilde{\nu}_\tau}}{m_W (v_1^2 + v_2^2)^{1/2}} \quad (6.3)$$

More mixing occurs with the charged Higgsino, proportional to

$$\frac{\langle \tilde{\nu}_\tau \rangle}{(v_1^2 + v_2^2)^{1/2}} \quad (6.4)$$

The Higgsino has the same couplings to the gauge bosons as the bare τ . Hence the 'tau' has the usual production rate and lifetime, and we have little constraint on $\langle v_\tau \rangle$ from this mixing.

Explicit R parity breaking¹²² requires additional terms in the superpotential of equation 1.3.

$$W \ni C_i LEL + D_i QDL \quad (6.5)$$

The term

$$LH_2 \quad (6.6)$$

is also allowed but can be eliminated by redefining the L and H_1 supermultiplets so that the 'L' is defined to be that combination which does not couple to H_2 . I shall therefore ignore this term. R parity could also be broken by the soft mass terms of equation 1.6

$$m_i^2 \phi_H \phi_{L_i} \quad (6.7)$$

Constraints on the coefficients C_i, D_i and m_i^2 arise from neutrino masses and from the absence of observed lepton number violating processes. The neutrinos acquire a tree level mass only if there is a non-zero sneutrino vev. The experimental limit on the tau neutrino mass is poorest,^{128*} I will assume only $\langle \tilde{\nu}_\tau \rangle \neq 0$ the mixing occurs between the zino, the photino, the two neutral Higgsinos and the τ neutrino. Under reasonable assumptions of the soft mass parameters are obtains the constraint^{126,127}

$$\langle \nu_\tau \rangle \gtrsim \text{few MeV}. \quad (6.8)$$

The constraints on $\langle \nu_\tau \rangle$ and $\langle \nu_\mu \rangle$ are much stricter, since the limits on the muon and electron neutrino masses are tighter.

The terms C_i and D_i can be constrained since they give rise to neutrino masses at one loop from the graphs of figure 6.1. A tighter constraint is obtained from the lepton number violating decays

$$\mu \rightarrow e\gamma \quad (6.9)$$

and

$$\mu^+ \rightarrow e^+ e^- e^+ \quad (6.10)$$

which proceed via the graphs of figure 6.2. The constraints from these processes can be satisfied if¹²²

*The lighter astrophysical constraint on the τ neutrino mass is not applicable if the tau neutrino is unstable.

$$C_i, D_i \lesssim O(10^{-3}) \quad (6.11)$$

These models with R parity breaking are unappealing. Nevertheless their phenomenology^{126,127} can be quite different from that of the standard supersymmetric models. Single production of sparticles via processes like

$$p\bar{p} \rightarrow \bar{q} + \tau + X \quad (6.2)$$

can occur, but the rates are small. Sparticle decays of the type

$$\bar{q} \rightarrow q\tau \quad (6.13)$$

are usually suppressed relative to $\bar{q} \rightarrow q + \tilde{g}$ by factors of order m_t/M_W , and are not likely to be important.¹²⁷

However, the lightest sparticle is not stable, consequently missing energy signatures are diluted. If I assume that the lightest sparticle is a photino, then it can decay via

$$\begin{aligned} \tilde{\gamma} &\rightarrow \gamma\nu \\ &\rightarrow q\bar{q}\nu \\ &\rightarrow u\bar{d}\ell^- \\ &\rightarrow \ell^+\ell^-\nu. \end{aligned} \quad (6.14)$$

The lifetime $\tau(\tilde{\gamma} \rightarrow \gamma\nu)$ is

$$\tau(\tilde{\gamma} \rightarrow \gamma\nu) \approx 10^{-9} \frac{1}{C_i^2} \left(\frac{m_{\tilde{q}}}{100\text{GeV}} \right)^4 \left(\frac{1\text{GeV}}{m_{\tilde{\gamma}}} \right)^3 \text{sec} \quad (6.15)$$

from the process of figure 6.3 and

$$\tau(\tilde{\gamma} \rightarrow \gamma\nu) \approx 10^{-9} \left(\frac{m_{\tilde{t}}}{100\text{GeV}} \right)^4 \left(\frac{1\text{GeV}}{m_{\tilde{\gamma}}} \right)^3 \left(\frac{10\text{GeV}}{\langle \tilde{\nu}_\tau \rangle} \right)^2 \text{sec} \quad (6.16)$$

from that of figure 6.4. The lifetime for $\tilde{\gamma} \rightarrow q\bar{q}\nu$, see figure 6.5 is

$$\tau(\tilde{\gamma} \rightarrow q\bar{q}\nu) \approx 10^{-11} \left(\frac{m_{\tilde{q}}}{100\text{GeV}} \right)^4 \left(\frac{1\text{GeV}}{m_{\tilde{\gamma}}} \right)^5 \frac{1}{D_i^2} \text{sec}. \quad (6.17)$$

The lifetimes are short enough so that the cosmological constraints of section 2 are evaded. Indeed if $m_{\tilde{\gamma}} > 10$ GeV or so, it is possible for the photino to decay inside a detector so that the missing energy signatures will be diluted. This is shown in figure 6.6,¹²⁶ which shows the distribution in missing p_t arising from

$$p\bar{p} \rightarrow \tilde{g}\tilde{g} + X$$

$$\hookrightarrow q + \tilde{g} + q + \bar{q} + \tilde{\gamma} + \tilde{\gamma} \quad (6.18)$$

followed by

$$\tilde{\gamma} \rightarrow \gamma\nu$$

or

$$\tilde{\gamma} \rightarrow q\bar{q}\nu$$

is displayed. It is clear that the current data cannot exclude a 40 GeV gluino if the decaying photino scenario occurs. The presence of extra photons may provide a good signal in one case.

Where can we look for a significant step in the search for supersymmetry? The searches discussed in section 3¹³⁰ can be carried out at the next generation of e^+e^- machines, LEP and SLC.¹²⁷ Particles with electro-weak charges and masses less than the beam energy should be produced copiously enough for a discovery to be made.

Using the same techniques as I discussed in Section 4, the Tevatron collider with center of mass energy of 2 TeV should be sensitive to squark and gluino masses less than about 140 GeV. A comparison of gluino production rates at the $Spp\bar{p}S$ and Tevatron colliders is given in figure 4.15 and for squark pairs in figure 6.7.

HERA¹³¹ will enable a search for supersymmetry in electron-proton collisions. The largest rate occurs for final states of a selectron and a squark which is produced via the processes of figure 6.8. The rate is model dependent, but a reasonable estimate can be obtained by neglecting the zino contribution and assuming that the photino is massless. The cross section is then given by^{4,80}

$$\frac{d\sigma}{du}(eq \rightarrow \tilde{e}\tilde{q}) = \frac{\pi Q_i^2}{s^2(t+m_{\tilde{e}}^2)^2} [ut + m_{\tilde{q}}^2 t + m_{\tilde{e}}^2 u] \quad (6.19)$$

where Q_i is the quark's electric charge. The resulting rate is shown in figure 6.9 where I have assumed that all squark flavors are degenerate. The present limits

$m_{\tilde{e}} > 20\text{GeV}$ and $m_{\tilde{q}} > 50\text{GeV}$ imply that HERA is left with a search in the mass region where the cross section is below 1 pb. The signal consists of a lepton and a jet(s) which have unbalanced transverse momenta. The final state squarks are dominantly u and d squarks so the limit $m_{\tilde{q}} > 50\text{GeV}$, which is arrived using in the assumption that all flavors are degenerate, may not be relevant. Nevertheless squarks with masses below 40 GeV will probably be found at LEP¹²⁹ or SLC¹³⁰ before HERA.

Squarks can be pair produced via the graph of figure 6.10 with a rate shown in figure 6.11. Given the current limits discussed in section four, the cross sections are likely to be less than 1 pb. The final states will involve jets with unbalanced transverse momenta. The small rates make it unlikely that HERA will be able to see this process.

Squarks can also be produced in association with gluinos via photo-production as shown in figure 6.12 with the rates shown in figure 6.13. Again it difficult to be optimistic about HERA's chances, since the cross-section are less than 1 pb for masses not ruled out by the previous analysis.

It has also been proposed to search for the final state of a selectron and a photino produced from the process $e+q \rightarrow \tilde{e}+q+\tilde{\gamma}$. The cross sections are given in reference 132 and are too small to be of much interest. This process is similar to the single production of sleptons in e^+e^- annihilation discussed in section three (c.f. equations 3.4). In conclusion it seems that, given the small rates for all these processes, it is difficult to be optimistic about HERA's prospects for finding supersymmetry. On the other hand, should supersymmetric particle be discovered elsewhere in the near future, HERA may be able to provide further insight into their properties.

I will conclude with a few comments about searches for supersymmetry at the SSC.¹³³ The production rates at this proposed high energy (40 TeV) high luminosity, ($10^{33}\text{cm}^{-2}\text{sec}^{-1}$) proton proton collider are very large. It will be possible even to search for sleptons up to rather high masses. The sleptons are pair produced in quark anti-quark collisions with the following cross-section

$$\frac{d\sigma}{dt}(q_i\bar{q}_i \rightarrow \tilde{e}\tilde{e}) = \frac{4\pi\alpha_{em}^2}{3s^2} \left[e_q^2 - \frac{e_q(L_q + R_q)(4\sin^2\theta_W - 1)}{8\sin^2\theta_W \cos^2\theta_W(1 - M_Z^2/s)} \right. \\ \left. + \frac{(L_q^2 + R_q^2)(1 + 8\sin^4\theta_W - \sin^2\theta_W)}{64\sin^4\theta_W \cos^4\theta_W(1 - M_Z^2/s)^2} \right] \left(\frac{ut - m_{\tilde{e}}^4}{s^2} \right) \quad (6.20)$$

where for charge $\frac{2}{3}$ quarks $R_q = 1 - \frac{4}{3}\sin^2\theta_W$, $L_q = -\frac{4}{3}\sin^2\theta_W$ and for charge $\frac{1}{3}$ quarks $R_q = -1 + \frac{2}{3}\sin^2\theta_W$, $L_q = \frac{2}{3}\sin^2\theta_W$. The final state consists of an electron-positron pair arising from the decay chain

$$pp \rightarrow \bar{e} + e + X$$

$$\quad \hookrightarrow e^+ + e^- + \tilde{\gamma} + \tilde{\gamma}$$

There is a background from W pair production, but sleptons of masses up to 400 GeV should be observable.⁷³

The searches for strongly interacting sparticles will involve techniques similar to those discussed in section four. Indeed the event rates are so high that it may be possible to look for rarer final states with cleaner signals. As an example, consider the search for a gluino of mass of order a few hundred GeV. The cross section for pair production is shown in figure 6.15. As was discussed in section four, the missing P_t signature can be diluted since the momenta carried off by the photinos in the decay chain

$$\tilde{g}\tilde{g} \rightarrow q\bar{q}q\bar{q} + \tilde{\gamma}\tilde{\gamma} \quad (6.21)$$

will tend to cancel if the gluinos are produced with appreciable momentum. In this case it may be better¹³⁴ to search for the final state

$$\tilde{g}\tilde{\gamma} \rightarrow q\bar{q} + \tilde{\gamma}\tilde{\gamma} \quad (6.22)$$

which has a much smaller production cross section (see figure 6.16) but a potentially cleaner signal.

A detailed analysis of supersymmetric signals at the SSC was carried out as part of the 1984 Snowmass Summer Study and may be consulted for more details.¹³⁴

Despite some false alarms, we still have no experimental evidence in favor of supersymmetry. Should we be discouraged? Probably not, since, as I indicated in section one, the natural mass scale for the superpartners is the W mass and searches have not yet reached this value. We are getting close however, and something has to show up soon. I hope that the extra energy range opened up by the Tevatron

collider will prove decisive, and that we do not have to wait for the SSC. Suppose nothing is found, when should theorist, give up? The mass range accessible at the SSC is so large that if it fails to find supersymmetry we can safely assume that supersymmetry is not relevant to the hierarchy problem, and that all the currently fashionably supersymmetric models are wrong.

Acknowledgments.

I am grateful to M. Barnett and S. Dawson for discussions. I would like to thank Pierre Ramond for organizing such a successful Summer School and all the students for enduring my accent for 7 hours. This work was supported by the Director, Office of High Energy and Nuclear Physics, Division of High Energy Physics of the U.S. Department of Energy under contract DE-AC03-76SF00098.

References

- [1] Howard E. Haber and G. L. Kane Phys. Rep. 117: (1985) 75.
- [2] D. V. Nanopoulos, and A. Savoy-Navarro, (Editors) Phys. Rep. 105 (1985) Nos. 1, 2; J. Ellis, CERN-TH-4017/84, Lectures given at Yukon Advanced Study Institute on Quarks and Leptons, Whitehorse, Yukon, Canada, Aug. 1984.
- [3] H. P. Nilles, Phys. Rep. 110: (1984) 1.
- [4] Ian Hinchliffe and L. Littenberg, "Phenomenological Consequences of Supersymmetry." Published in Proc. of DPF Summer Study on Elementary Particle Physics and Future Facilities, Eds. R. Donaldson and F. Paige (Fermilab, 1982).
- [5] For a review, see M. Turner Lectures given at the 1984 Summer School on concepts in High Energy Physics (St. Croix) and at this school.
- [6] G. Ross, Lectures at this school.
- [7] S. Weinberg, Phys. Rev. Lett. 19 (1967) 1267; A. Salam in Elementary Particles Physics Ed. N. Sgrtholm, Almquist and Wiksell (Stockholm 1967); S. L. Glashow, Nucl. Phys. B22 (1961) 579.
- [8] Julius Wess and Jonathan Bagger "Supersymmetry and Supergravity" Princeton Univ. Press. (1982).
- [9] R. D. Peccei and Helen R. Quinn, Phys. Rev. Lett. 38 (1977) 1440, Phys. Rev. D16: (1977) 1791.
- [10] For a review of axions see the lectures of P. Sikivie, this school, or Frank Wilczek, "The U(1) Problem; Instantons, Axions, and Familons. Erice Lecture 1983. Santa Barbara preprint NSF-ITP-84-14, 1983.
- [11] L. Girardello and M. Grisaru, Nucl. Phys. B194, (1982) 65.
- [12] K. Wilson, Phys. Rev. D3 (1971) 1818 .
- [13] E. Cremmer et al., Phys. Lett. 116B (1982) 231 . R. Barbieri, S. Ferrara, and C. Savoy, Phys. Lett. 119B (1983) 342. L. Hall, J. Lykken, and S. Weinberg, Phys. Rev. D27 (1983) 2359.
- [14] K. Inoue, A. Kakuto, H. Komatsu and S. Takeshita, Prog. Theor. Phys. 68 (1982) 927 (E-ibid 70 (1983) 330) and Prog. Theor. Phys. 71(1984) 413.
- [15] L. Alvarez-Gaumé, M. Claudson and M. B. Wise, Nucl. Phys. B207 (1982) 96; L. Alvarez-Gaumé, J. Polchinski and M. B. Wise, Nucl. Phys. B221 (1983) 495; J. Ellis, J. S. Hagelin, D. V. Nanopoulos and K. Tamvakis, Phys. Lett. 125B (1983) 275; L. E. Ibáñez and C. Lopez, Nucl. Phys. B233 (1984) 511.
- [16] S. Kobayashi and K. Maskawa, Prog. Theor. Phys. 49 (1963) 562.
- [17] H. Georgi and S. Glashow, Phys. Rev. Lett. 32 (1974) 438.
- [18] R. Barbieri, L. Girardello and A. Masiero, Phys. Lett. 127B (1983) 429.
- [19] S. Weinberg Phys. Rev. Lett. 50 (1983) 387.
- [20] S. Deser and B. Zumino, Phys. Rev. Lett. 38 (1977) 1433.
- [21] J. Gunion and H. Haber, SLAC Pub. 3404 (Aug. 1984).
- [22] F. Wilczek , Phys. Rev. Lett.39(1977) 1304.
- [23] Parthasarathi Majumdar and Prohir Roy, Phys. Rev. D30 (1984) 2432.
- [24] J. D. Bjorken, Proc. of 1976 SLAC Summer Institute, ed. M. Zipf.
- [25] J. Ellis in Prof. of DPF. Summer study on Design and Utilization of the SSC. Ed. R. Donaldson and J. Morfin, FNAL (1985).
- [26] G. Steigman, Ann. Rev. of Nuclear and Particle Science 29 (1979) 313; S. Weinberg, Gravitation and Cosmology (Wiley, 1972).
- [27] B. W. Lee and S. Weinberg, Phys. Rev. Lett.39 (1977) 165.
- [28] J. Ellis et al., Nucl. Phys. B238 (1984) 453.
- [29] H. Goldberg, Phys. Rev. Lett. 50 (1983) 1419; L. Krauss, Nucl. Phys. B227 (1983) 556.
- [30] J. Silk and M. Srednicki, Phys. Rev. Lett. 53 (1985) 62.
- [31] S. Wolfram, Phys. Lett. 82B (1979) 65.
- [32] P. F. Smith and J. R. J. Bennett, Nucl. Phys. B149 (1979) 525.

- [33] J. S. Hagelin, G. L. Kane and S. Raby, Nucl. Phys. B241 (1984) 638.
- [34] S. Weinberg, Phys. Rev. Lett. 48 (1982) 1303; J. Primack and H. Pagels, Phys. Rev. Lett. 48 (1982) 223.
- [35] J. Ellis, J. E. Kim and D. V. Nanopoulos, Phys. Lett. 145B 181 (1985).
- [36] A. Guth, Phys. Rev. D23 (1981) 347; A. D. Linde Phys. Lett. 108B (1982) 389; A. Albrecht and P. J. Steinhardt, Phys. Lett. 140B (1984) 44.
- [37] B. A. Ovrut and P. J. Steinhardt in Proc of the 'Inner Space Outer Space' Workshop FNAL 1984. Pennsylvania (preprint UPR-9260T(July 1984)).
- [38] For a review of Big Bang Nucleosynthesis see D. N. Schramm and R. V. Wagner Ann. Rev. Nucl. Sci. 27 (1977) 37.
- [39] E. N. Kolb and R. J. Scherrer, Phys. Rev. D25 (1982) 1481.
- [40] M. Yu Khlopov and A. D. Linde Phys. Lett. 138B (1984) 265.
- [41] J. Ellis, D. V. Nanopoulos and S. Sakar, Nucl. Phys. B259 (1985) 175.
- [42] H. Aihara et al., Phys. Rev. Lett. 53 (1985) 130.
- [43] F. Balestra et al., CERN EP/84-108 (1984).
- [44] M. Yoshimura, Phys. Rev. Lett. 41, (1978) 281; A. D. Sakharov, JETP 49, (1979) 594; S. Dimopoulos and L. Susskind, Phys. Lett. 81B, (1979) 416. A. Yu. Ignatiev, V. A. Kuzmin and M. E. Shaposhnikov, Phys. Lett. 87B, (1979) 114; B. Toussaint, S. B. Treiman, F. Wilczek and A. Zee, Phys. Rev. D19 (1979) 1036; S. Weinberg, Phys. Rev. Lett. 42 (1979) 850.
- [45] J. Ellis, M. K. Gaillard and D. V. Nanopoulos, Phys. Lett. 80B (1979) 360; S. Barr, G. Segré and H. A. Weldon, Phys. Rev. D20 (1979) 2494; A. Yildiz and P. Cox, Phys. Rev. D21 (1980) 906; R. Barbieri, D. V. Nanopoulos and A. Masiero, Phys. Lett. 98B (1981) 191; J. A. Harvey, E. W. Kolb, D. B. Reiss and S. Wolfram, Nucl. Phys. B201 (1982) 16; J. F. Nieves, Phys. Rev. D25 (1982) 1417; E. W. Kolb and M.S. Turner Ann. Rev. Nucl. and Partr. Sci. 33 (1983) 645.
- [46] A. Masiero and T. Yanigida, Phys. Lett. 112B (1982) 336; M. Claudson, L. Hall and I. Hinchliffe, Nucl. Phys. B241 (1984) 309; P. A. Kosower, L. Hall and L. Krauss, Phys. Lett. 150B (1985) 435.
- [47] G. D. Coughlan, et al., Phys. Lett. 158B (1985) 401; *ibid* 100B (1985) 249; R. Holmon, P. Ramond, G. Ross, Phys. Lett. 137B (1984) 343; S. Mahajan LBL-20179 (Sept. 1985) Phys. Rev. D (to appear).
- [48] I. Affleck and M. Dine, Nucl. Phys. B269 (1985) 36; A. D. Linde, Phys. Lett. 160B (1985) 243.
- [49] P. Fayet and G. Farrar, Phys. Lett. 89B (1980) 191.
- [50] R. Brandelik, et al., Phys. Lett. 117B (1982) 365; H. J. Behrend, et al., Phys. Lett. 114B (1982) 287. B. Adeva et al., Phys. Lett. 152B (1985) 439. W. Bartel et al., Phys. Lett. 152B (1985) 385, 392.
- [51] W. Bartel, et al, Phys. Lett. 139B (1984) 327.
- [52] M. K. Gaillard, L. Hall and I. Hinchliffe, Phys. Lett. 116B (1982) 279; J. Salati, and M. Waller, Phys. Lett. 122B (1983) 397.
- [53] C. Weizsacker and E. T. Williams, Z. Phys. 88 (1934) 612.
- [54] L. Gladney, et al., Phys. Rev. Lett. 51 (1983) 2253.
- [55] JADE Collaboration reported by S. Yamada, in Proc. of 1983 International Lepton/Photon symposium. (Cornell, 1983).
- [56] J. Ellis and G. G. Ross, Phys. Lett. 117B (1982) 397.
- [57] W. Bartel, et al., Phys. Lett. 139B (1984) 327.
- [58] E. Reya, Phys. Lett. 133B (1984) 245.
- [59] B. Adeva, et al., Phys. Rev. Lett. 53 (1984) 1806.
- [60] J. Ellis and J. Hagelin, Phys. Lett. 122B (1983) 303; K. Grassie and P. N. Pandita, Phys. Rev. D30 (1984) 22.
- [61] G. Barta, et al., SLAC PUB 3817 (1985), Phys. Rev. Lett. (to appear).
- [62] E. Ma and J. Okada, Phys. Rev. Lett. 41 (1978) 287; K. J. F. Gaemers and R. Gastmans and F. Renard, Phys. Rev. D19 (1979) 1650.
- [63] R. M. Barnett, H. E. Haber, and K. Lackner, Phys. Rev. Lett. 51 (1983) 176; Phys. Rev. D29 (1984) 1381.

- [64] P. Nelson and P. Osland, Phys. Lett. 115B (1982) 407; J. Ellis and S. Rudaz, Phys. Lett. 128B (1983) 248.
- [65] W. Keung, Phys. Rev. D28 (1983) 1129.
- [66] S. D. Drell and T. M. Yan. Ann. Phys. 66 (1971) 595.
- [67] C. N. Cabbibo, et al., Phys. Lett. 132B (1983) 195.
- [68] P. R. Harrison and C. H. Llewellyn Smith, Nucl. Phys. B213 (1983) 223 (E: B223 (1983) 542).
- [69] G. L. Kane and J. P. Leveille, Phys. Lett. 112B (1982) 227.
- [70] S. Dawson, E. Eichten, and C. Quigg, Phys. Rev. D31 (1985) 1581.
- [71] I. Antoniadis, L. Baulieu, and F. DelduC, Z. Phys. C23 (1984) 119.
- [72] P. Bagnaia, et al., Z. Phys. C20 (1983) 117; P. Bagnaia, et al., Phys. Lett. 139(1984) 430; G. Arnison, Phys. Lett. 123B (1983) 115; G. Arnison, Phys. Lett. 132B (1983) 214.
- [73] E. Eichten, I. Hinchliffe, K. Lane, and C. Quigg, Rev. Mod. Phys. 56 (1984) 579.
- [74] A. Abramowicz, et al., 1983, Z. Phys. C17 (1983) 283.
- [75] G. Altarelli, R. K. Ellis, and G. Martinelli, Nucl. Phys. B143 (1978) 521; 146 544(E) (1978).
- [76] For a review see J. Ritchie in Proc. of 1984 DPF Summer study on the design and utilization of the SSC, Ed. R. Donaldson and J. Morfin (FNAL 1984); A. Kernan and G. van Delen, Phys. Rep. 106 (1984) 297.
- [77] F. Herzog and Z. Kunszt, Phys. Lett. 157B (1985) 430.
- [78] G. Altarelli and G. Parisi, Nucl. Phys. B126 (1977) 285.
- [79] V. Barger, S. Jacobs, J. Woodside, and K. Hagiwara, Wisconsin preprint MAD/PH/232 (1985).
- [80] C. Kounaus and D. A. Ross Nucl Phys. B217 (1983) 145.
- [81] J. Collins, D. Soper, and G. Sterman, University of Oregon preprint OITS-292 (June 1985).
- [82] A. De Rújula and R. Petronzio, Nucl. Phys. B261 (1985) 587.
- [83] H. Albrecht et al., Phys. Lett. 150B (1985) 225. C. Bebek et al. Phys. Rev. Lett. 49(1985) 610. H. Yamamoto Ph. D. Thesis (1986).
- [84] H. Aihara et al. Z. Phys. C27 (1985) 495.
- [85] J. F. Owens Phys. Lett. 76B (1978) 85; T. Vematson, Phys. Lett. 79B(1978) 97.
- [86] C. Peterson, et al., Phys. Rev. D27 (1983) 105.
- [87] K. Hagiwara and S. Jacobs (in preparation).
- [88] For a review see H. Aihara/Ph. D Thesis UT-HE-84/15 (1985).
- [89] P. Fayet, Phys. Lett. 86B (1979) 272.
- [90] R. C. Ball, et al., Phys. Rev. Lett. 53 (1984) 1314; F. Bergsma, et al., Phys. Lett. 121B (1983) 429. A. M. Cooper-Sakar et al., Phys. Lett. 100B (1985) 212.
- [91] M. Chanowitz and S. Sharpe, Phys. Lett. 126B (1983) 225.
- [92] H. R. Gustafson, et al., Phys. Rev. Lett. 37 (1976) 747; J. Appel, et al., *ibid* 32 (1974) 428.
- [93] J. Ellis and H. Kowalski, Phys. Lett. 142B (1984) 441; Nucl. Phys. B246 (1984) 189; Phys. Lett. 157B (1985) 437; Nucl. Phys. B259 (1985) 109. E. Reya and D. P. Roy, Phys. Rev. Lett. 51 (1983) 867; (E: 51 (1983); 1307 Dortmund preprint DO-TH 85/23 (1985); V. Barger, K. Hagiwara and J. Woodside, Phys. Rev. Lett. 145B (1985) 147; V. Barger, K. Hagiwara and W. -Y. Keung, Phys. Lett. 145B (1984) 147; V. Barger, K. Hagiwara, W. -Y. Keung and J. Woodside, Phys. Rev. D32 (1985) 528; D32 (1985) 806; A. R. Allan, E. W. N. Glover and A. D. Martin, Phys. Lett. 146B (1984) 247; A. R. Allan, E. W. N. Glover, and S. L. Grayson, Durham preprint DTP/84/28 (1984); N. D. Tracas and S. D. P. Vlassopoulos, Phys. Lett. 149B (1984) 253; X. N. Maintas and S.D. P. Vlassopoulos, Phys. Rev. D32 (1985) 604; F.

- Delduc, H. Navelet, R. Peschanski and C. Savoy, Phys. Lett. 155B (1985) 173.
- [94] R. M. Barnett, H. Haber and G. L. Kane, LBL-20102 (August 1985). Nucl. Phys. B (to appear).
- [95] G. Arnison, et al, Phys. Lett. 129B (1983) 130; 132B (1983) 214, 132B (1983) 223; 136B (1983) 294.
- [96] J. Rohlf in Proceedings of the 1985 meeting of the Division of Particles and Fields of the APS. Oregon July 1985 CERN EP/85-160; C. Rubbia Talk at Lepton-Photon Symposium, Kyoto, Japan, August 1985.
- [97] S. D. Ellis, R. Kleiss and W. J. Stirling CERN TH-4170/85 (May 1985), Phys. Lett. 154B (1985) 435.
- [98] R. M. Barnett, H. E. Haber, and G. L. Kane, Phys. Rev. Lett. 54 (1985) 1983; M. J. Herrero, L. E. Ibanez, C. Lopez and F. J. Yndurain, Phys. Lett. 132B (1983) 199; 145B (1984) 430; J. Ellis and H. Kowalski, Phys. Lett. 157B (1985) 437.
- [99] T. Kinoshita et al., Phys. Rev. Lett. 52 (1984) 717.
- [100] J. Bailey, et al., Nucl. Phys. B150 (1979).
- [101] R. Barbieri and L. Maiani, Phys. Lett. 117B (1982) 203; P. Fayet, Phys. Lett. 84B (1979) 416.
- [102] D.A. Kosower, L. M. Krauss and N. Sakai, Phys. Lett. 133B (1983) 305.
- [103] C. Prescott, et al., Phys. Lett. 77B (1978) 347.
- [104] R. N. Cahn and F. Gilman, Phys. Rev. D17 (1978) 1313;
- [105] M. Duncan, Nucl. Phys. B214 (1983) 21. M. Suzuki, Phys. Lett. 115B (1982) 40.
- [106] M. Box, et al., Nucl. Phys. A260 (1976) 412.
- [107] E. G. Adelberger, et al., Phys. Rev. Lett. 34 (1975) 402.
- [108] Particle Data Group Rev. Mod. Phys. 56(1984).
- [109] E. Ranco and M. Mangano, Phys. Lett. 135B (1985) 445; J. Barber and R. Schrock, Phys. Lett. 139B (1984) 427.
- [110] B. A. Campbell, Phys. Rev. D28 (1983) 209.
- [111] J. Ellis and D. V. Nanopolous, Phys. Lett. 110B (1982) 44.
- [112] M. Suzuki Berkeley preprint UCB-PTH-82/8 (1982).
- [113] J. F. Donohue, H. P. Nilles and D. Wyler, Phys. Lett. 128B (1983) 55.
- [114] H. Goldberg, Phys. Lett. 147B (1984) 289.
- [115] J. M. Gerard, et al., Phys. Lett. 140B (1984) 349.
- [116] M. Dugan, B. Grinstein and L. Hall, Nucl. Phys. B255 (1985) 413.
- [117] M. K. Gaillard, et al., Phys. Lett. 123B (1983) 241.
- [118] J. Ellis and J. Hagelin, B217 (1983) 189.
- [119] L. S. Littenberg, Brookhaven preprint BWL 35086 (unpublished) (1984).
- [120] M. B. Gavela, et al, CERN Preprint CERN-TH-4093/85.
- [121] L. Hall and J. Polchinski, Phys. Lett. 152B (1985) 335; S. Nandi, Phys. Rev. Lett. 54 (1985) 2493; J. Ellis and M. Sher, Phys. Lett. 148B (1984) 390
- [122] L. Hall and M. Suzuki, Nucl. Phys. B23 (1984) 419; I. Lee, Nucl. Phys. B246 (1984) 120.
- [123] C. Aulakh and R. Mohaputra, Phys. Lett. 119B (1982) 136.
- [124] H. Georgi, S. Glashow and S. Nussinov, Nucl. Phys. B193 (1981) 247; M. Fukusita, et al., Phys. Rev. Lett. 48 (1982) 1527.
- [125] G. G. Ross and J. Valle, Phys. Lett. 151B (1985) 375.
- [126] S. Dawson, Nucl. Phys. B261 (1985) 297
- [127] J. Ellis, et al., Phys. Lett. 150B (1984) 142.
- [128] S. Abachi et al. ANL-HEP-PR-85-115 (1986).
- [129] Proc. of 1978 LEP Summer Study CERN 79-01.

- [130] Proc. of the SLC Workshop SLAC Pub 247 (1983).
- [131] R. J. Cashmore et al. Phys. Rep. **122** (1985) 275.
- [132] P. Salati and M. Wallet Phy. Lett. **122B** (1985) 397.
- [133] M. Tigner IEEE Proc. on Nucl. Sci NS-32 (1985) 1556.
- [134] S. Dawson and A. Savoy Navarro in Proc of 1984 Summer Study on the Design and Utilization of the SSC. Ed by J. Morfin and R. Donaldson FNAC.
- [135] L. Feyard Presentation at the 1985 SLAC Summer Institute. Ed. M. Zipf (1986)

Figure Captions

- Figure 1.1 Diagrams showing contributions to gluon masses from a loop of quarks and squarks, the suffices L and R refer to chirality states.
- Figure 1.2 Diagrams showing contributions to gluino masses from loops involving gravitinos \tilde{G} .
- Figure 1.3 Diagram showing the scattering of χ_0 states from a nucleon.
- Figure 1.4 (a) Diagram showing the decay $\tilde{\gamma} \rightarrow f\bar{f}\tilde{H}^0$.
(b) Diagram showing a contributions to $\tilde{\gamma} \rightarrow \tilde{H}\gamma$.
- Figure 2.1 Feynman graphs contributing to the annihilation of neutrinos. The first graph is relevant only if $m_\nu > m_\ell$.
- Figure 2.2 The quantity f (see equation 2.22) plotted against x for various values of the parameters appearing in equation 2.22.
- Figure 2.3 Feynman diagram to the annihilation process $\tilde{\gamma}\tilde{\gamma} \rightarrow f\bar{f}$ where f is a quark or lepton.
- Figure 2.4 Figure showing the region of squark and photino masses which is allowed by the cosmological considerations of section 2.³⁰ All squarks and sleptons are taken to be degenerate and the photino is assumed to be stable.
- Figure 2.5 Feynman diagrams showing the annihilation of Higgsino pairs.

- Figure 2.6 Feynman diagram showing a contribution to the annihilation of sneutrino pairs.
- Figure 2.7 Feynman graphs showing regeneration of gravitinos by scattering of other fields.
- Figure 3.1 Feynman diagrams for the process $e^+e^- \rightarrow \tilde{\ell}\tilde{\ell}$. The first graph is relevant only for final states of selectron pairs.
- Figure 3.2 Excluded regions in slepton- χ_0 space.⁵⁰ The data assume that $m_{\tilde{L}}^2$ and $m_{\tilde{R}}^2$ are degenerate and decay via $\tilde{\ell} \rightarrow \ell + \chi_0$ where the χ_0 escapes undetected. The solid line applies to selectrons and the dashed to smuons.
- Figure 3.3 Feynman diagram contributing to the process $e^+e^- \rightarrow \tilde{e}\tilde{\gamma}e^+$.
- Figure 3.4 Feynman diagrams showing the pair production of neutral inos in e^+e^- annihilation.
- Figure 3.5 Feynman diagram showing a contribution to the process $e^+e^- \rightarrow \gamma + \tilde{\gamma} + \tilde{\gamma}$.
- Figure 3.6 Radiative Bhabha scattering. This process is a background to that of figure 3.5 if the outgoing e^+e^- pair is undetected.
- Figure 3.7 The excluded region⁶¹ in photino-selectron masses from the non-observation of the process of figure 3.5. \tilde{e}_L and \tilde{e}_R are assumed to be degenerate.
- Figure 3.8 Feynman diagram showing a contribution to the decay $\tilde{\nu} \rightarrow \nu + \tilde{\gamma}$.
- Figure 3.9 Feynman diagram showing a contribution to the process $\tilde{\nu} \rightarrow e + q + \bar{q} + \tilde{g}$ or $\tilde{\nu} \rightarrow e + q + \bar{q} + \tilde{\gamma}$.
- Figure 4.1 Figure showing the missing transverse momentum (p_T) distribution arising from the process $p\bar{p} \rightarrow Z + X \rightarrow \tilde{e} + \tilde{e} + X \rightarrow e^+ + e^- + \tilde{\gamma} + \tilde{\gamma} + X + x$. The photino is taken to be massless, and the electron mass is GeV. The curves are normalized to 100 events in the channel $Z \rightarrow e^+e^-$. The solid line corresponds to electron position pair masses of 10-30 GeV and the dashed line to 50-70 GeV.⁶⁷
- Figure 4.2 The transverse momentum distribution of electrons arising from the process $p\bar{p} \rightarrow W + x \rightarrow \tilde{e} + \tilde{\nu} + x \rightarrow e + X$ with $m_{\tilde{e}} = 40\text{GeV}$ $m_{\tilde{\nu}} =$

10GeV (dashed line). The solid line shows the distribution from $W \rightarrow ev$ for comparison. The curves are normalized to the same area.⁶³

Figure 4.3 Diagram showing the process $pp \rightarrow X + X + \text{anything}$ (see equation 4.3).

Figure 4.4 Curves showing the x dependence of the structure functions $f_i(x, Q^2)$.

Figure 4.5 Comparison of the jet cross-section measured at the CERN $Spp\bar{S}$ collider⁷² with the prediction using the structure functions of ref. 73. Shown is $d\sigma/dp_t dy$ at $y = 0$ and $\sqrt{s} = 540\text{GeV}$.

Figure 4.6 Feynman diagram showing a contribution to the process $g + g \rightarrow g + \tilde{g} + \tilde{g}$.

Figure 4.7 Feynman diagram showing the formation of a squark in a gluino quark collision.

Figure 4.8 A comparison of the exact and leading log approximations for the rate $p\bar{p} \rightarrow \tilde{g} + \tilde{q} + X$ at $\sqrt{s} = 630\text{GeV}$. The squark mass has been set to 100 GeV.

Figure 4.9 The distribution⁸³³ in $x = p_0/p_{\text{max}}$ of D mesons seen e^+e^- annihilation at 10.5 GeV (CLEO) (diamonds) 10 GeV (ARGUS) (squares) and 29 GeV (DELCO) (stars). For comparison the distribution of π 's from the TPC (crosses) is shown.⁸⁴ The quark which initiates the hadronic shower is at $x = 1$.

Figure 4.10 The fragmentation function at $D(z, Q)$ for gluino⁷⁹ at $Q = 40\text{GeV}$. The solid lines have $\epsilon_j = \epsilon_b(\frac{m_b}{m_j})^2$, and the dashed has $\epsilon_j = \frac{9}{4}\epsilon_b(\frac{m_b}{m_j})^2$.

Figure 4.11 The cross-section for producing a pair of gluinos in proton proton collisions at low energy. The dependence upon $m_{\tilde{g}}$ is slight, it has been set to 50 GeV.

Figure 4.12 The excluded region in squark and gluino masses arising from the beam dump experiments discussed in the text.⁹⁰

Figure 4.13 Contour plot showing the number of missing transverse energy events per 100 nb^{-1} of luminosity in $p\bar{p}$ collisions at 630 GeV. The cuts are described in the text. Figure courtesy of M. Barnett.⁹⁴

Figure 4.14 The cross section $p\bar{p} \rightarrow \tilde{g} + \tilde{g} + X$ as a function of gluino mass for $m_{\tilde{q}} = 100\text{GeV}$. The curves are insensitive to the precise values of the squark mass.

Figure 5.1 Feynman diagram showing a contribution to the muon $(g-2)$ from smuon loops. There are other contributions involving winos.

Figure 5.2 Feynman graphs showing a contributions to electron proton scattering which results in a different cross-section for left and right handed electrons.

Figure 5.3 Graphs showing contributions to a parity violating interaction between quarks.

Figure 5.4 Graphs showing a contribution to the process $\mu \rightarrow e\gamma$ due to the mixing terms of equation 5.17.

Figure 5.5 Diagrams showing supersymmetric contributions to the $K_L - K_S$ mass matrix.

Figure 5.6 Graphs showing a contribution to the renormalization of $m_{\tilde{d}}$ by u-quarks and Higgs particles. The contribution is proportional to m_u^2 .

Figure 5.7 Diagram showing the process $K \rightarrow \pi + \tilde{\gamma} + \tilde{\gamma}$.

Figure 6.1 Figure showing the contribution to neutrino masses from radiative corrections involving the terms of equation 6.3.

Figure 6.2 Contributions to the process $\mu \rightarrow e\gamma$ from the terms of equation 6.3.

Figure 6.3 Diagram showing a contribution to the decay process $\tilde{\gamma} \rightarrow \gamma + \nu$ from the terms C_i of equation 6.3.

Figure 6.4 Diagram showing a contributing to the decay process $\tilde{\gamma} \rightarrow \gamma + \nu$ from a non zero sneutrino vev.

Figure 6.5 Diagram showing a contribution to the decay process $\tilde{\gamma} \rightarrow q + \bar{q} + \nu$ from the terms D_i of equation 6.4.

Figure 6.6 The missing transverse momentum spectrum¹²⁶ from the process $p\bar{p} \rightarrow \tilde{g} + \tilde{g} + X$ at $\sqrt{s} = 540\text{GeV}$ with $m_{\tilde{q}} = 100\text{GeV}$, $m_{\tilde{g}} = 40\text{GeV}$ and $m_{\tilde{\gamma}} = 1\text{GeV}$. The solid line is due to the decay $\tilde{g} \rightarrow q + \bar{q} + \tilde{\gamma}$ where

the photino is stable. The dashed line has the decay $\tilde{\gamma} \rightarrow \gamma + \nu$ and the dot-dashed line $\tilde{\gamma} \rightarrow q + \bar{q} + \nu$.

Figure 6.7 The cross section for the process $p\bar{p} \rightarrow \tilde{q}\tilde{q} + X$. The solid lines have $m_{\tilde{q}} = m_{\tilde{q}}$ and the dashed lines have $m_{\tilde{q}} = 100\text{GeV}$.

Figure 6.8 Feynman diagram showing the process $ep \rightarrow \tilde{e} + \tilde{q} + X$.

Figure 6.9 Cross section from the process $ep \rightarrow \tilde{e} + \tilde{q} + X$ at $\sqrt{s} = 318\text{GeV}$. The photino mass as assumed to be zero.

Figure 6.10 Feynman diagram showing to process $ep \rightarrow e + \tilde{q} + \tilde{q} + X$.

Figure 6.11 The cross-section for the process $ep \rightarrow e + \tilde{q} + \tilde{q} + X$ at $\sqrt{s} = 318\text{GeV}$.

Figure 6.12 Parton diagram showing the process $ep \rightarrow e + \tilde{g} + \tilde{q} + X$.

Figure 6.13 The cross-sections for the process $ep \rightarrow e + \tilde{g} + \tilde{q} + X$ at $\sqrt{s} = 318\text{GeV}$.

Figure 6.14 The cross-sections for $pp \rightarrow \tilde{e}\tilde{e} + X$ as a function of the selectron mass at $\sqrt{s} = 10, 20, 40\text{TeV}$.

Figure 6.15 The cross-section $pp \rightarrow \tilde{g} + \tilde{g} + X$ as a function of gluino mass. The squark mass has been set to 1 TeV.

Figure 6.16 The cross section $pp \rightarrow \tilde{g} + \tilde{\gamma} + X$ as a function of photino mass. The gluino and photino masses are equal to the squark mass.

Table 1

Particle	decay mode	lifetime sec
\tilde{e}	$e + \tilde{\gamma}$	$2 \times 10^{-22} \frac{m_{\tilde{e}}^3}{(m_{\tilde{e}}^2 - m_{\tilde{\gamma}}^2)^2} \left(\frac{1}{a^2}\right)$
\tilde{q}	$q + \tilde{g}$	$6 \times 10^{-24} \frac{m_{\tilde{q}}^3}{(m_{\tilde{q}}^2 - m_{\tilde{g}}^2)^2}$
	$q + \tilde{\gamma}$	$3 \times 10^{-22} \frac{m_{\tilde{q}}^3}{(m_{\tilde{q}}^2 - m_{\tilde{\gamma}}^2)^2} \left(\frac{1}{a^2}\right)$
	$q + \tilde{W}$	$6 \times 10^{-23} \frac{m_{\tilde{q}}^3}{(m_{\tilde{q}}^2 - m_{\tilde{W}}^2)^2}$
\tilde{g}	$\tilde{g} + q$	$4 \times 10^{-23} \frac{m_{\tilde{g}}^3}{(m_{\tilde{g}}^2 - m_{\tilde{q}}^2)^2}$
\tilde{g}	$q + \bar{q} + \tilde{\gamma}$	$10^{-11} \left(\frac{m_{\tilde{q}}}{M_W}\right)^4 \frac{1}{m_{\tilde{\gamma}}^5} \left(\frac{1}{\alpha^2}\right)$

Table Caption

Lifetime estimates for sparticle decays.⁴ Quarks and lepton masses and neglected. If the photino is not the lightest state a reasonable approximation is obtained by including the factor in parenthesis. The term a is given by equation 1.30. All masses are GeV.

Table 2

Sparticle	Excluded Mass Region	Comment
$\tilde{\gamma}$	$2 \text{ GeV} \gtrsim m_{\tilde{\gamma}} \gtrsim 100 \text{ eV}$	$m_{\tilde{\gamma}} \approx 20 \text{ GeV}$
	$5 \text{ GeV} \gtrsim m_{\tilde{\gamma}} \gtrsim 100 \text{ eV}$	$m_{\tilde{\gamma}} \approx 70 \text{ GeV}$
\tilde{H}^0	$5.5 \text{ GeV} \gtrsim m_{\tilde{H}^0} < 100 \text{ eV}$	valid if $v_1 \neq v_2$
	$m_t \gtrsim m_{\tilde{H}^0} \gtrsim 100 \text{ eV}$	valid if $v_1 = v_2$
\tilde{e}, \tilde{q}	$m_{\tilde{e}, \tilde{q}} \lesssim 350 \text{ GeV}$	
		valid only if lightest
\tilde{g}	$m_{\tilde{g}} \lesssim 350 \text{ GeV}$	shadron is charged
$\tilde{\nu}$	$10 \text{ MeV} \gtrsim m_{\tilde{\nu}} \gtrsim 100 \text{ eV}$	

Table Caption

Limits on superparticles from cosmology. The limit stated on each sparticle assumes that it is the lightest and is absolutely stable.

Table 3

Process	UA1 ⁹⁶	UA2 ¹³⁵	Theory	Theory
			L0	H0
$\sigma(p\bar{p} \rightarrow W^\pm + x)B(W \rightarrow e\nu)$	$630 \pm 50 \pm 90$	$529 \pm 64 \pm 49$	310	403
$\sigma(p\bar{p} \rightarrow Z + x)B(Z \rightarrow e^+e^-)$	$79 \pm 21 \pm 12$	$110 \pm 39 \pm 9$	38	49

Table Caption

A comparison of the predicted cross-sections for W and Z production at the CERN $S\bar{p}\bar{p}S$ collider with those observed by the UA1 and UA2 collaborations at $\sqrt{s} = 630 \text{ GeV}$. The predictions indicated by L0(H0) are without (with) the higher order QCD corrections. All cross-sections are given in picobarns.

Table 4

Particle	Excluded Mass Range	Comment
$\tilde{e}, \tilde{\mu}, \tilde{\tau}$	< 20 GeV	Valid provided decay is $\tilde{\ell} \rightarrow \ell + \chi_0$ or $\tilde{\ell} \rightarrow \ell + \gamma + \chi_0$
\tilde{e}	< 50 GeV	Valid if $m_{\tilde{\gamma}}$ is small and $\tilde{\gamma}$ is an eigenstate of mass.
\tilde{g}	≥ 60 GeV	valid provided decays are $\tilde{q} \rightarrow \bar{q} + \chi$ or $\tilde{g} \rightarrow \tilde{q} + q$
\tilde{q}	≥ 60 GeV	or $\tilde{g} \rightarrow q + \tilde{q} + \chi$ or $\tilde{q} \rightarrow q + \bar{g}$ χ must be long lived.
$\tilde{\gamma}$	$100 \text{ ev} < m < \text{few GeV}$	Valid if $\tilde{\gamma}$ stable
\tilde{H}	$100 \text{ ev} < m < \text{few GeV}$	Valid if \tilde{H} stable
$\tilde{\nu}$	$100 \text{ ev} < m < 10 \text{ MeV}$	Valid if $\tilde{\nu}$ stable

Table Caption

Limits on sparticle mass from the processes discussed in sections 2-5. This table assumes that all squarks masses are approximately equal, that R parity is not broken.

Appendix

This appendix given the renormalization group equations which determine the evolution of the masses and coupling constants^{15,14} discussed in section one. For simplicity I will assume that the superpotential contains only two terms viz

$$W = \lambda Q u H_2 + \mu H_1 H_2 \quad (A1)$$

where Q is a quark doublet, U is a right handed quark and H_1 and H_2 are Higgs doublets: I will further assume that the supersymmetry is broken in the appearance of the following terms. Scalar masses:

$$m_Q^2 |Q|^2 + m_{H_1}^2 |H_1|^2 + m_u^2 |u|^2 + m_{H_2}^2 |H_2|^2. \quad (A2)$$

Soft Operators:

$$A \lambda m Q u H_2 + B_{\mu m} H_1 H_2 + h.c. \quad (A3)$$

The scale m has been introduced so that B is dimensionless.

Gaugino masses:

$$\frac{1}{2} M_3 \bar{\psi}_{\tilde{g}} \psi_{\tilde{g}} + \frac{1}{2} M_2 \bar{\psi}_{\tilde{W}} \psi_{\tilde{W}} + \frac{1}{2} M_1 \bar{\psi}_{\tilde{B}} \psi_{\tilde{B}} \quad (A4)$$

Here B is the gauge boson associated with the group $U(1)_Y$. If we assume that there are 3 generations of quarks and leptons, then the evolution of the gauge coupling constants α_i is given by

$$\frac{d}{dt} \alpha_i(t) = \frac{b_i}{2\pi} \alpha_i^2(t) \quad (A5)$$

where $t = \log Q^2$ and $b_1 = \frac{33}{5}$, $b_2 = 1$ and $b_3 = -3$. I have assumed that there are 3 generations of quarks and leptons. Note that the coupling constant $\alpha_1 = g_1/4\pi$ is normalized so that if the theories grand unified at scale M_G .

$$\alpha_i(M_G) = \alpha_G$$

for all i. Hence $\frac{5}{3} g'^2 = g_1^2$. The gaugino masses evolve according to

$$\frac{d}{dt} \left(\frac{M_i}{\alpha_i} \right) = 0 \quad (A6)$$

The Yukawa coupling λ evolves according to

$$\frac{d\lambda}{dt} = \frac{\lambda}{4\pi} \left[-\frac{16}{3} \alpha_3 - 3\alpha_2 - \frac{13}{15} \alpha_1 + \frac{6\lambda^2}{4\pi} \right] \quad (A7)$$

The other superpotential parameter μ evolves according to

$$\frac{d\mu}{dt} = \frac{\mu}{4\pi} \left[-3\alpha_2 - \frac{3}{5} \alpha_1 + \frac{3\lambda^2}{4\pi} \right] \quad (A8)$$

A and B evolve as

$$\frac{dA}{dt} = \frac{1}{4\pi} \left[-\frac{32}{3} \alpha_3 M_3 - 6\alpha_2 M_2 - \frac{26}{15} \alpha_1 M_1 + \frac{12\lambda^2 A}{4\pi} \right] \quad (A9)$$

$$\frac{dB}{dt} = \frac{1}{4\pi} \left[-b\alpha_2 M_2 - \frac{6}{5} \alpha_1 M_1 + \frac{6\lambda^2 A}{4\pi} \right] \quad (A10)$$

Finally the scalar masses

$$\frac{d}{dt} \begin{pmatrix} m_H^2 \\ m_U^2 \\ m_Q^2 \end{pmatrix} = -\frac{2}{\pi} \sum_i \alpha_i T_{ai}^2 M_i^2 + \frac{\lambda^2}{8\pi^2} \begin{pmatrix} 3 \\ 2 \\ 1 \end{pmatrix} (m_{H_2}^2 + m_u^2 + m_Q^2 + A^2) \quad (A11)$$

$$\frac{d}{dt} m_{H_1}^2 = -\frac{2}{\pi} \sum_A T_{ia}^2 \alpha_i M_i^2 \quad (A12)$$

Here $T_{ai}^2 = \sum_A T_{ia}^A T_{ia}^A$ is the quadratic casimir of the a^{th} scalar with respect to the i^{th} gauge group. As a consequence of equation A11, models which have large gaugino masses at M_G tend to have squark masses where are comparable at low energy. The equations given in this appendix are valid to lowest order in $\alpha_i \lambda^2$ A and B.

Figures

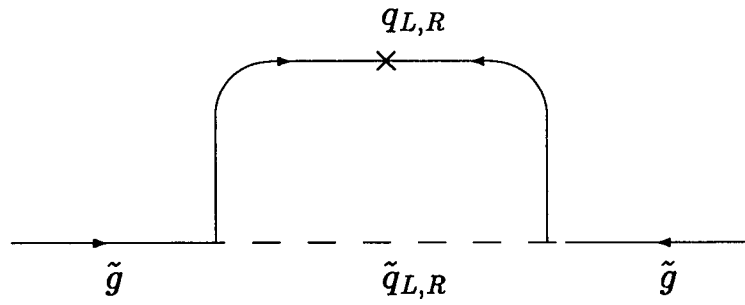


Figure 1.1

84

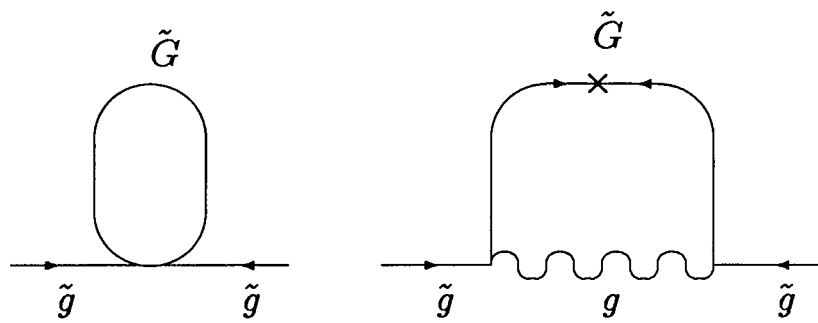


Figure 1.2

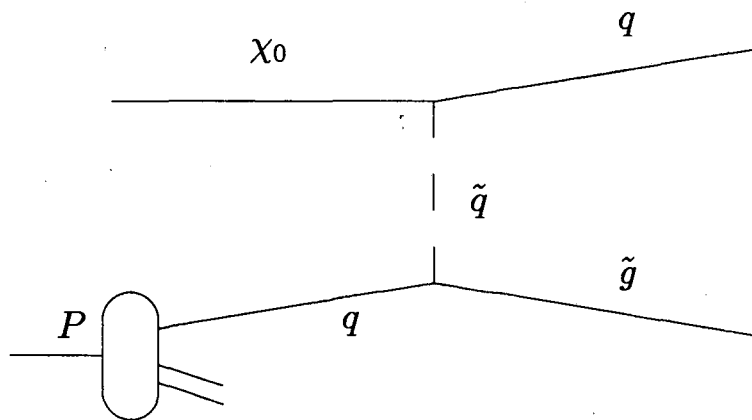
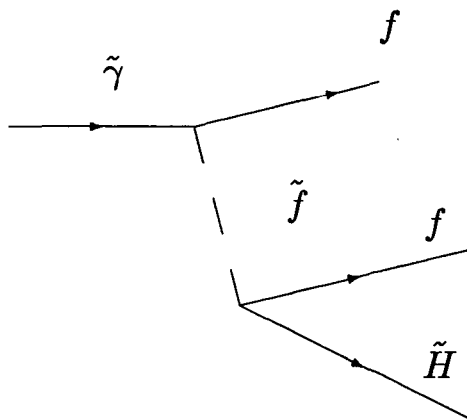
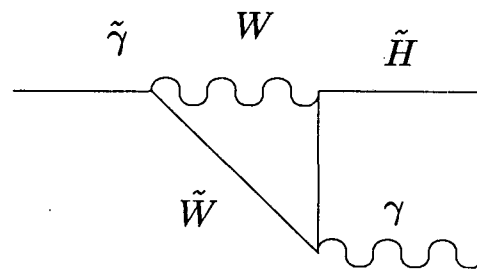


Figure 1.3

85



(a)



(b)

Figure 1.4

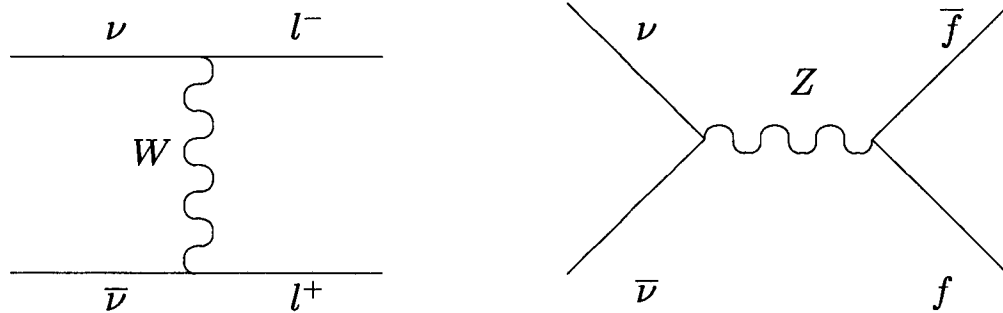


Figure 2.1

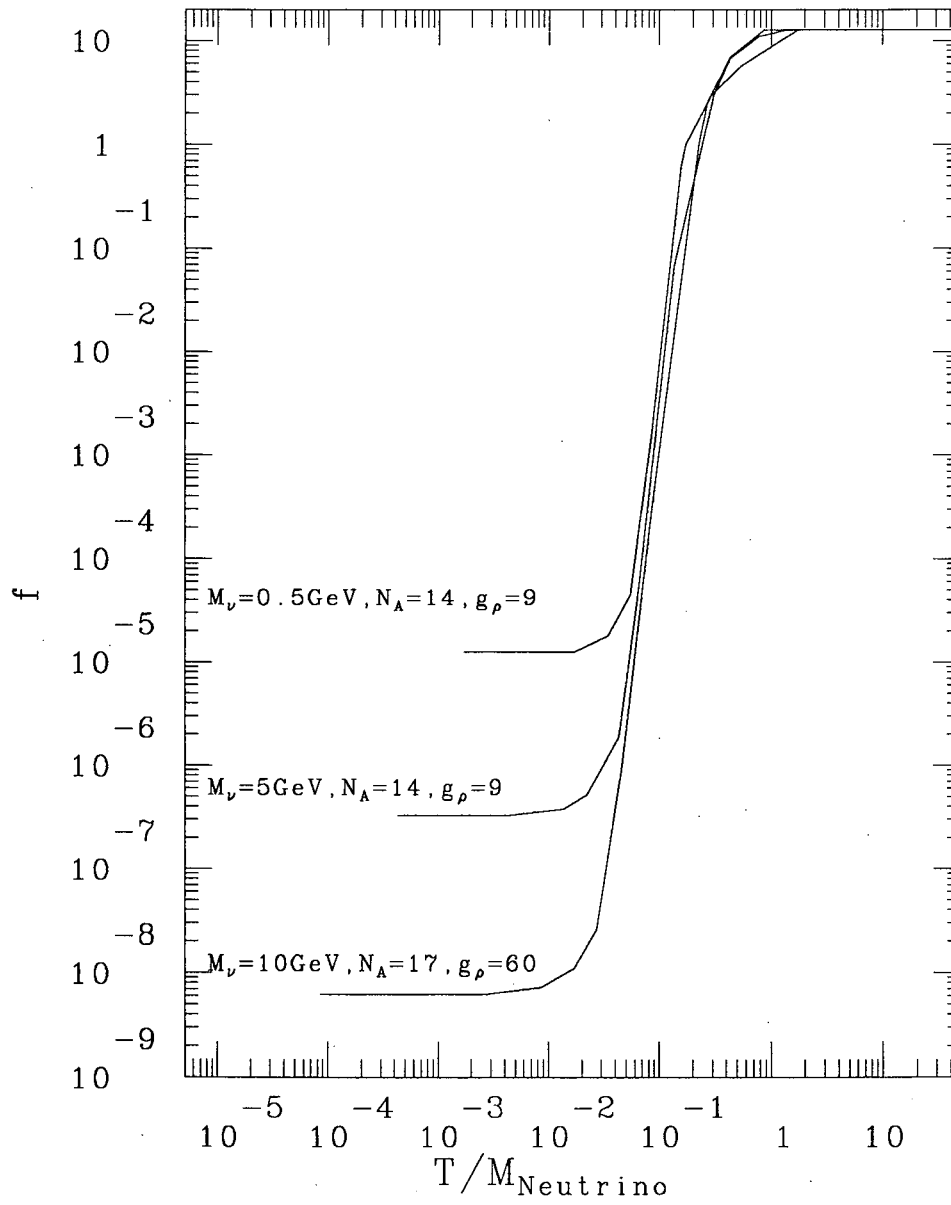


Figure 2.2

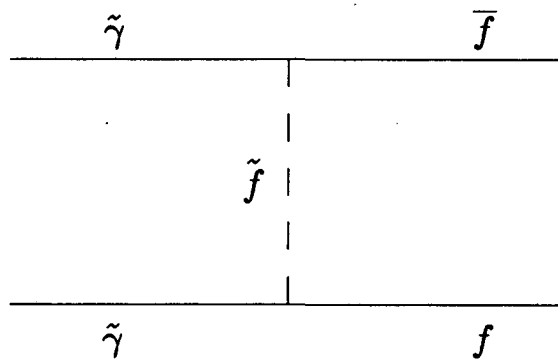


Figure 2.3

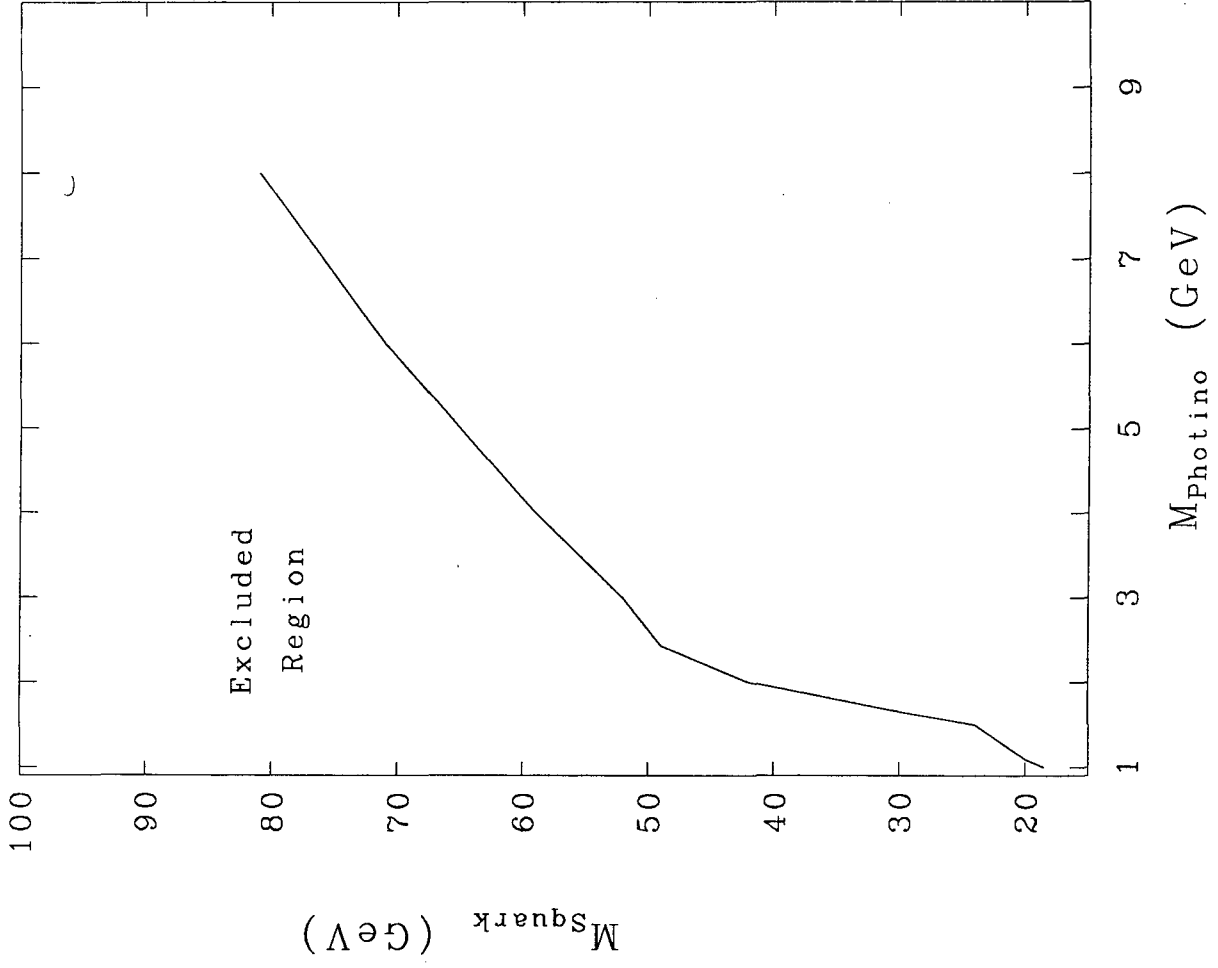


Figure 2.4

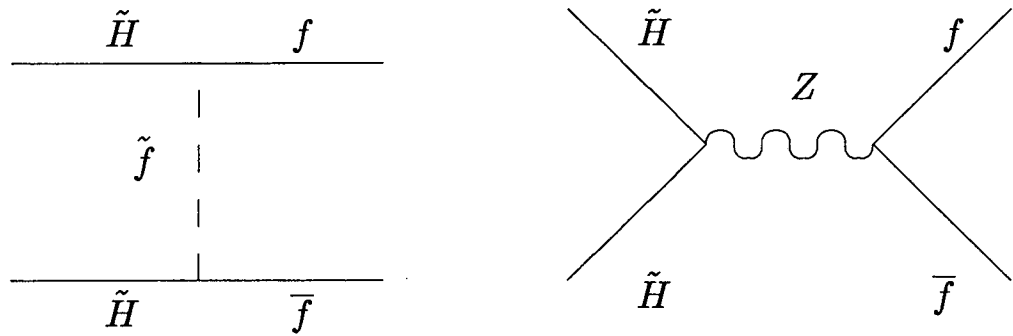


Figure 2.5

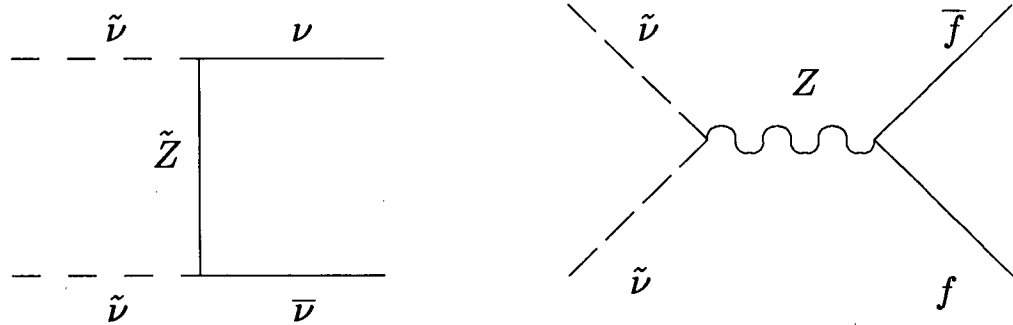


Figure 2.6

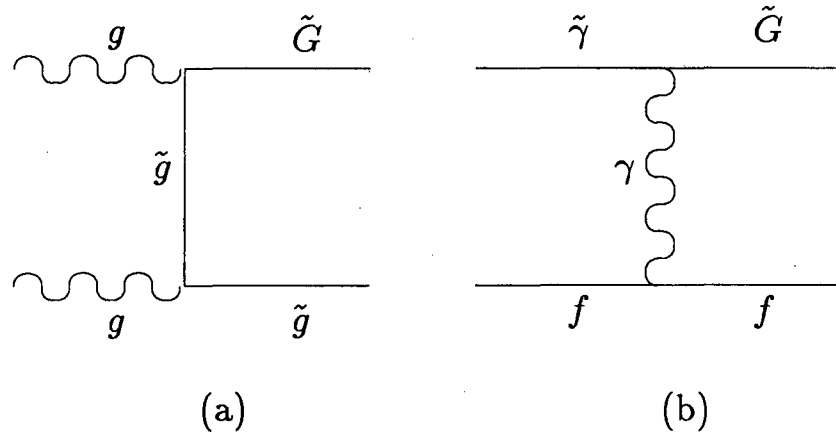


Figure 2.7

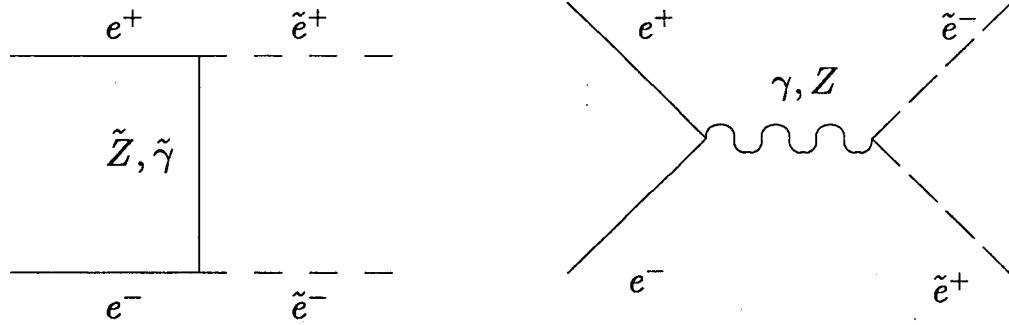
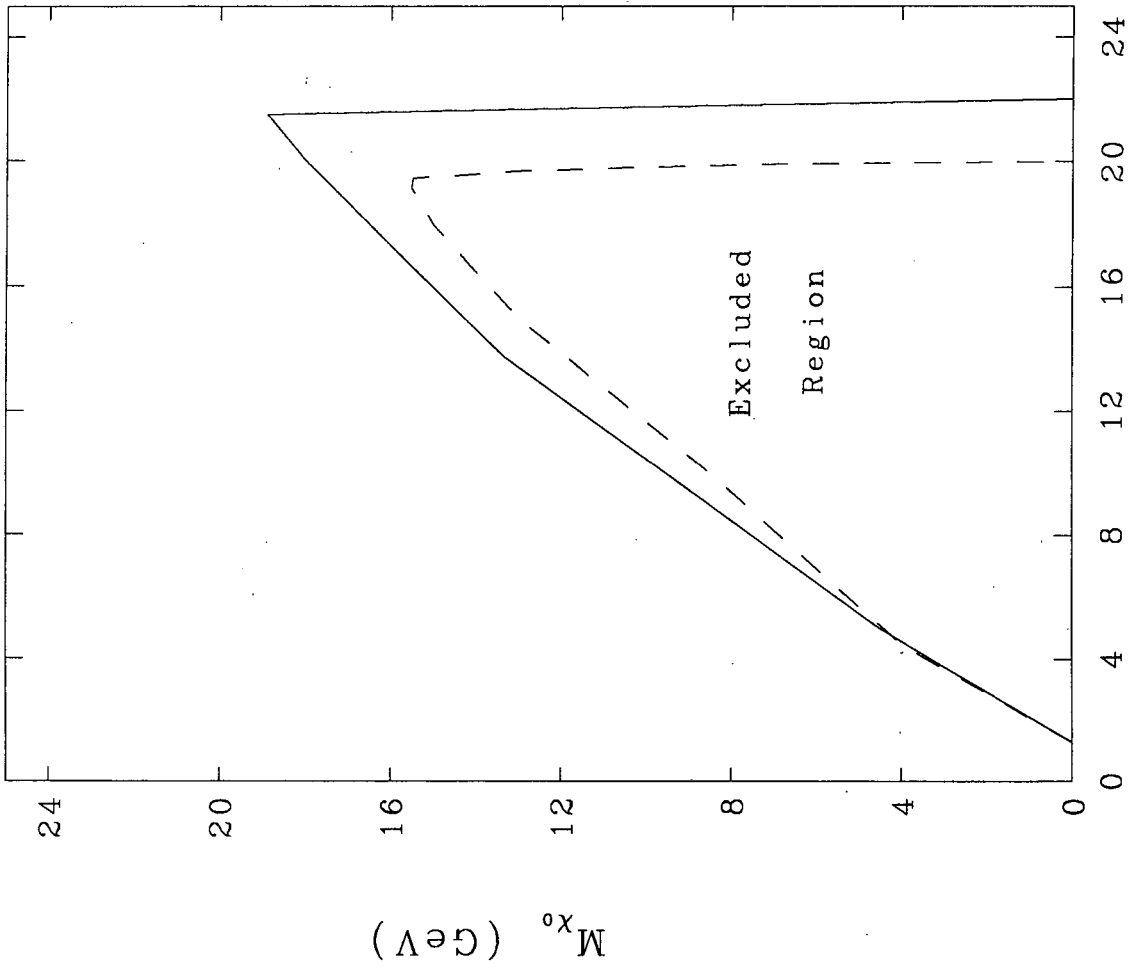


Figure 3.1



$M_{Slepton}$ (GeV)

Figure 3.2

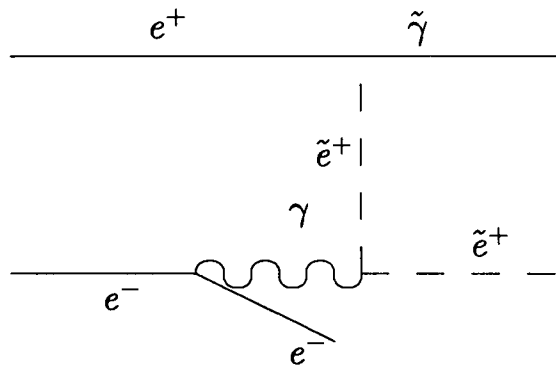


Figure 3.3

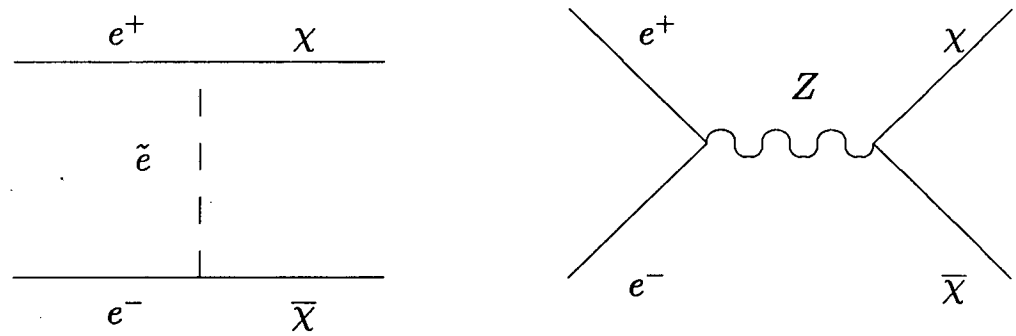


Figure 3.4

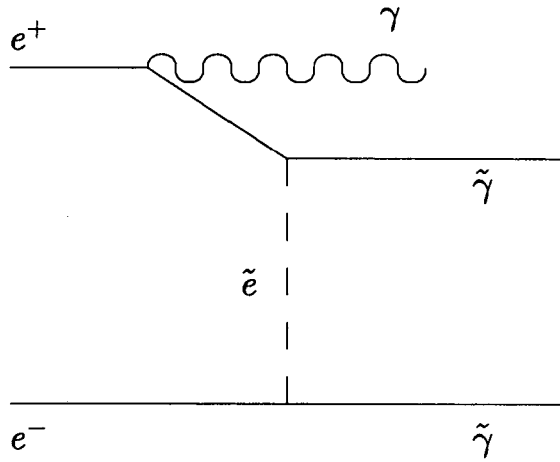


Figure 3.5

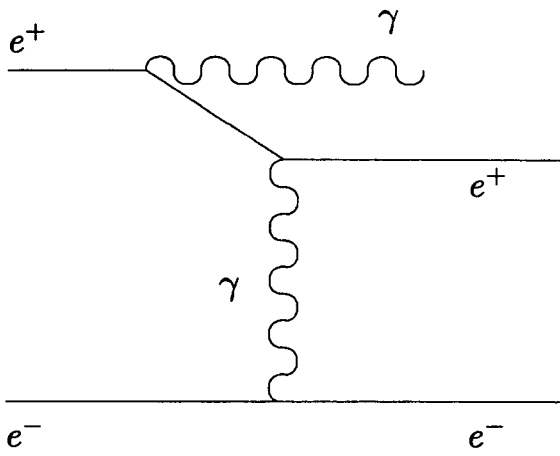


Figure 3.6

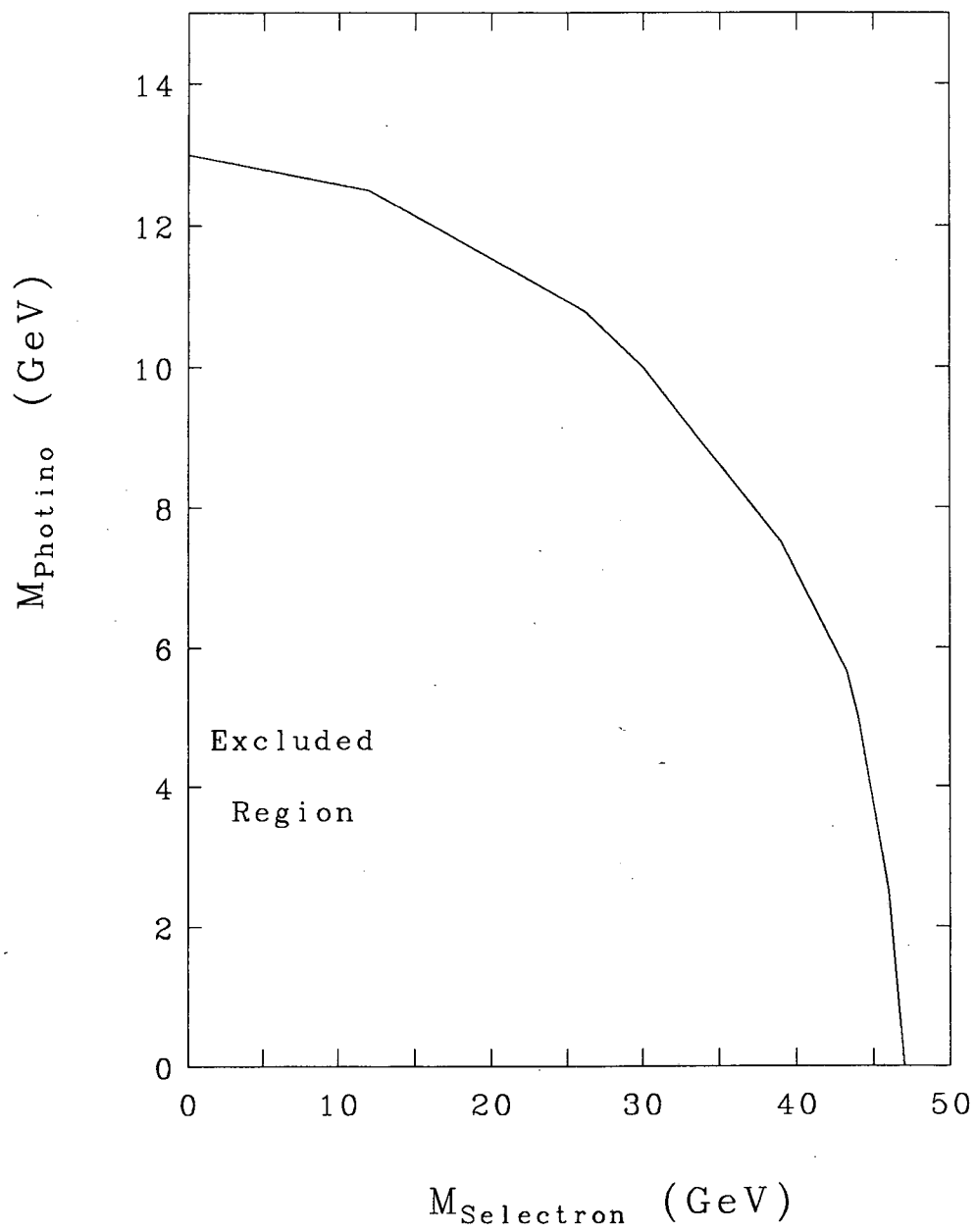


Figure 3.7

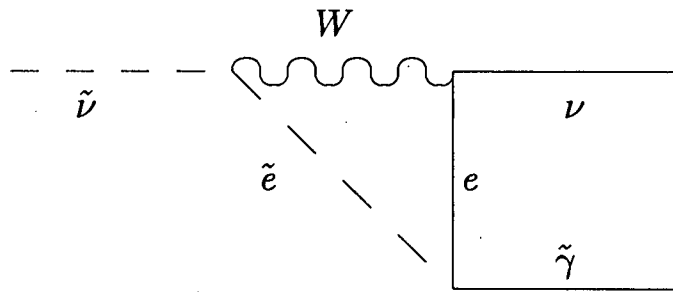


Figure 3.8

97

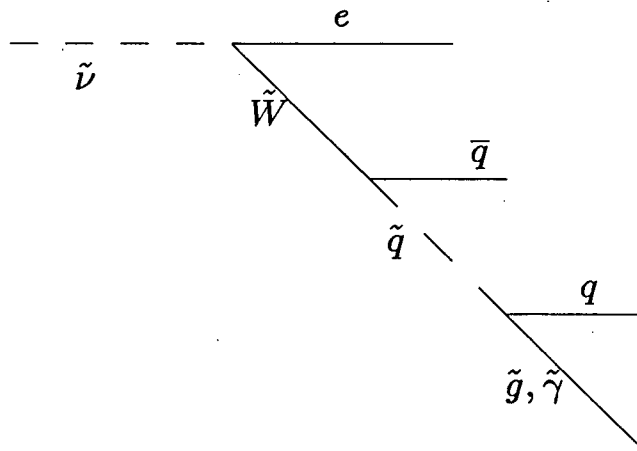


Figure 3.9

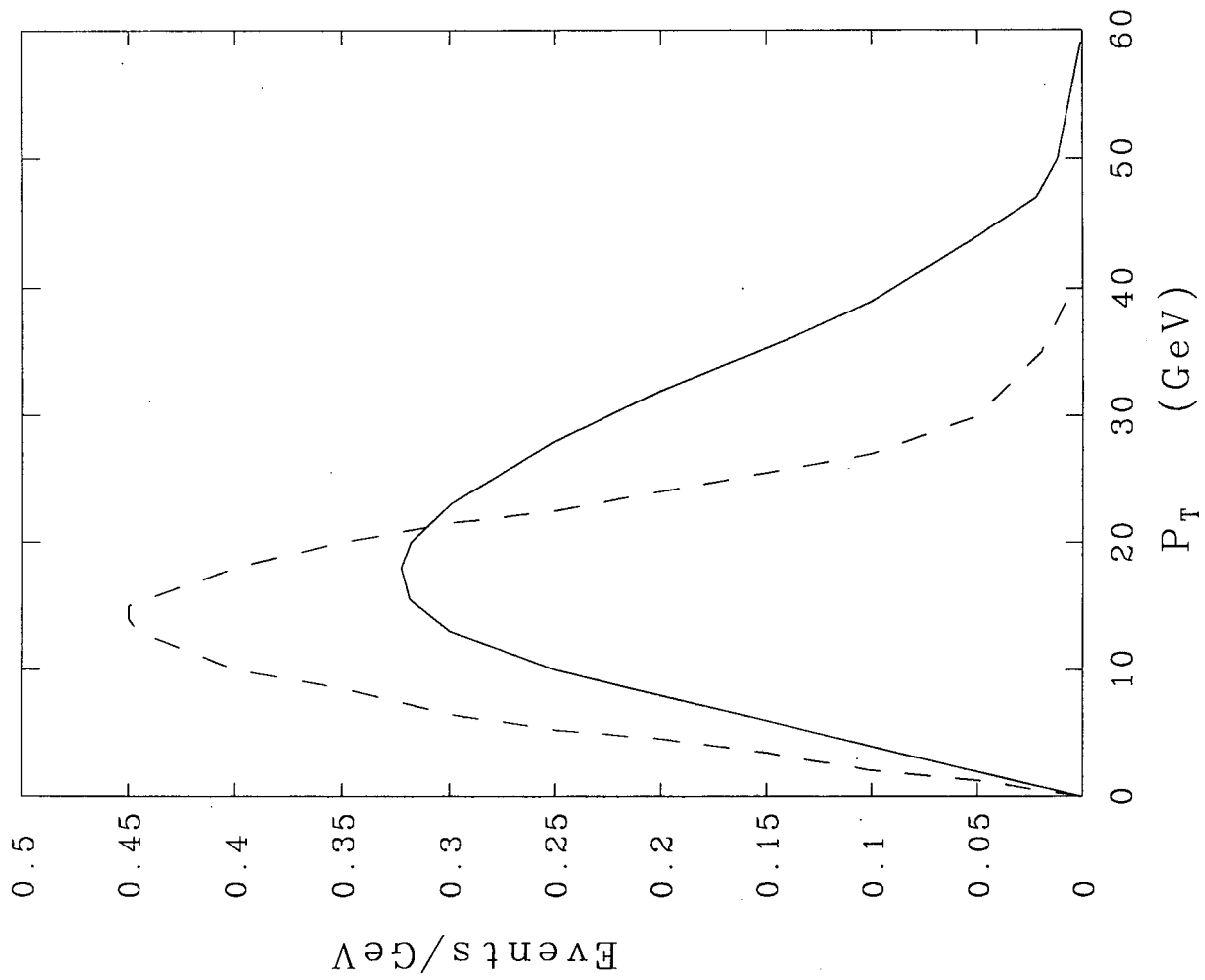


Figure 4.1

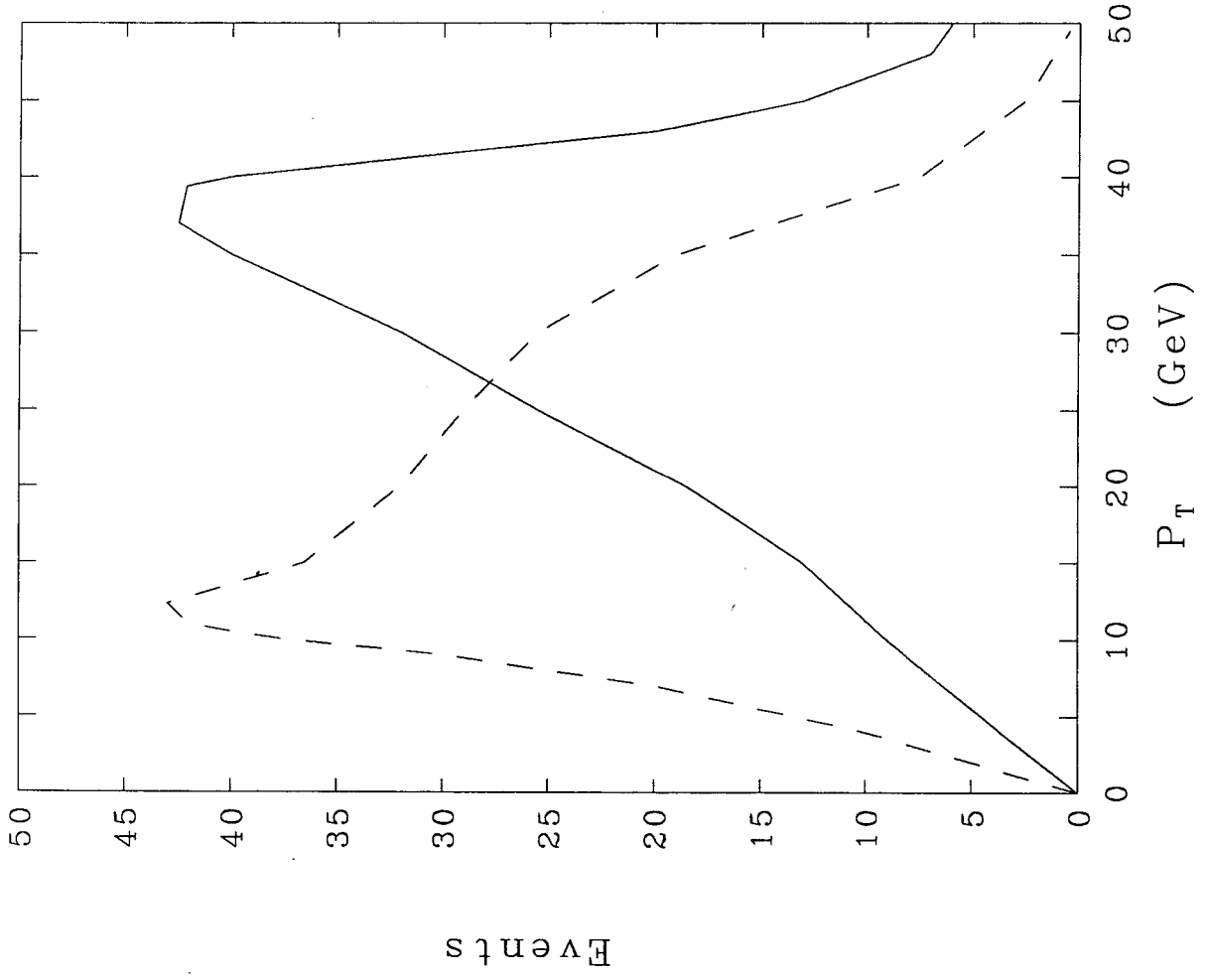


Figure 4.2

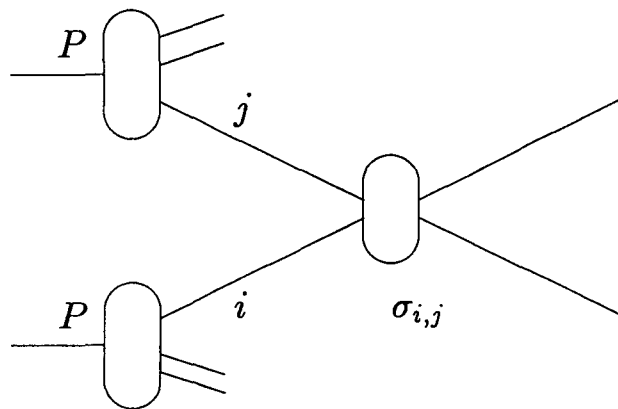


Figure 4.3

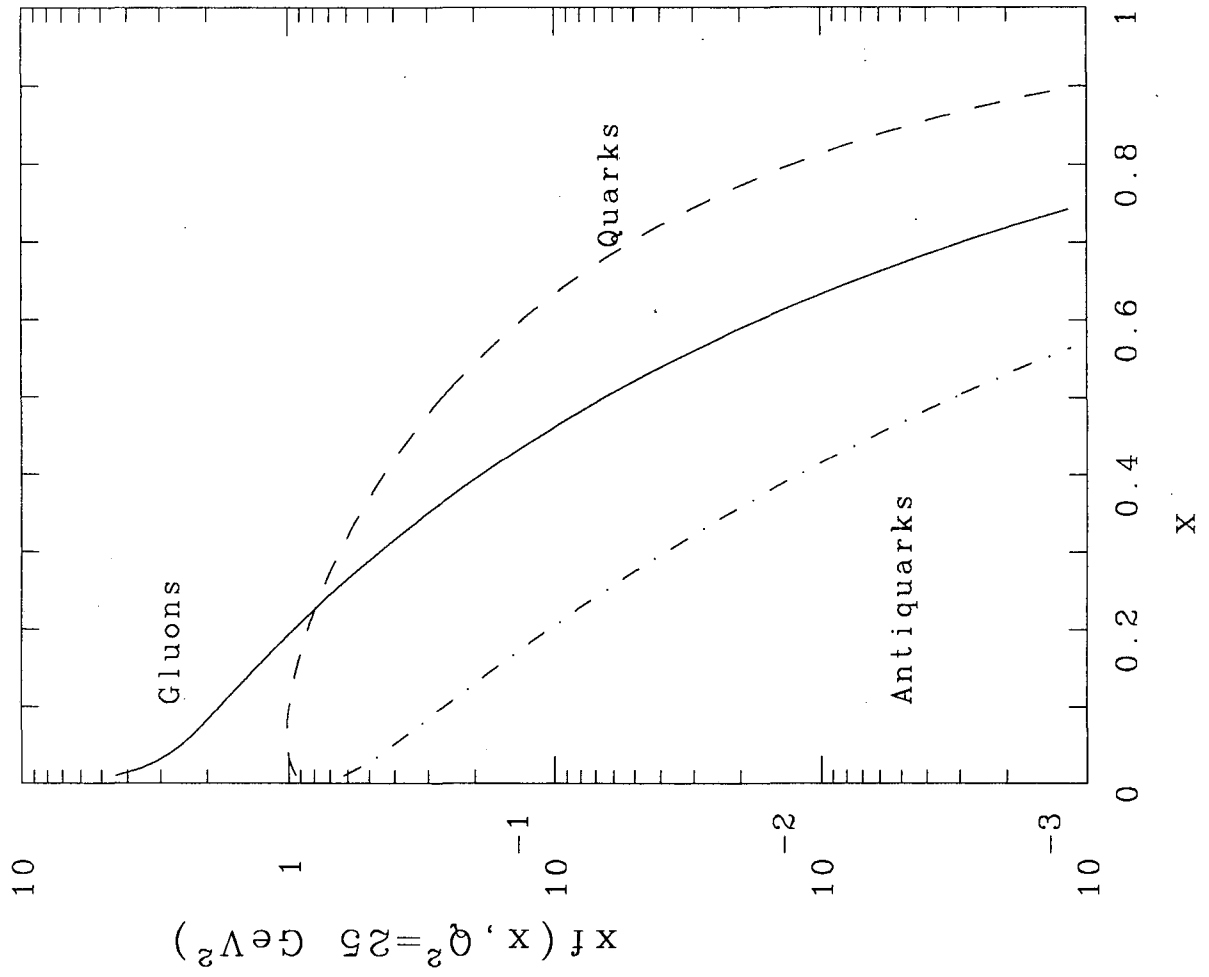


Figure 4.4

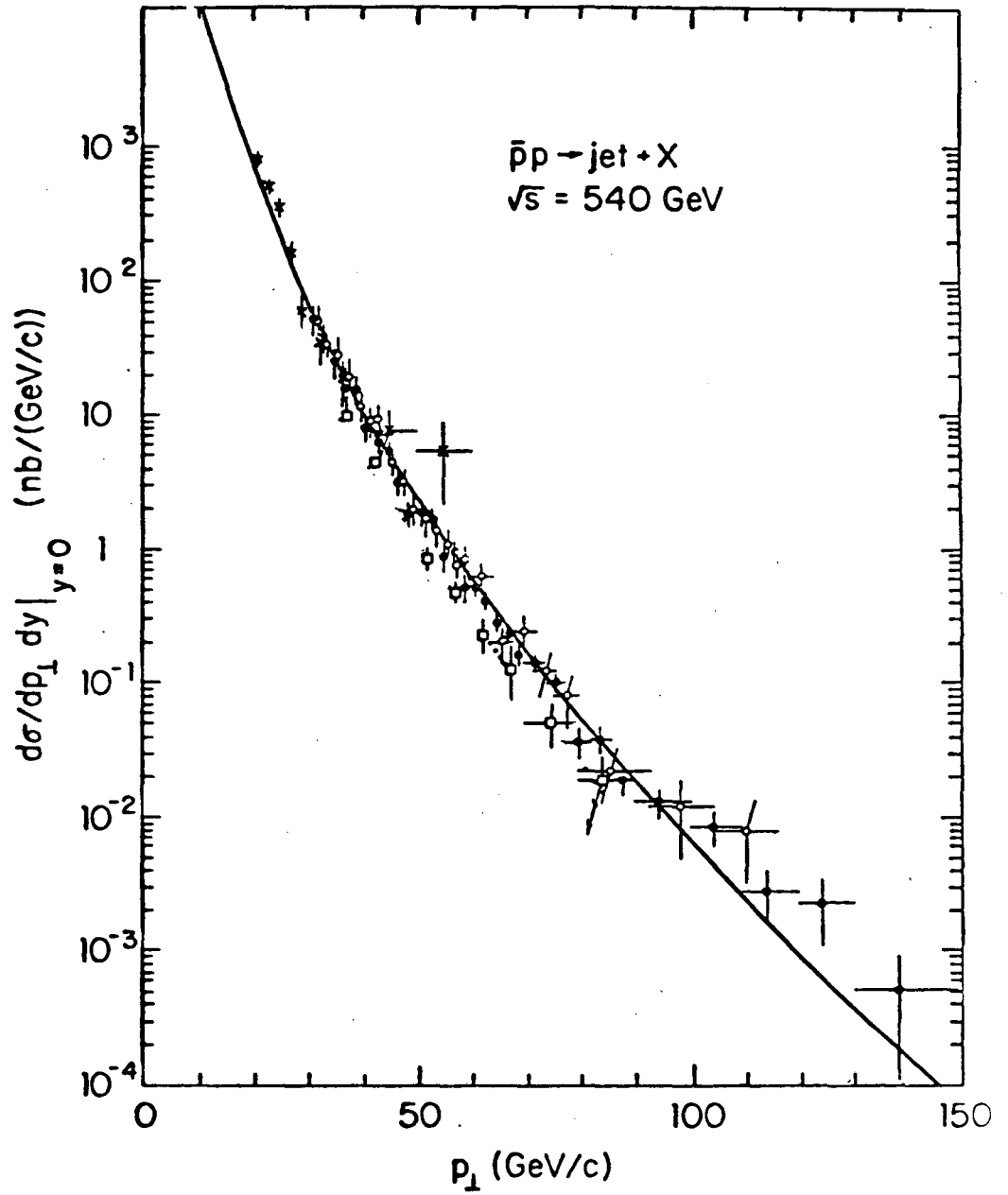


figure 4.5

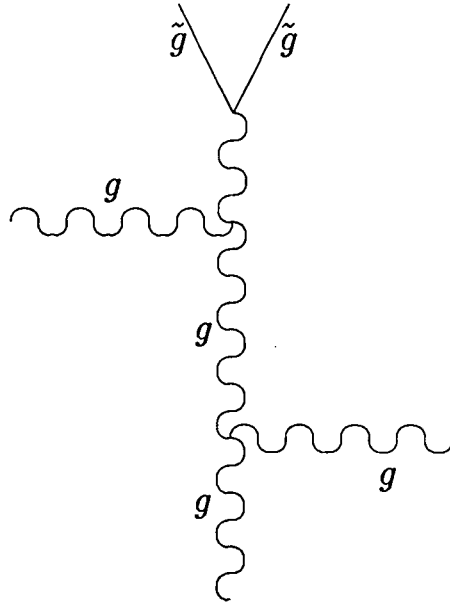


Figure 4.6

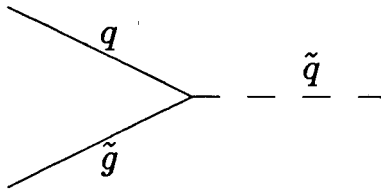


Figure 4.7

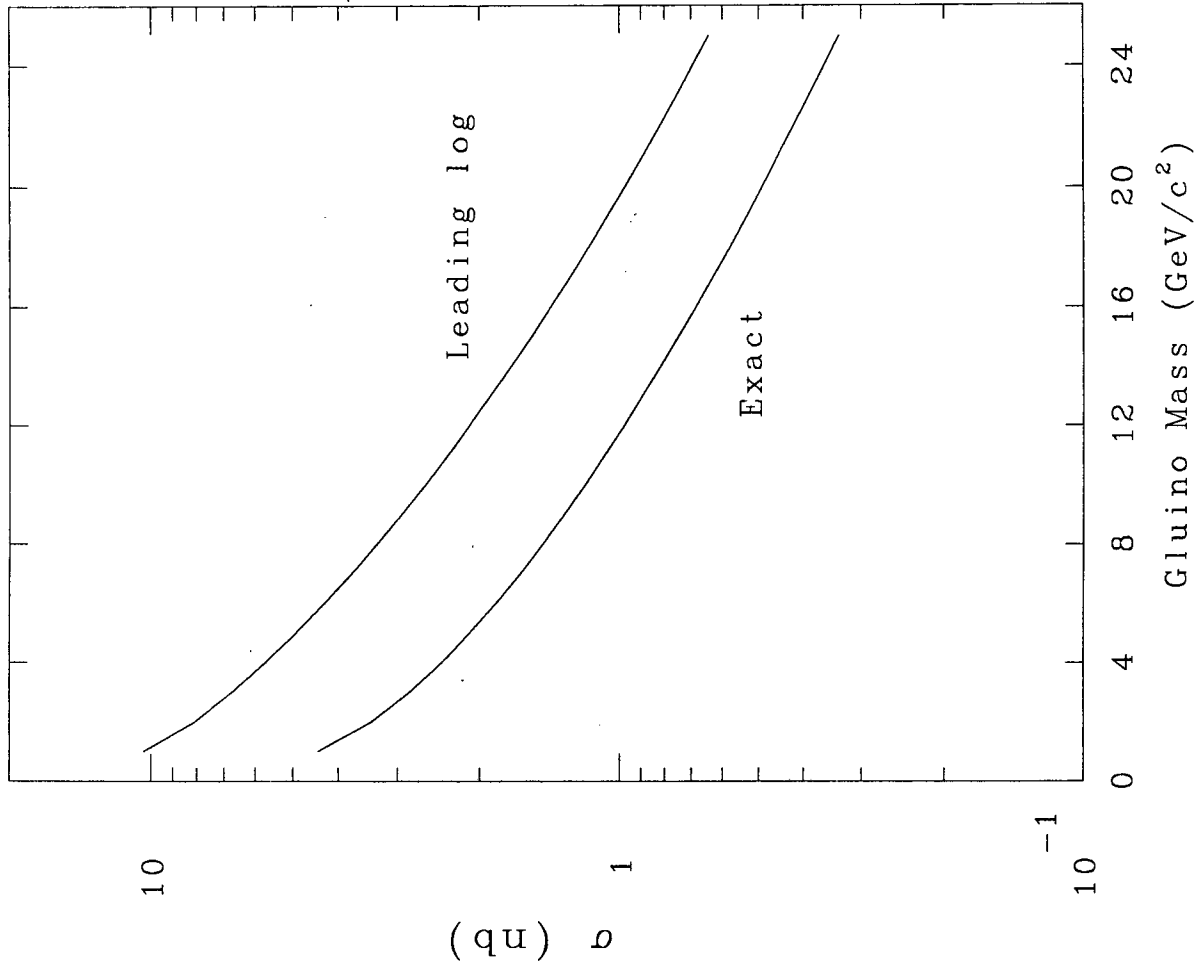


Figure 4.8

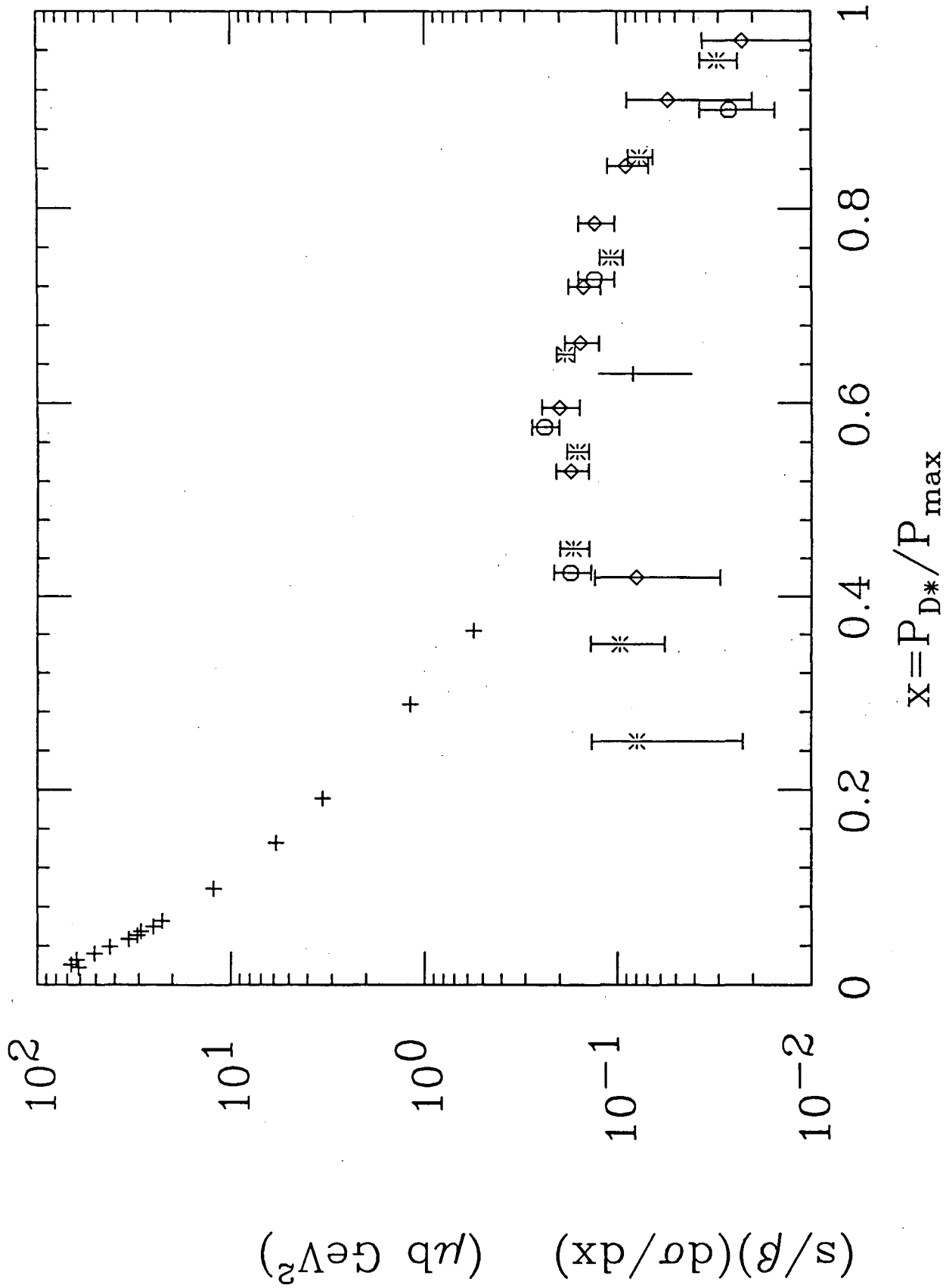


Figure 4.9

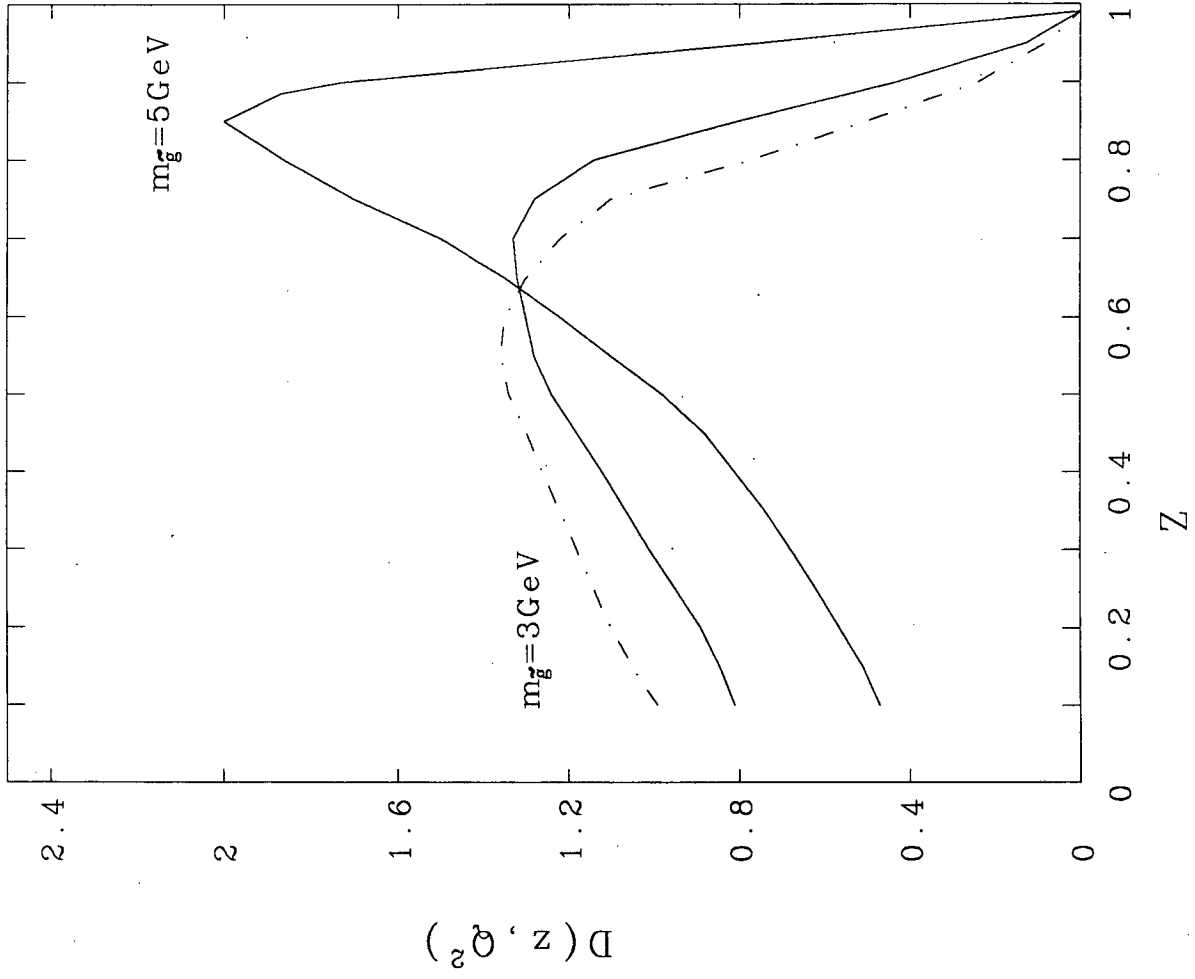


Figure 4.10

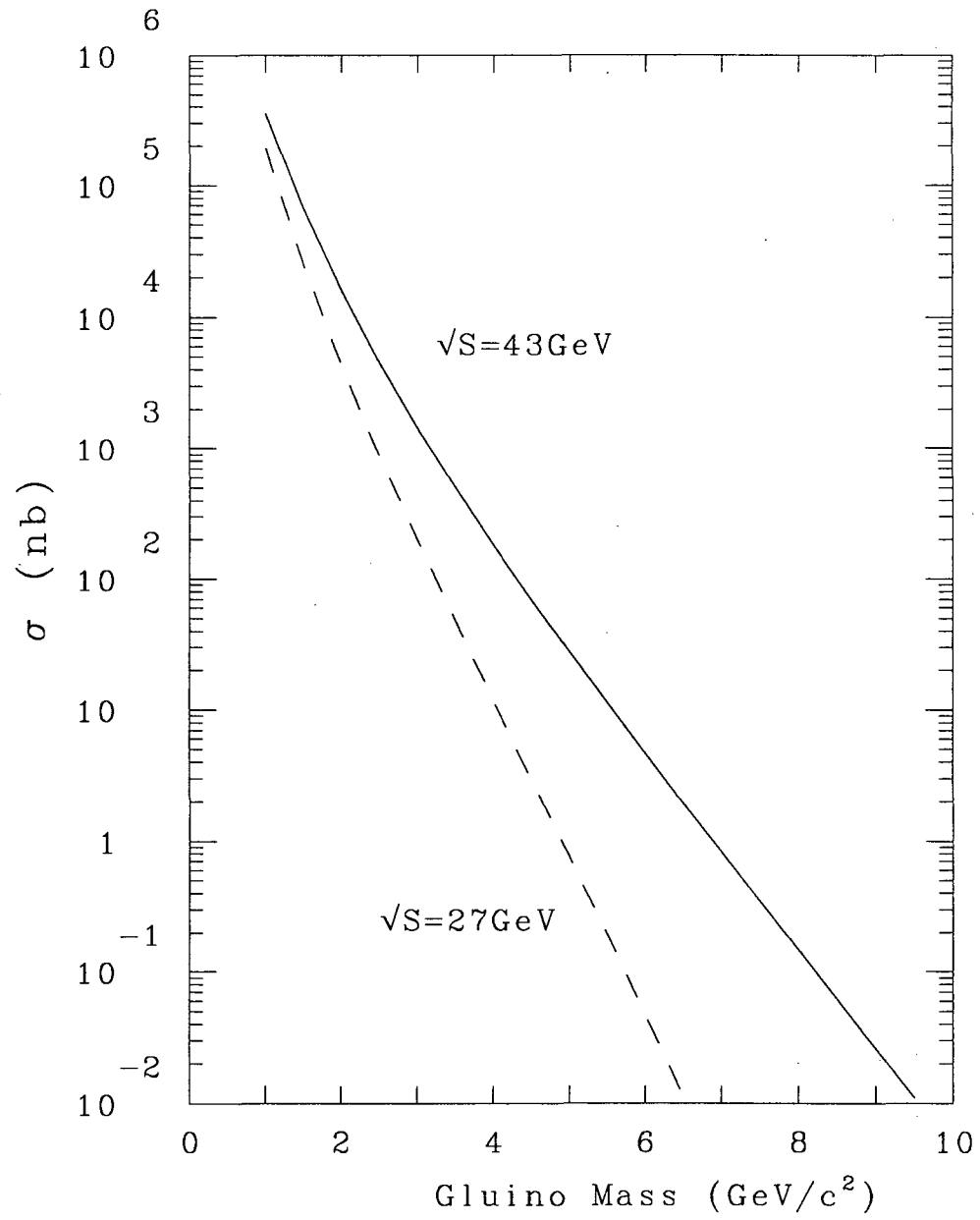


Figure 4.11

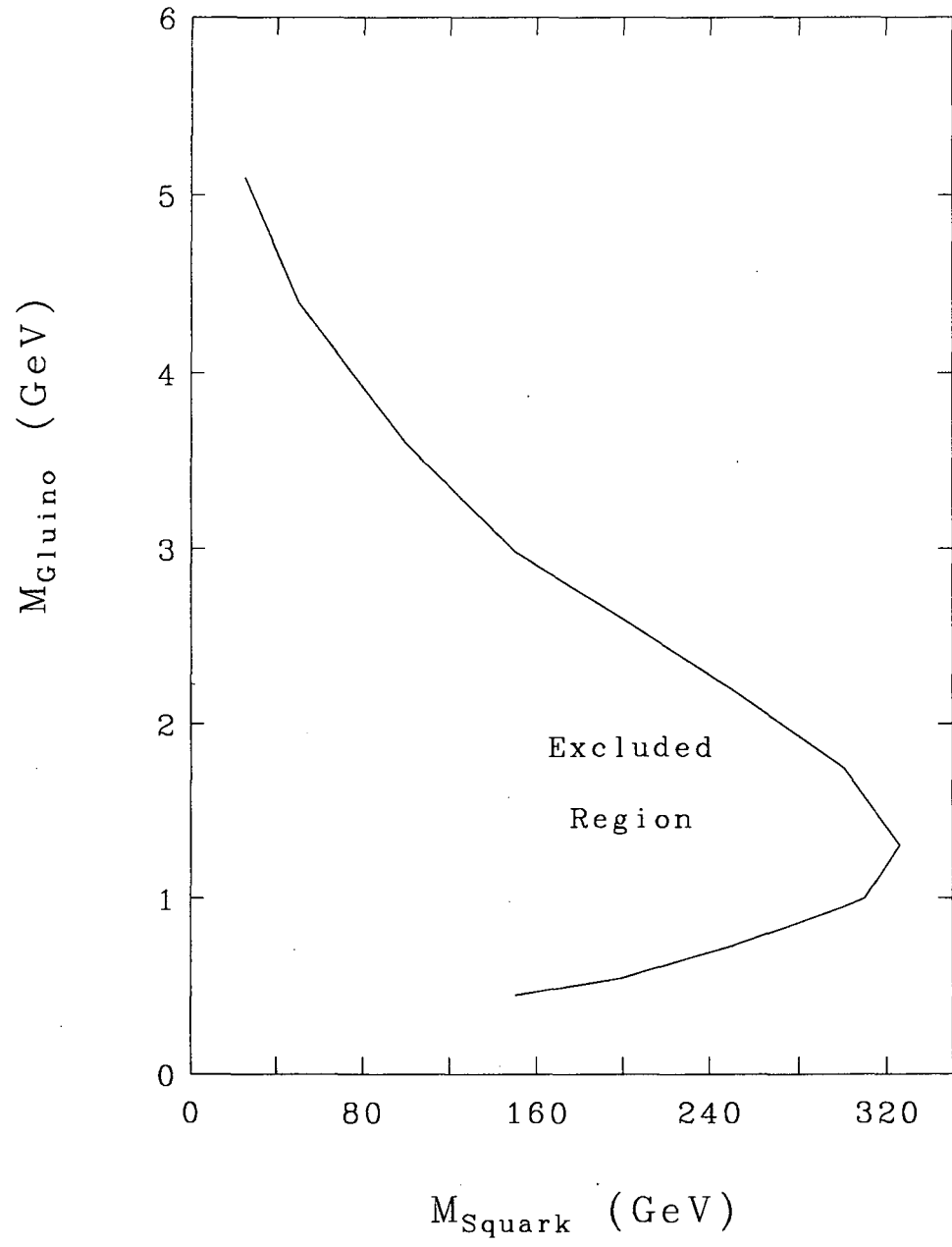


Figure 4.12

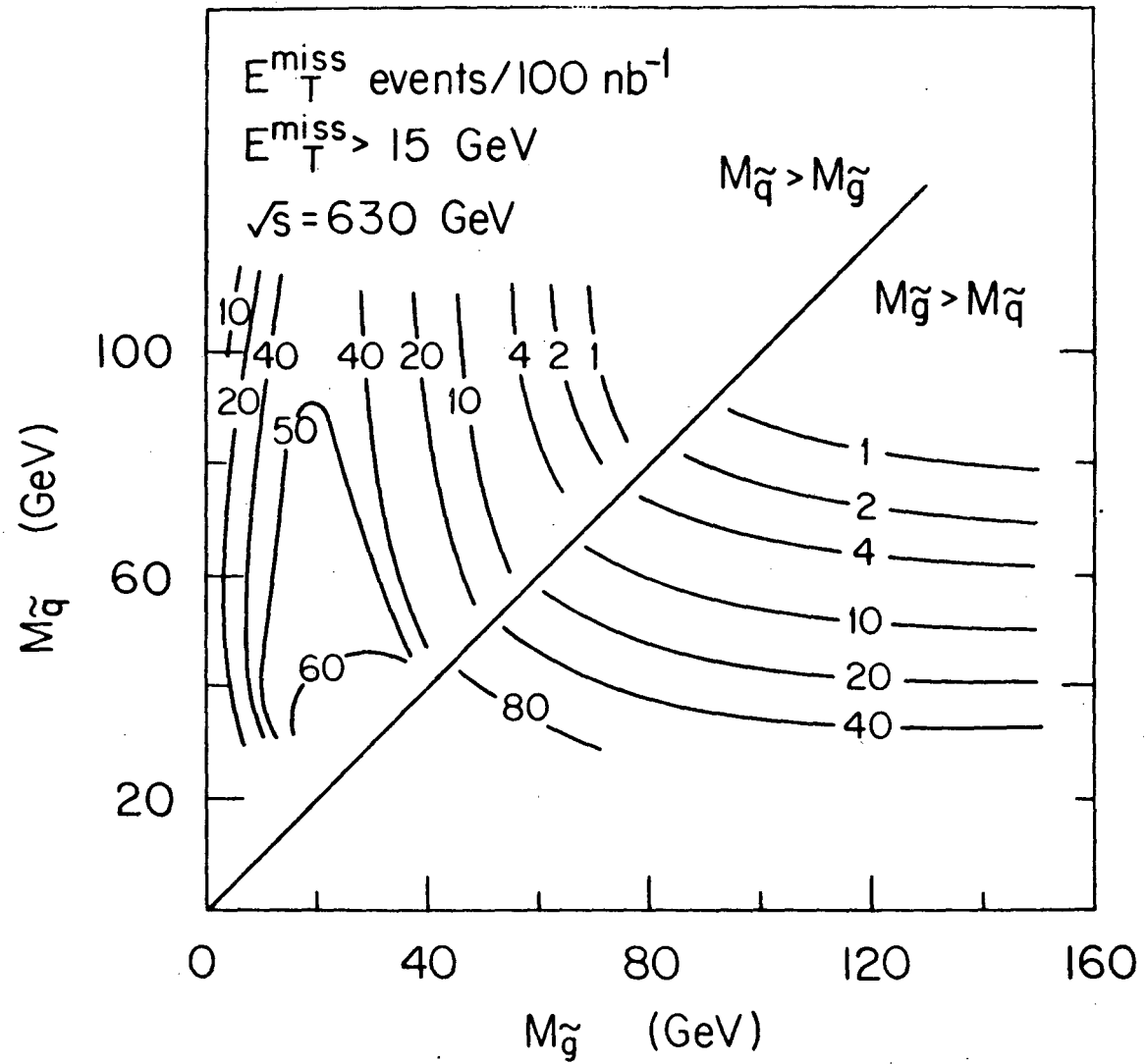


figure 4.13

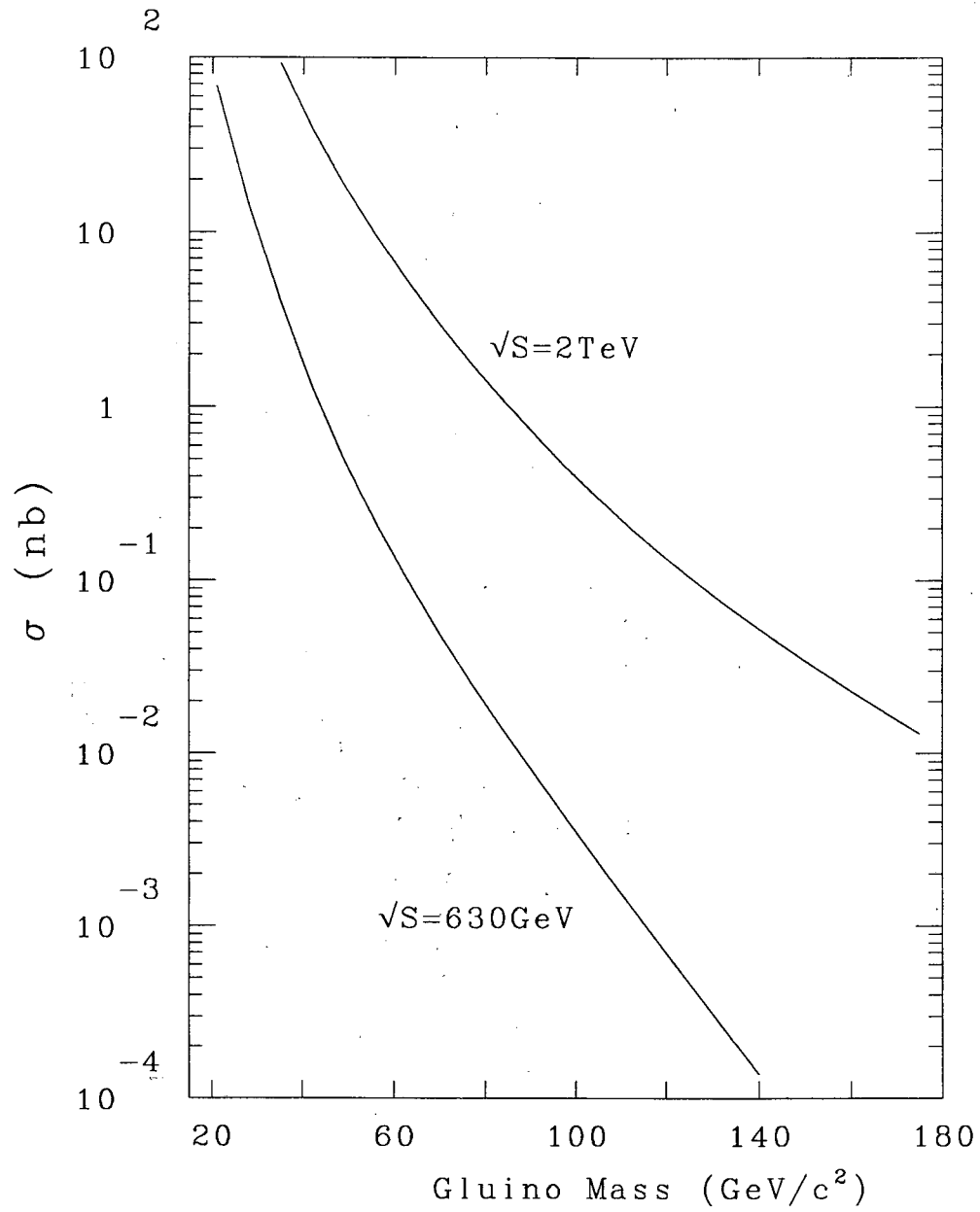


Figure 4.14

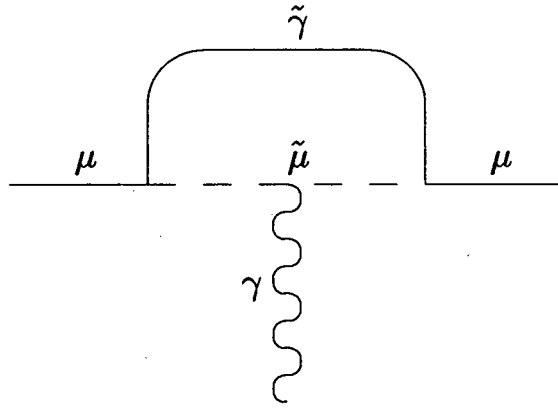


Figure 5.1

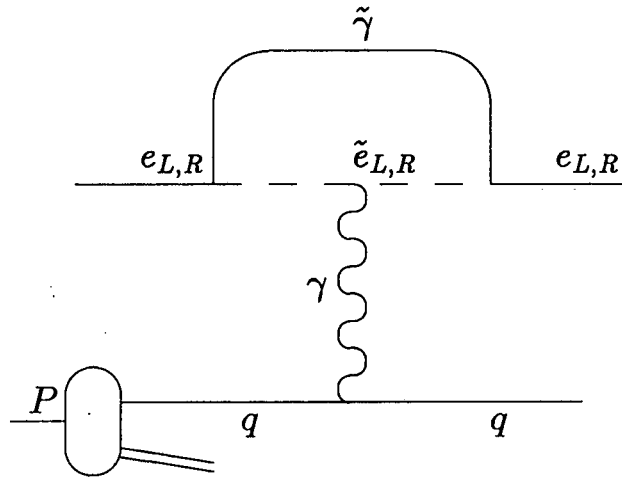


Figure 5.2

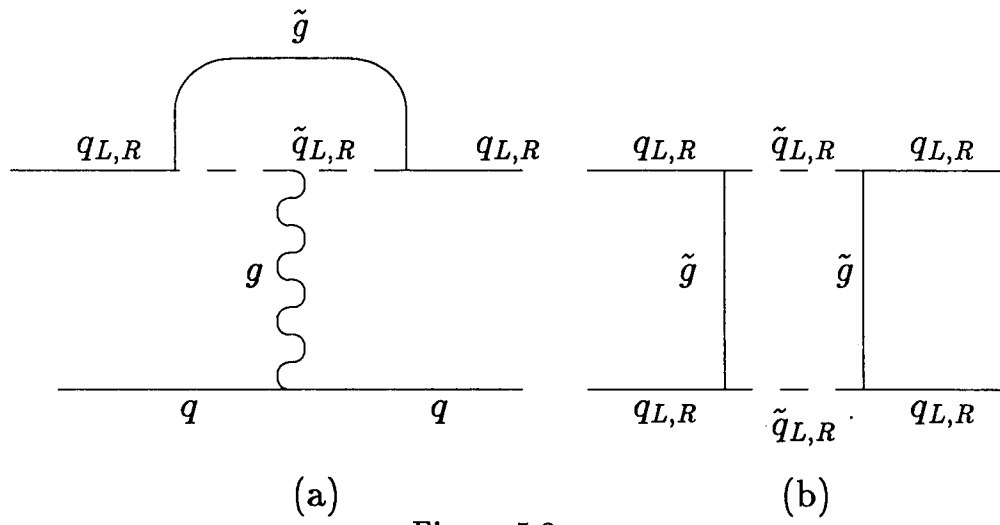


Figure 5.3

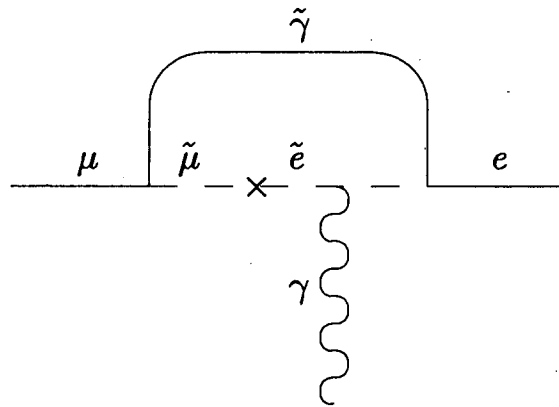


Figure 5.4

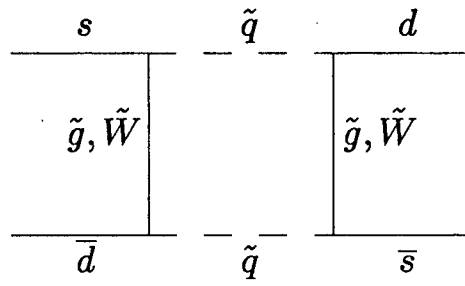


Figure 5.5

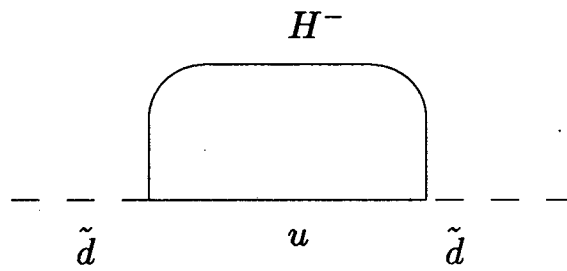


Figure 5.6

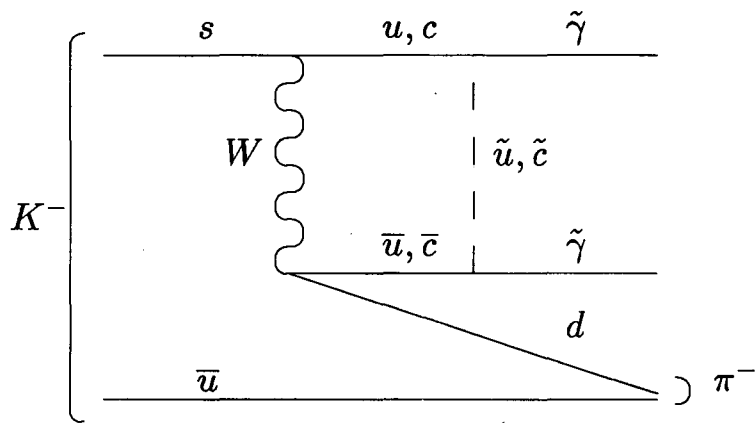


Figure 5.7

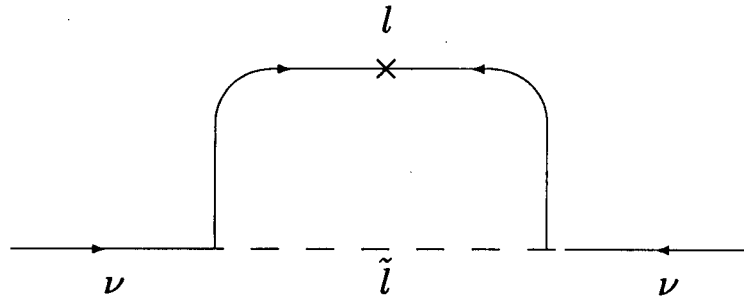


Figure 6.1

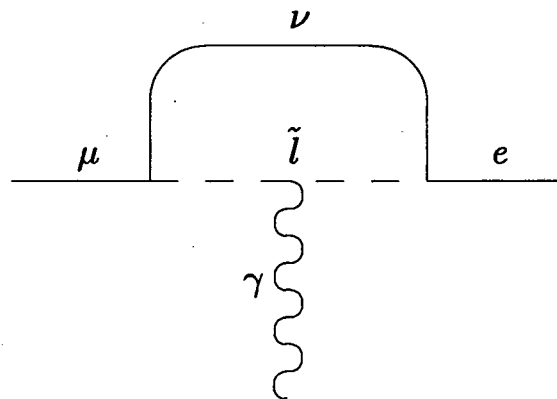


Figure 6.2

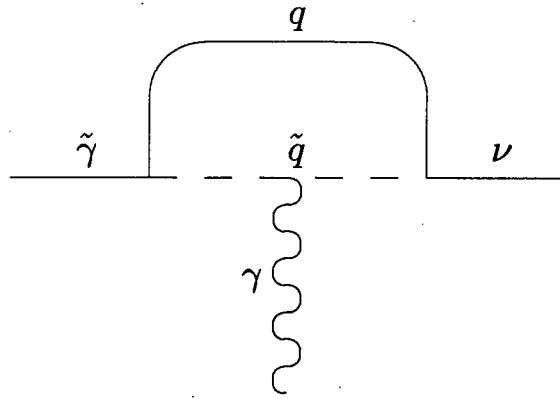


Figure 6.3

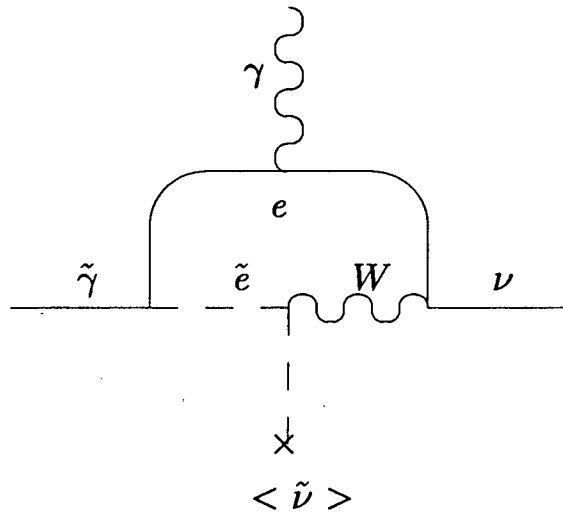


Figure 6.4

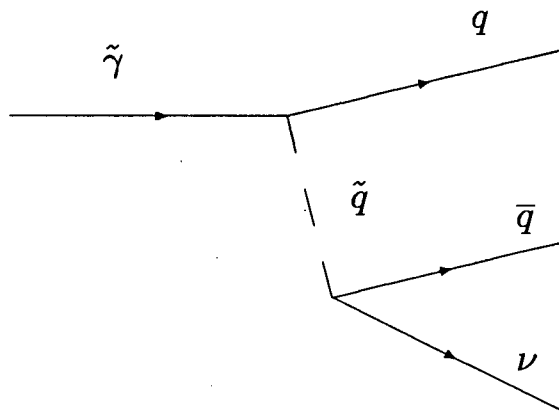


Figure 6.5

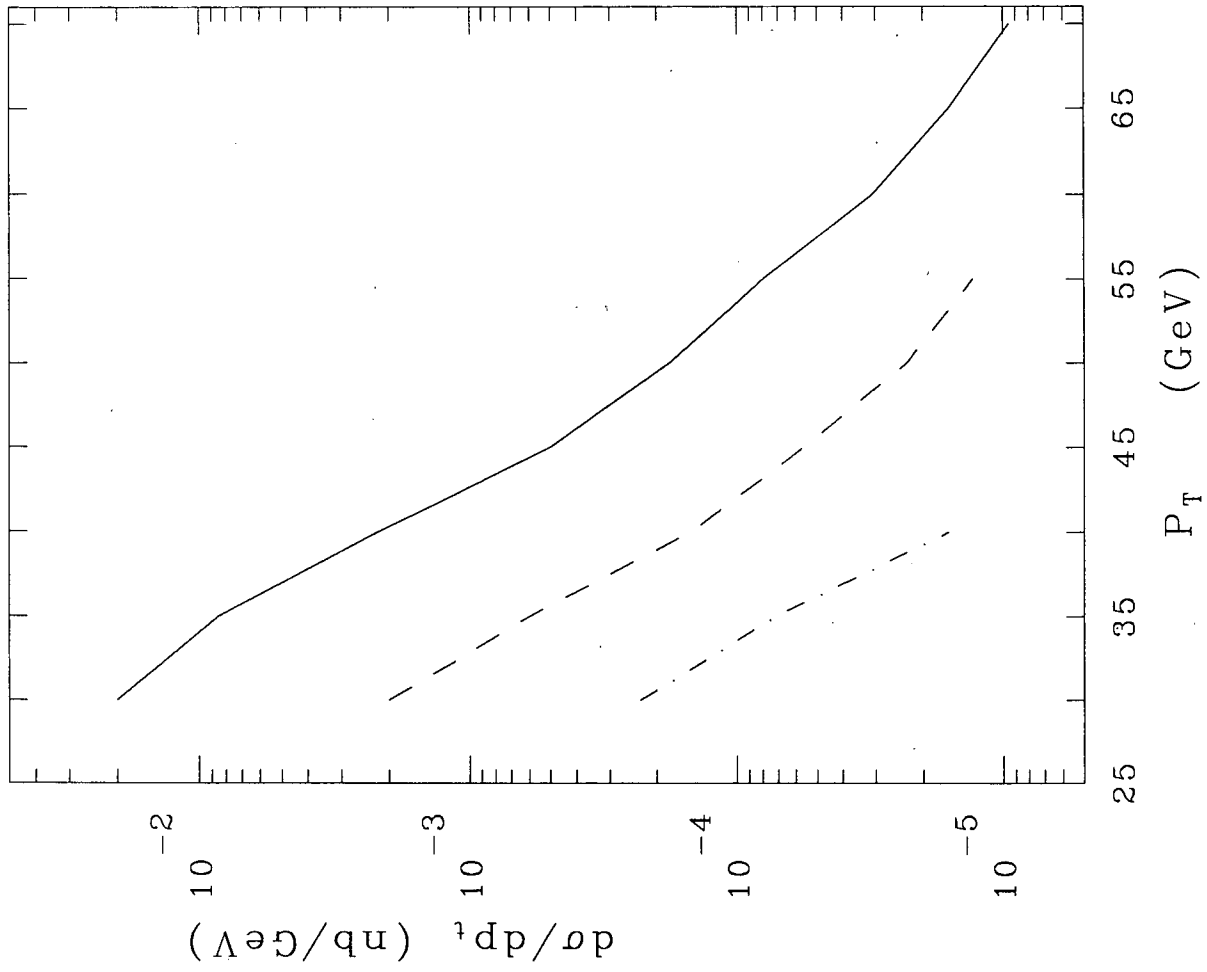


Figure 6.6

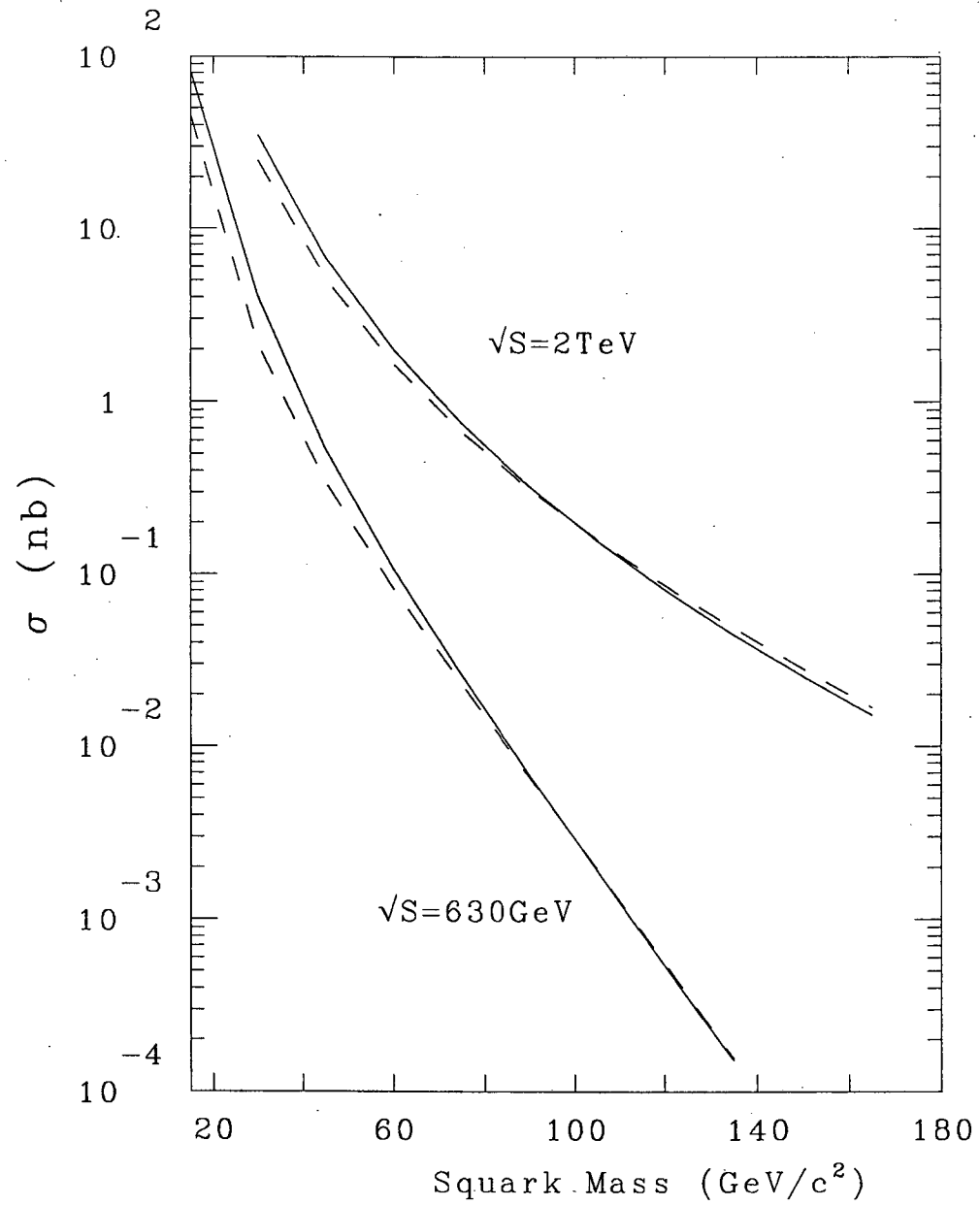


Figure 6.7

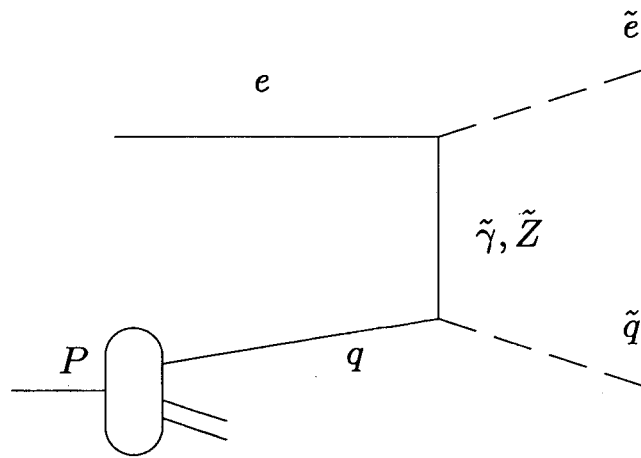


Figure 6.8

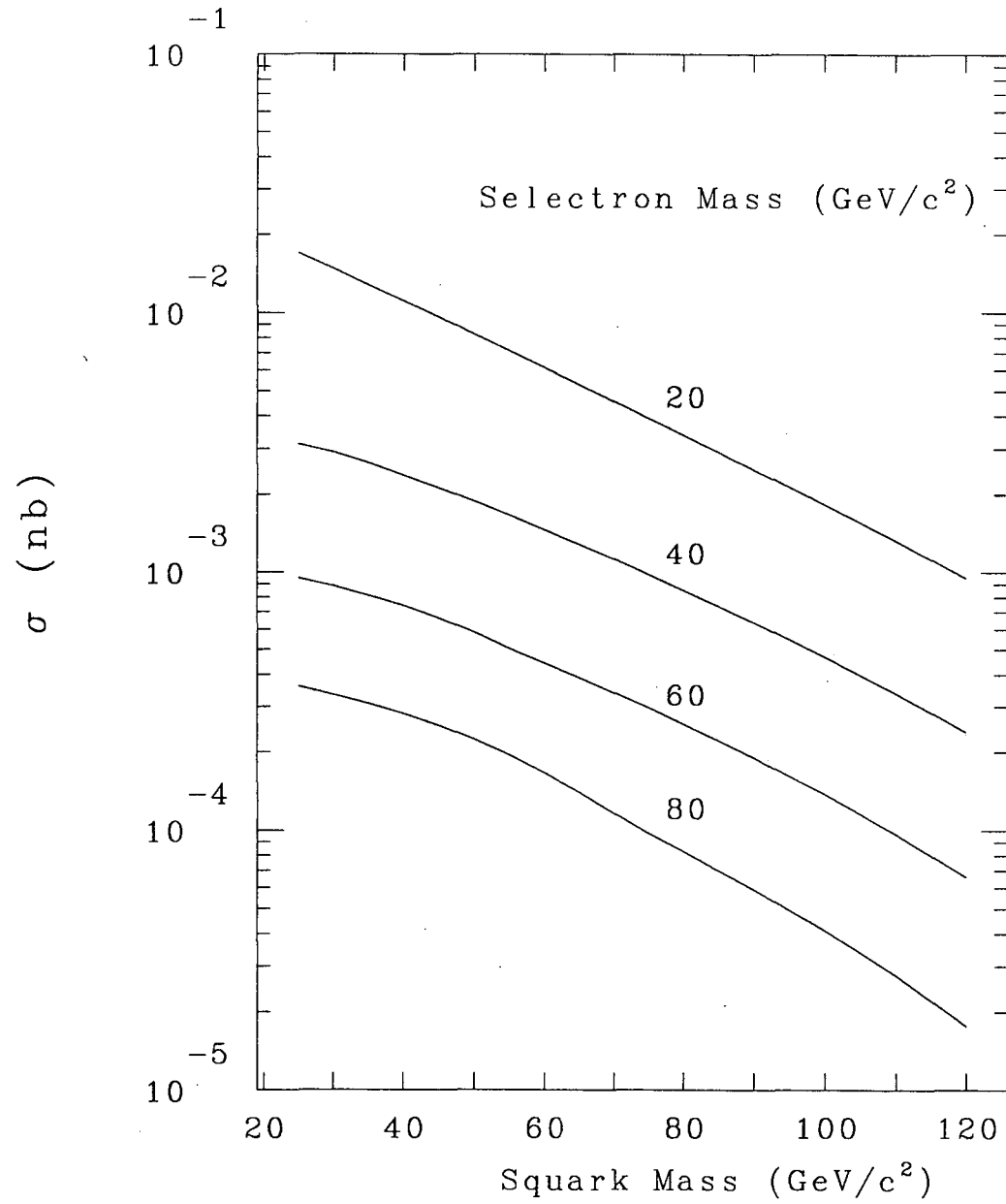


Figure 6.9

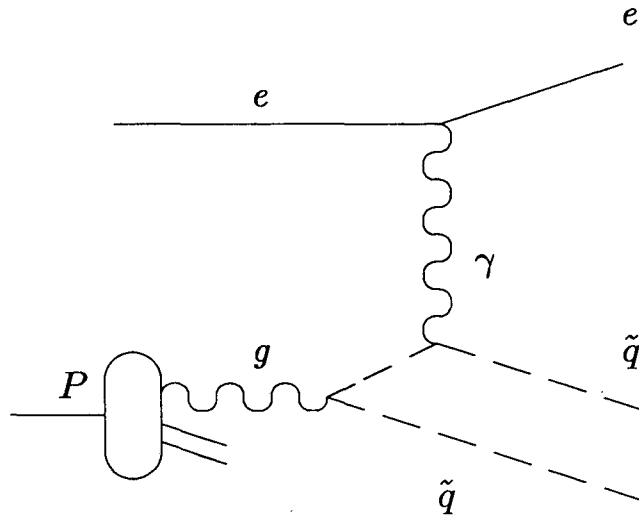


Figure 6.10

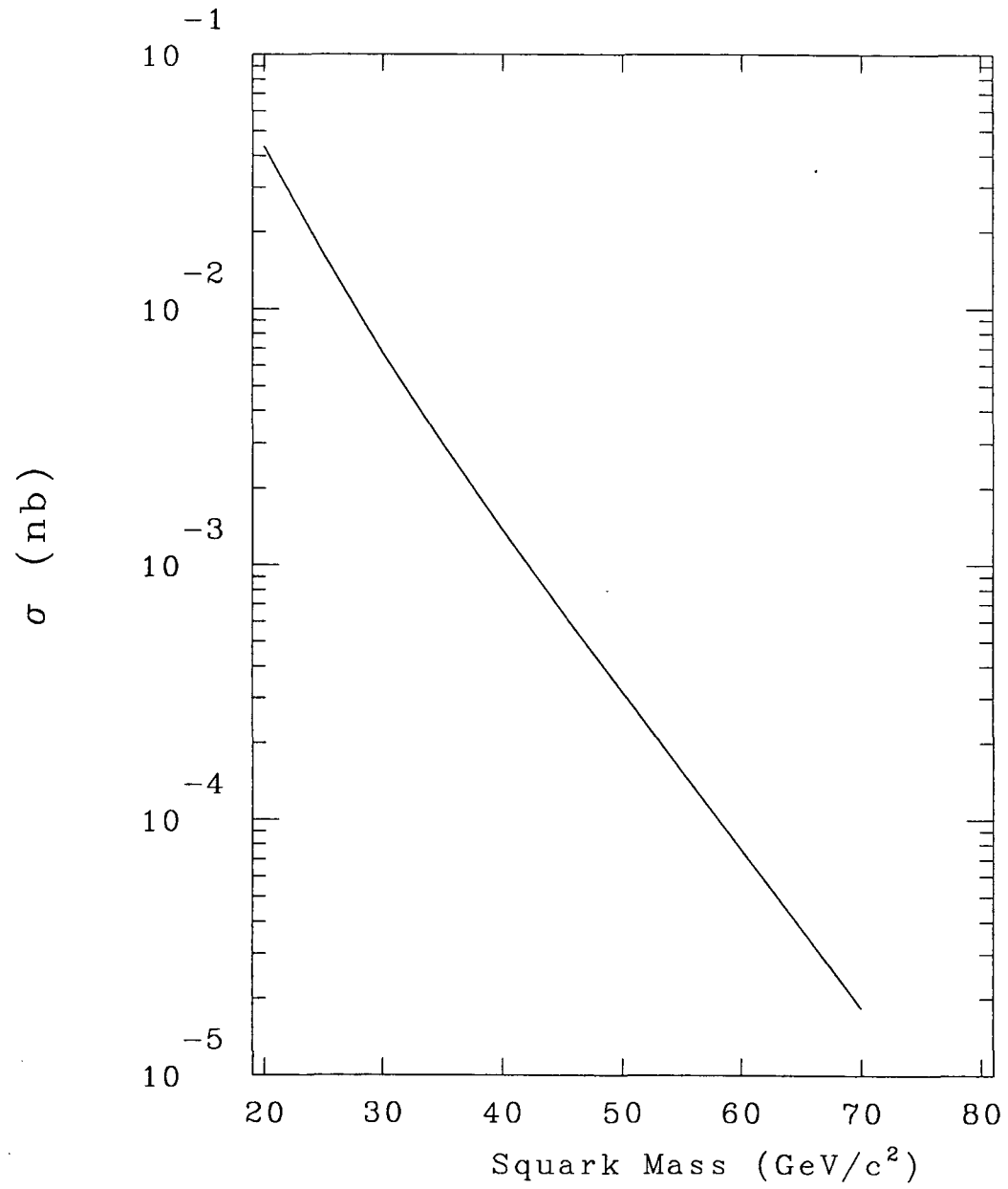


Figure 6.11

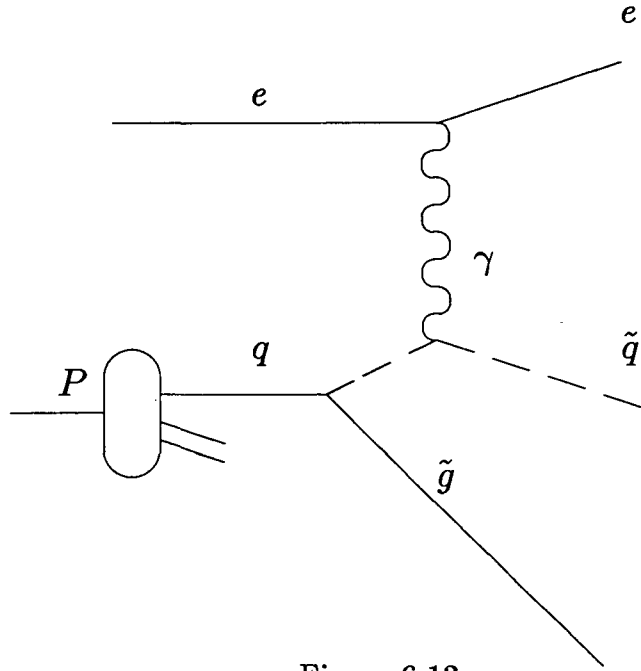


Figure 6.12

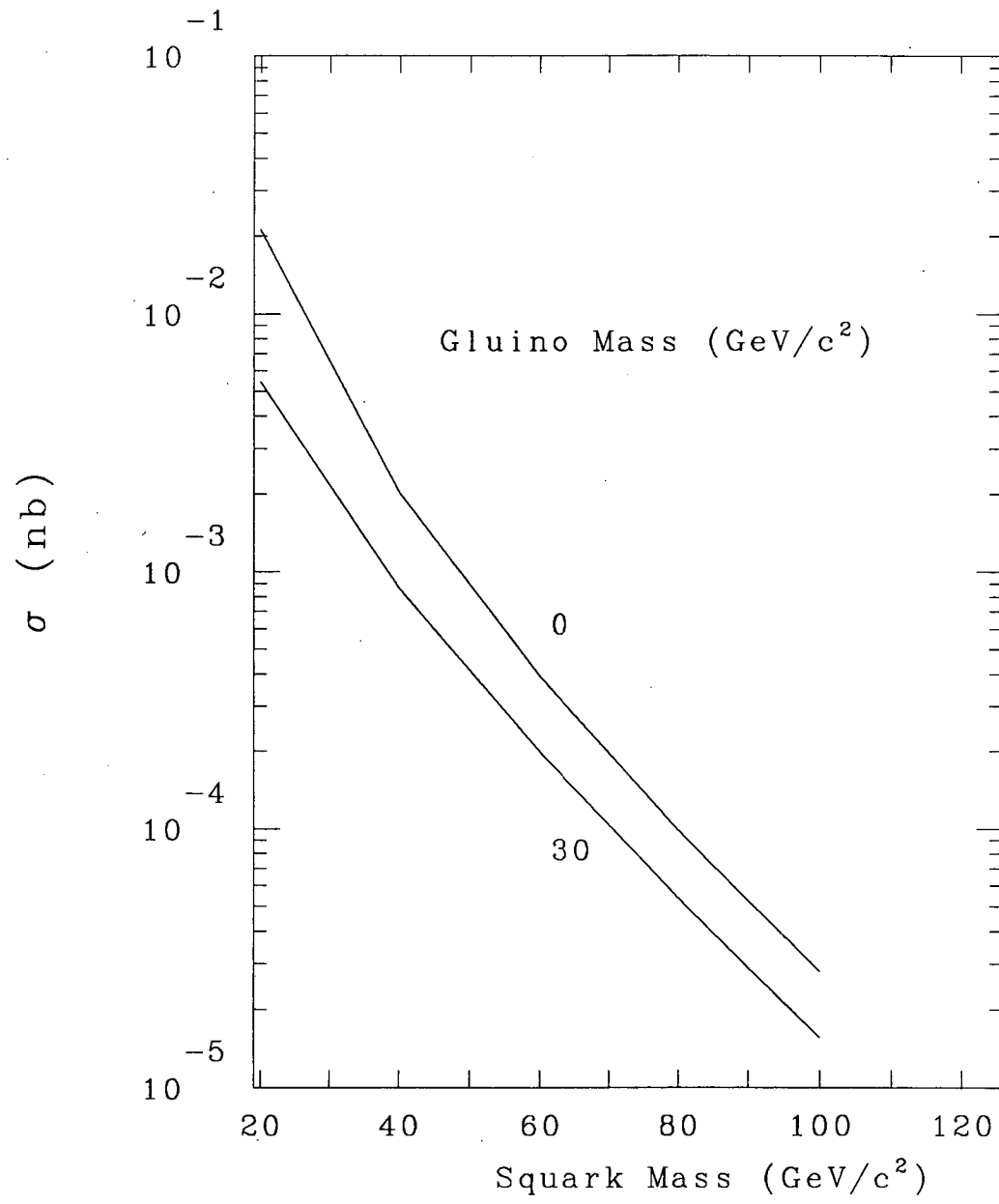


Figure 6.13

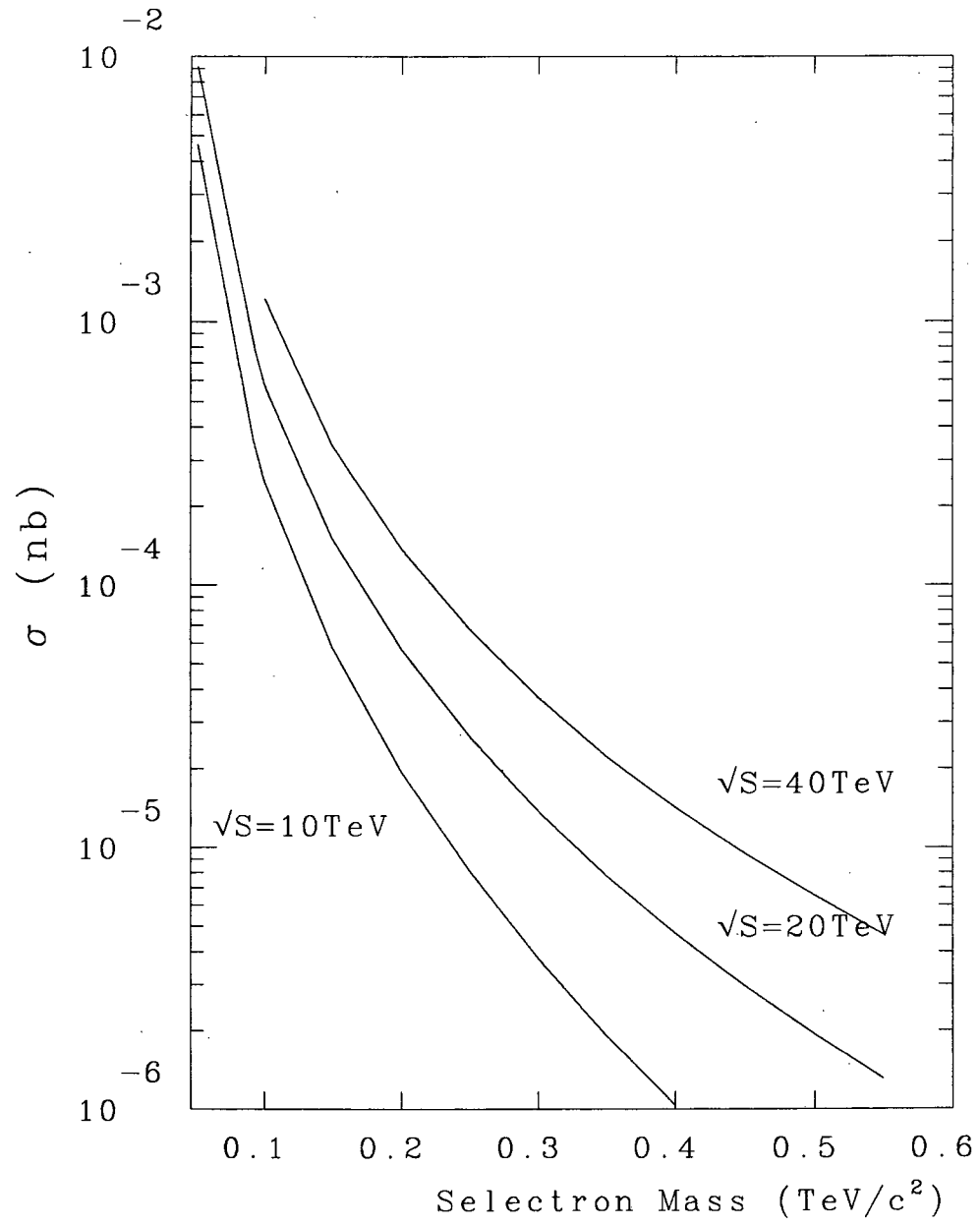


Figure 6.14

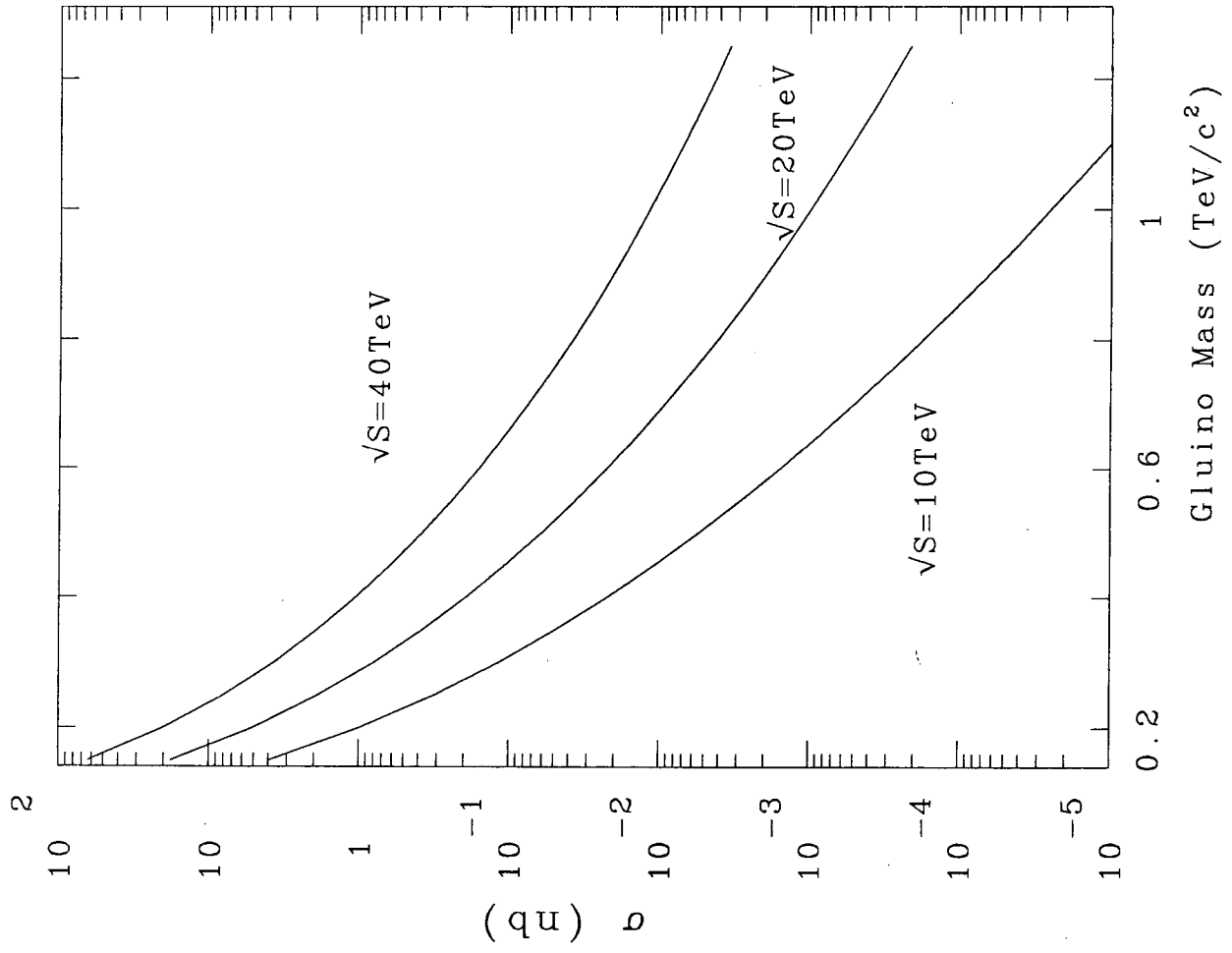


Figure 6.15

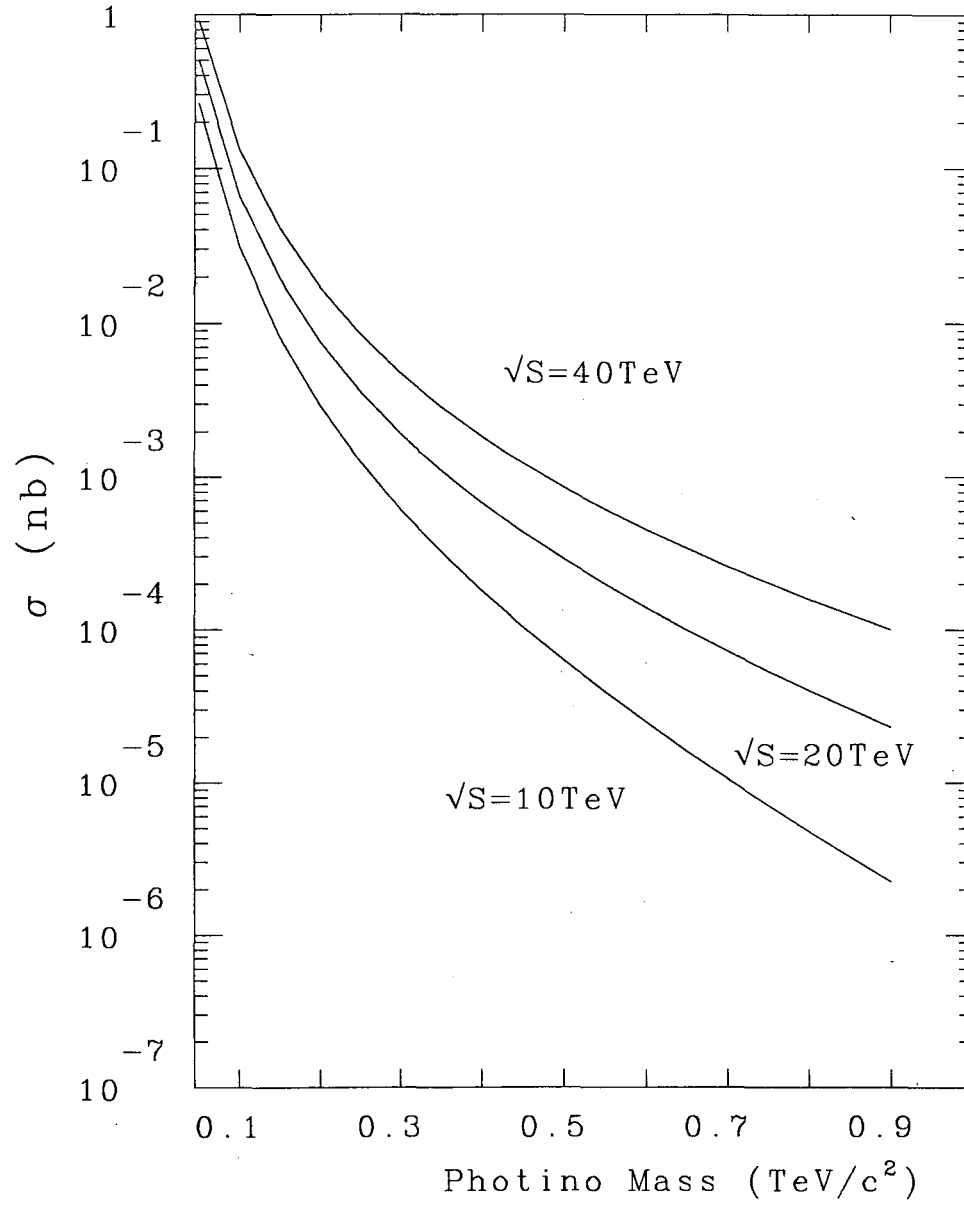


Figure 6.16

This report was done with support from the Department of Energy. Any conclusions or opinions expressed in this report represent solely those of the author(s) and not necessarily those of The Regents of the University of California, the Lawrence Berkeley Laboratory or the Department of Energy.

Reference to a company or product name does not imply approval or recommendation of the product by the University of California or the U.S. Department of Energy to the exclusion of others that may be suitable.

*LAWRENCE BERKELEY LABORATORY
TECHNICAL INFORMATION DEPARTMENT
UNIVERSITY OF CALIFORNIA
BERKELEY, CALIFORNIA 94720*